4-5-2017

Activation of Human Vγ9Vδ2 T Cells by Phosphoantigen Prodrugs

Ashley M. Kilcollins
University of Connecticut, ashley.kilcollins@uconn.edu

Activation of Human Vγ9Vδ2 T Cells by Phosphoantigen Prodrugs

Ashley Marie Kilcollins, Ph.D.

University of Connecticut, 2017

Vγ9Vδ2 T cells are a subset of T cells which recognize cells containing small charge-negative phosphorous compounds known as phosphoantigens. These phosphoantigens include (*E*)-4-hydroxy-3-methyl-but-2-enyl diphosphate (HMBPP) and isopentenyl diphosphate (IPP) which are produced primarily by microbial organisms (HMBPP) and at low levels in human cells (IPP), but are increased some in cancer cells. The mechanisms involved in Vγ9Vδ2 T cell activation are widely unknown and are continually being uncovered. Here, we investigate the signaling involved in Vγ9Vδ2 T cell activation in both the T cell as well as signaling in the target cell. Using live imaging and flow cytometry in human cells, our studies elucidate the signaling pathways, the pathway of cellular uptake of charge-negative phosphoantigens, and the significance of the phosphoantigen binding protein BTN3A1, in phosphoantigen mediated Vγ9Vδ2 T cell activation. As these phosphoantigens are charge-negative, we also investigate several charge-neutral phosphoantigen prodrugs including POM_2-C-HMBP, which readily cross the plasma membrane. These studies show the effects of phosphoantigen prodrugs on Vγ9Vδ2 T cell expansion, target cell lysis by Vγ9Vδ2 T cells, and toxicity in several human cell lines. *In vivo* analysis has also shown little toxicity of these prodrugs and a humanized mouse model has been established to test expansion of Vγ9Vδ2 T cells and cancer treatment *in vivo*. Together, these studies expand the knowledge of Vγ9Vδ2 T cell signaling and activation and provide a basis for future studies, particularly the advancement of immunotherapies utilizing Vγ9Vδ2 T cell.

Activation of Human Vγ9Vδ2 T Cells by Phosphoantigen Prodrugs

Ashley Marie Kilcollins

B.S., University of Connecticut, **2010**

A Dissertation

Submitted in Partial Fulfillment of the

Requirements for the Degree of

Doctor of Philosophy

at the

University of Connecticut

2017

APPROVAL PAGE

Doctor of Philosophy Dissertation

Activation of Human Vγ9Vδ2 T Cells by Phosphoantigen Prodrugs

Presented by

Ashley Marie Kilcollins, B.S.

Major Advisor

_____

Andrew J. Wiemer, Ph.D.

Associate Advisor

_____

Randall S. Walikonis, Ph.D.

Associate Advisor

_____

Akiko Nishiyama, M.D., Ph.D.

Associate Advisor

_____

Olga Vinogradova, Ph.D.

Associate Advisor

_____

Steven Szczepanek, Ph.D.

University of Connecticut

2017

Table of Contents

CHAPTER I

INTRODUCTION

Immunological synapse

In Greek, "synapse" means conjunction or to clasp. Biological synapses therefore, can be described as a tight interaction between two cells, most commonly associated with the interaction between two neurons (Oxford English Dictionary). Here, at the synapse, information from one cell is passed to the next in order to illicit a response. This same concept applies when T cells, natural killer (NK) cells, or B cells interact with antigen presenting cells, and has been termed the immunological synapse. It is at this interaction between the effector immune cell and the target cell presenting antigen that several proteins cluster together [1-3]. Proteins from each side of the synapse interact with each other and ultimately determine whether the effector cell will become stimulated/activated or whether it will detach without activation [1-4].

In αβ T cells, there are a number of receptor molecules located at the synapse, these include; 1) antigen receptors, e.g. T cell receptors (TCRs), 2) adhesion molecules, e.g. lymphocyte function-associated antigen 1 (LFA-1), and 3) costimulatory molecules, e.g. CD28. The TCR is located at the center of the synapse and interacts with major histocompatibility complex (MHC) molecules on the opposing cell [3, 5]. Costimulatory molecules like CD28 are located just outside of the TCRs and interact with their ligands, which in the case of CD28 are CD80 and CD86, both of which are B7 proteins found on the target cell [6-8]. Both the TCRs and costimulatory molecules are located at the area of the synapse known as the central supramolecular activation cluster (cSMAC). Adhesion molecules, such as LFA-1, are located just outside of the cSMAC at the peripheral supramolecular activation center (pSMAC) and interact with their binding proteins, i.e. intracellular adhesion molecule 1 (ICAM-1), on the opposing cell [3, 9].

It has been well accepted that specificity of the immune response is governed by the TCR-MHC complex. Costimulatory molecules alone are unlikely to sustain an immunological synapse, but instead act to strengthen it once established by the TCR-MHC complex and its cellular signaling to the adhesion molecules. However, a lack of co-stimulation, in αβ T cells, leads to anergy, an unresponsiveness of the T cell [9].

The synapse as a whole is important for the function of T cells, not only because it leads to stimulation or activation of the T cell, but it has been shown that once activated, cytotoxic T cells lyse and kill target cells by secreting cytotoxic granules that are released at the synapse directly [10]. Another function of T cells is to secrete cytokines, once an immunological synapse is formed some cytokines, specifically interferon γ (IFN-γ), are secreted directed toward the synapse, however secretion of other cytokines, such as tumor necrosis factor α (TNF-α) are not [11].

Overall, immunological synapses are the site of important interactions between effector immune cells and their antigen-presenting and/or target cells. If these synapses are non-functioning, it could result in pathogenic infections of the organism or even cancer [12, 13]. Here, I will examine the immunological synapse between a specific type of effector immune cells, the γδ T cells, and their target cells.

γδ T cells

γδ T cells are a unique subset of T cells, often referred to as "non-traditional" or "non-canonical" T cells. These cells differ from αβ T cells in that they express a TCR with a γ chain instead of an α chain, and a δ chain instead of a β chain. There are several distinct types of γδ T cells, each type based off their specific γδ T cell receptors. For example, humans utilize up to seven Vγ chains, Vγ2, Vγ3, Vγ4, Vγ5, Vγ8, Vγ9, and Vγ11, and three Vδ chains, Vδ1, Vδ2, and Vδ3, to make up their γδ T cell receptor repertoire [14-16]. However, few of the antigens, or activating

ligands, for each specific TCRs have been found. TCR subunits and their known activating ligands include: Vδ1 TCRs recognize MHC class I polypeptide-related sequence A (MICA) [17], CD1c [18], CD1d [19], and lipohexapeptides [20]; Vδ2 recognize UL16 binding protein 4 (ULBP4) [21]; Vγ4Vδ5 recognize endothelial protein C receptor (EPCR) [22]; and Vγ9Vδ2 recognize phosphoantigens [23] and potentially F1-ATPase [24], though the latter report remains to be verified.

Once γδ T cells interact with their antigen directly, or in some cases, with cells containing these antigens, there are several different responses that can occur. Each γδ may respond in a manner of its own, based on the TCR it expresses, the type of synapse that is formed with the target cell, and/or the subset of T cell it is at the time (i.e. naïve, memory or effector). These different responses include, but are not limited to: proliferation; cytokine/chemokine production; interaction with B cells, leading to IgE production; interaction with dendritic cells, leading to dendritic cell maturation; interaction with αβ T cells, priming them via antigen presentation; and lysis of target cells [25]. The underlying mechanisms of each γδ T cell and its function are still widely unknown, but here, I hope to elucidate these mechanisms further in the specific subset of γδ T cells, the Vγ9Vδ2 T cells.

Vγ9Vδ2 T cells

The most common combination of the γδ T cell receptor is the Vγ9Vδ2 T cell receptor, which is found on approximately 75% of γδ T lymphocytes circulating the blood [26]. These cells are specifically sensitive to other cells containing phosphoantigens [27]. Phosphoantigens are small phosphorus containing molecules that can be found in cells infected with a microorganism. These microorganisms produce the phosphoantigen (*E*)-4-hydroxy-3-methyl-but-2-enyl diphosphate (HMBPP), an intermediate in the 2-*C*-methyl-D-erythritol 4-phosphate (MEP)

pathway of isoprenoid biosynthesis (Figure 1). Phosphoantigens can also be naturally occurring in human cells, the phosphoantigen isopentenyl diphosphate (IPP) [23, 28-30] is an intermediate in the mevalonate pathway of isoprenoid biosynthesis in human cells (Figure 1). However, at normal physiological levels, IPP is unable to stimulate Vγ9Vδ2 T cells, this is in part due to the levels of IPP itself, but also due to the potency of IPP as a phosphoantigen. In some instances, the level of IPP can increase, such as the case with some cancerous cells [31, 32] or following treatment with certain drugs, such as bisphosphonates that inhibit the enzyme farnesyl diphosphate synthase [33, 34]. These cells have an increase in production of IPP, which results in the recognition of these cells by Vγ9Vδ2 T cells. Phosphoantigens found inside the target cell then interact with a membrane bound protein, known as butyrophilin subfamily 3 member A1 (BTN3A1), at the cytoplasmic face of the plasma membrane [35]. This interaction ultimately leads to the activation of the Vγ9Vδ2 T cell via an inside-out mechanism which is still widely undefined [35-37].

BTN3A1 and the target cell

BTN3A1 and its isoforms, BTN3A2 and BTN3A3, are B7 family proteins, whose three distinct genes are located on chromosome 6 at the MHC region [38, 39]. This protein is membrane bound and stabilized at the membrane by the GTPase Rho B [37]. Here, two molecules of BTN3A1 form a homodimer [37] and interact with phosphoantigens at the intracellular B30.2 domain, as shown in Figure 2. Unlike αβ T cells, and even some subsets of γδ T cells where the target cell interacts with the respective antigen via an extracellular MHC molecule, Vγ9Vδ2 T cells do not interact with antigen presenting MHC molecules, instead they are somehow triggered by cells containing phosphoantigen interacting with BTN3A1 [40-44] by an unknown mechanism.

In nature, phosphoantigens are found within the target cell due to microbial infection, or in some malignant cells. However, it is also possible to study Vγ9Vδ2 T cells and their response to

the target cell, by treating/loading the target cell with exogenous phosphoantigen. These negatively charged phosphoantigens are not found at high enough levels naturally within these specific cells and therefore are somehow traversing the cell membrane to enter the cytoplasm, likely by endocytosis. Once there, they interact with the positively charged shallow binding pocket within the B30.2 domain of BTN3A1 [35]. Once phosphoantigens interact with the B30.2 domain of BTN3A1, a conformational change is seen, ultimately resulting in the stimulation or activation of the Vγ9Vδ2 T cells. However, the mechanism from this point until the target cell stimulates the Vγ9Vδ2 T cell is still not clear. This protein, BTN3A1, is not well understood but has been shown to be required for Vγ9Vδ2 T cell stimulation in response to primary peripheral blood cells [35]. In Chapter IV of this dissertation, I elucidate this mechanism further.

Vγ9Vδ2 T cells and the response to phosphoantigen stimulation

Once Vγ9Vδ2 T cells sense BTN3A1/phosphoantigen presenting target cells, they coordinate an immune response. This immune response begins at the γδ T cell receptor, at which point a γδ T cell receptor signal cascade is initiated. This results in the activation of signaling cascades including zeta-chain-associated protein kinase 70 (ZAP-70), phospholipase C γ (PLCγ), protein kinase B (Akt), nuclear factor kappa-light-chain-enhancer of activated B cells (NFκB), mitogen-activated protein kinase (MAPK), and extracellular regulated kinase 1 (Erk1) [45] all of which are also activated in the αβ T cell immune response, as seen in figure 3. These signals ultimately lead to the response of the Vγ9Vδ2 T cell. The Vγ9Vδ2 T cell can respond by proliferating, producing cytokines and chemokines, lysing the target cell, co-stimulating NK or dendritic cells, and acting as an antigen presenting cell [46]. As Vγ9Vδ2 T cells are yet to be fully characterized, it is possible that they have many other functions in addition to those listed above

in response to phosphoantigen stimulation. Here, our focus on the cellular functions of proliferation, production of cytokines and the lysis of target cells.

Vγ9Vδ2 T cells found in the blood are known to produce several chemokines, these include: chemokine ligand 3 (CCL3), which has receptors on macrophages; chemokine ligand 4 (CCL4), which has receptors primarily on macrophages and NK cells; c-x-c motif chemokine ligand 10 (CXCL10), which has receptors primarily on macrophages, NK cells, and T cells; and lastly, c-x-c motif chemokine ligand 13 (CXCL13), which has receptors on B cells [47]. The cytokines produced by the Vγ9Vδ2 T cell depend on cellular subtype and polarization. If the cell is exposed to interleukin 2 (IL-2) or IL-12, it will likely gain a Th1 phenotype and produce IFN-γ, IL-2, and TNF-α, if it is exposed to IL-4, it will gain a Th2 phenotype and produce IL-2, IL-4, IL-5, and IL-13, and exposure to IL-1β/transforming growth factor β (TGF-β), IL-6, or IL-23 leads to a Th17 phenotype and production of IL-17, IL-22, and TNF-α [48]. Some of the studies shown here (Chapter IV) determine which lineage phosphoantigen stimulated Vγ9Vδ2 T cells belong.

Less is known about the mechanism(s) by which Vγ9Vδ2 T cells use to lyse phosphoantigen-containing target cells. It is well-established that the lysis of the target cell results from the perforin/granzyme pathway [49] as well as an antibody dependent mechanism [50], ultimately leading to the same result, death of the target cell. Here, I will further investigate the mechanism by which Vγ9Vδ2 T cells lyse target cells, specifically looking at the effects of different phosphoantigen stimulation on lysis, the requirement of BTN3A1 and which Src kinases are required for lysis.

Vγ9Vδ2 T cell cancer therapy

As cancer is one of the leading causes of death in the United States, it is imperative to find new and more effective cancer therapies. Vγ9Vδ2 T cells are of great interest as they can

specifically target cells with elevated levels of IPP, as seen in some cancerous cells [31, 32]. Thus, they have been designed by nature to have a key role in immunosurveillance. Theoretically, a patient's own Vγ9Vδ2 T cells could be expanded and used as an immunotherapy for cancer; however more research needs to be done to determine if this would truly work. Another opportunity for clinical intervention could be to use specially designed non-charged phosphoantigen prodrugs, like those described by Hsiao et al [51] and those described here, to stimulate and activate Vγ9Vδ2 T cells within the patient. These prodrugs, readily cross the cell membrane and once inside the cell would be enzymatically cleaved into an active phosphoantigen. These prodrugs also have some flexibility in design in regard to the protecting groups utilized. This would potentially allow for some cell specificity depending on the design of the phosphoantigen prodrug, e.g. altering the enzyme required for the cleavage of the active phosphoantigen, conjugating a cell specific antibody, etc. [52].

Summary

Vγ9Vδ2 T cells and/or the phosphoantigens that activate them may be an effective immunotherapy, but first both of these topics need to be elucidated more, specifically the mechanism behind the interaction between phosphoantigen and BTN3A1, as well as the interaction between the target cell and the Vγ9Vδ2 T cell. Also, the testing of novel phosphoantigens and phosphoantigen prodrugs in both cell culture as well as *in vivo* will be necessary if we hope to create more efficient immunotherapeutics.

The following chapters provide further details of my graduate research to investigate these topics further. Specifically, I have investigated the mechanisms behind Vγ9Vδ2 T cell "stop signal" induction as well as involvement of Src kinases in activation of Vγ9Vδ2 T cell mediated lysis. I tested a fluorescent phosphoantigen prodrug, which appears to be a very potent Vγ9Vδ2 T

cell activator. I was also able to investigate the requirement for BTN3A1 in the lysis of target cells and have addressed the specificity of Vγ9Vδ2 T cells to target phosphoantigen loaded cells. Additionally, I examined the mechanism by which exogenous phosphoantigens enter the target cell and compared how long different phosphoantigens remain active within the cell. I then analyzed the activity of several novel HMBPP analogs in proliferation and lysis assays and advanced the testing of some novel phosphoantigen prodrugs to *in vivo* mouse models.

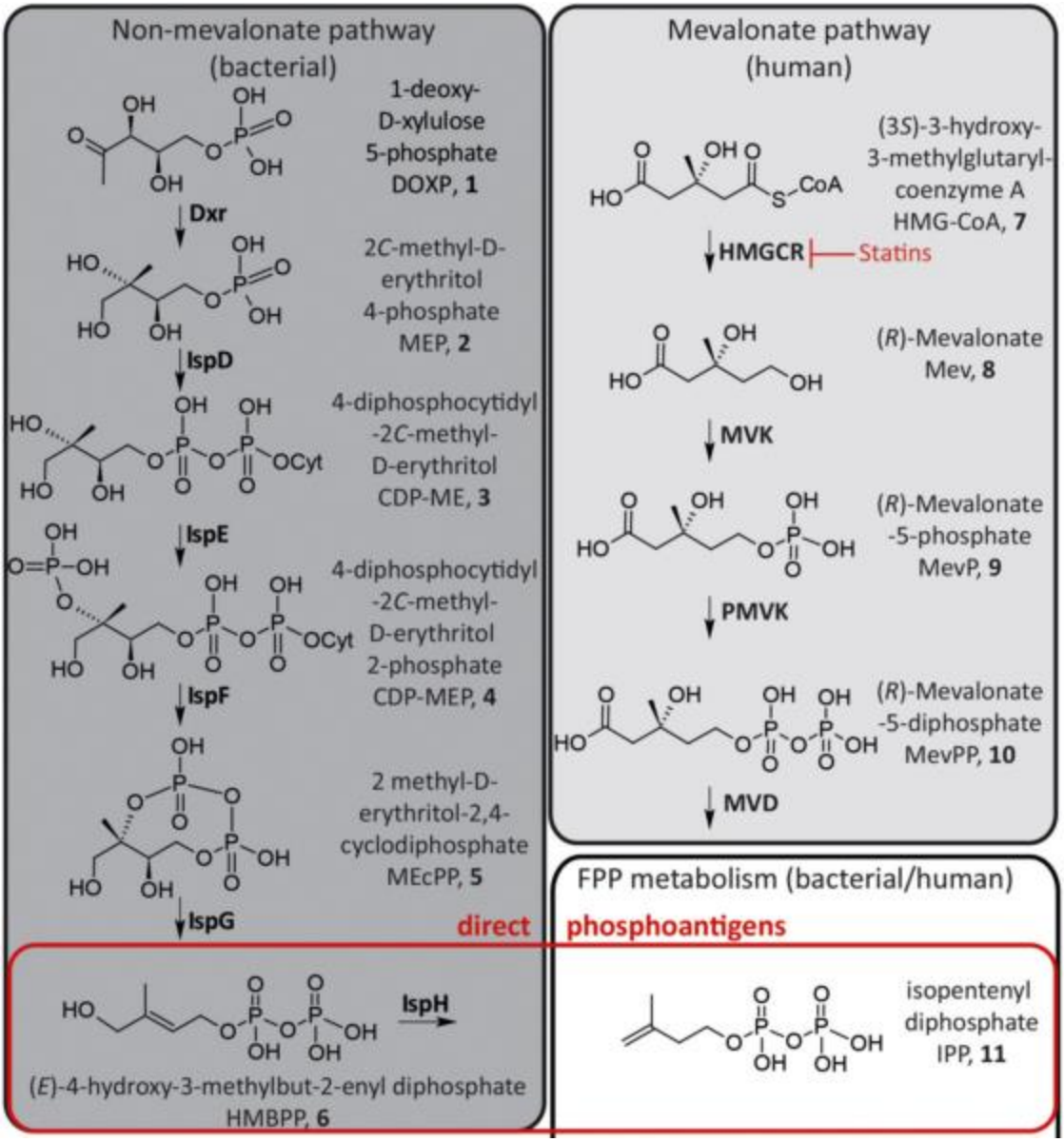

Figure 1. Biosynthetic pathways of HMBPP and IPP.

HMBPP is produced via the non-mevalonate pathway (left) while IPP is produced via the mevalonate pathway (right). Figure was modified from Wiemer and Wiemer, 2014 [53].

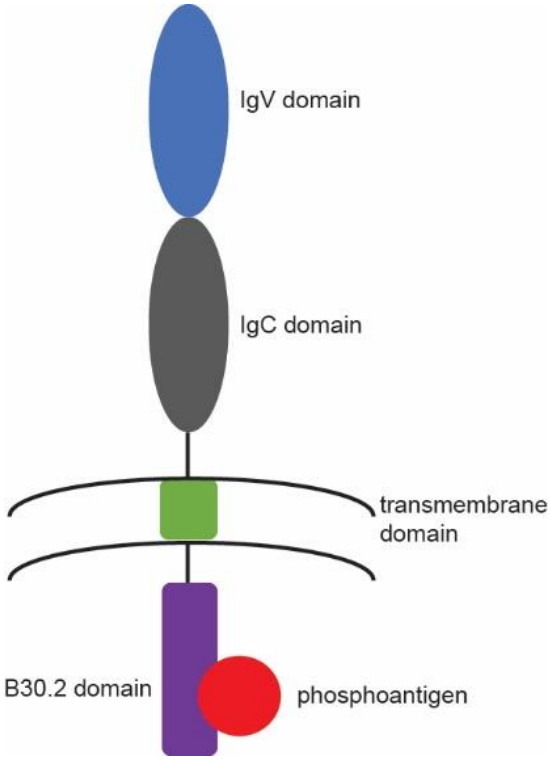

Figure 2. BTN3A1 schematic with phosphoantigen binding at the B30.2 domain.

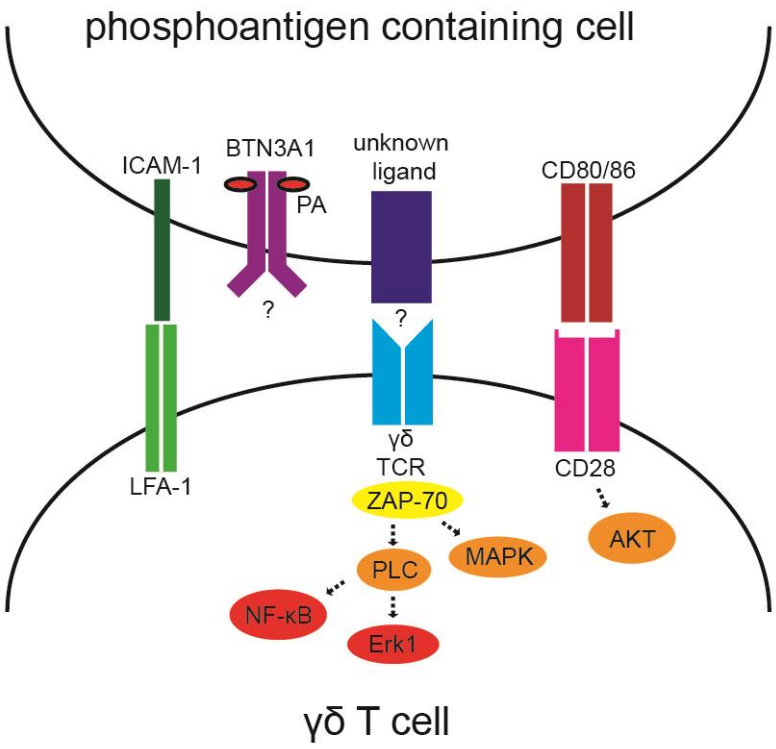

Figure 3. Schematic of interaction between the γδ T cell and phosphoantigen containing cell.

Known signaling molecules are shown, however interactions are based off previous αβ T cell signaling [54, 55].

CHAPTER II

SIGNALING PAHTWAYS INVOLVED IN Vγ9Vδ2 T CELL ACTIVATION

Introduction

Vγ9Vδ2 T cell receptor-induced signaling within the γδ T cell is widely uncharacterized. As the immune response of a Vγ9Vδ2 T cell is very similar to that of the cytotoxic αβ T cell, it is likely that the γδ T cell receptor signaling pathway is comparable to the T cell receptor signaling pathway of the cytotoxic T cell, but it is important to characterize this fully.

One of the first steps in activation of T cells is synapse formation. This occurs when a migrating T cell interacts with an adjacent cell. If the adjacent cell is "presenting" an antigen, the TCR will be stimulated, ultimately reversing the polarity of the migrating T cell, and increasing adhesion of the T cell and antigen presenting cell. This change in migration and polarity is known as a "stop signal" [56]. In αβ T cells, once the TCR is activated and a stop signal is induced, a series of downstream protein kinases are activated, resulting in phosphorylation of further downstream proteins.

This immune response is similar in Vγ9Vδ2 T cells, although the full signaling cascade has yet to be identified, some proteins involved in signaling have been identified as active in response to Vγ9Vδ2 T cell stimulation. Decaup et al. found that zeta-chain-associated protein kinase 70 (ZAP-70), phospholipase C γ (PLCγ), protein kinase B (Akt), nuclear factor kappa-light-chain-enhancer of activated B cells (NFκB), mitogen-activated protein kinase (MAPK), and extracellular regulated kinase 1 (Erk1), were all phosphorylated in Vγ9Vδ2 T cells stimulated by the phosphoantigen bromohydrin pyrophosphate (BrHPP) or anti-BTN3A activating antibody [45]. Each of these proteins are also phosphorylated in the αβ T cell immune response, showing striking similarity between the two TCR signaling pathways.

These downstream signals of a T cell "stop signal" ultimately lead to a cellular response. In Vγ9Vδ2 T cells, the response can be a number of things, proliferation, production of cytokines and chemokines, target cell lysis, co-stimulation of NK or dendritic cells, or even acting as an antigen presenting cell themselves [46]. These functions are only those known as of now, and as Vγ9Vδ2 T cells become fully characterized, it is possible for others to be revealed.

This chapter will focus first on the unknown signaling events involved in "stop signal" induction and migration, then will focus on the signaling requirement for Src kinases in the lysis of target cells by Vγ9Vδ2 T cells.

Materials and Methods

Reagents and supplies

RPMI-1640, Fetal Bovine Serum, nonessential amino acids, pyruvate, penicillin streptomycin, HEPES, BME, and HMBPP were obtained through Fisher Scientific. IL-2 and the MACS γδ T cell negative selection kit was obtained through Miltenyi Biotec. FITC-Annexin V was from eBioscience. Daudi cells were from American Type Culture Collection, while Research Blood Components (Boston, MA) supplied blood. DiD and calcein AM were obtained through Life Technologies. PP2 and PMA were obtained from Sigma-Aldrich. SKI-1 was obtained from EMD Millipore.

Vγ9Vδ2 T cell expansion and purification

Human PBMCs from healthy anonymous donors were isolated from heparinized blood using Lymphoprep (Axis-Shield) within 24 hours of collection. Cells were counted by hemocytometer in the presence of trypan blue, then aliquoted in freezing media (10% DMSO, 20% FBS, 70% media), and stored in liquid nitrogen. PBMCs were resuspended at 1×10^6 cells/mL in fresh T cell media (RPMI 1640, 10% heat-inactivated FBS, 1x HEPES, pyruvate, nonessential

amino acids, and BME). Cells were stimulated with 0.01 μM HMBPP or 0.01 μM POM_2-C-HMBP for 3 days and cultured for another 4-18 days after compound removal. Fresh IL-2 (5 ng/mL) was provided every 3 days. After 7-21 days, Vγ9Vδ2 T cells were purified by negative selection. Experiments were performed at least three times using at least two donors.

Daudi cell culture

Daudi cells were cultured in RPMI 1640, 10% FBS, and 1% penicillin/streptomycin and maintained between 0.3 and 2-3 x 10^6 cells per mL.

Migration assay

ICAM-1 was obtained by protein G sepharose purification of Chinese hamster ovary cell spent media as described [57, 58]. 384-well clear bottom plates were coated with 5 μg/μL (ICAM-1) for 60 min. Plates were washed with PBS and blocked with 2% BSA at 37 ºC for 30 minutes. Purified Vγ9Vδ2 T cells were added and treatments were added to each individual well as described. Cells were visualized using an Andor confocal microscope (Andor) set up for multi-dimension acquisition and live imaging at the University of Connecticut Flow Cytometry and Confocal Microscopy Facility. Images were taken every 30-60 seconds for 30-240 minutes at 37 ºC.

Lysis assay

Daudi cells were stained with DiD (2 minutes in 4 μM DiD in BSA/PBS), quenched by addition of an equal volume of FBS, and washed twice in T cell media. Daudi cells were mixed with γδ T cells at an effector: target ratio of 3:1 in 200 μL. Treatments were added to these mixtures and were then incubated for 4 hours at 37 ºC. After 4 hours, tubes were placed on ice for 5 minutes. FITC-Annexin V (3 μL) was added for 15 minutes on ice, then cells were diluted by addition of 200-300 μL binding buffer (BD Biosciences) and analyzed by flow cytometry using the BD

Fortessa (BD Biosciences). Results were analyzed by FlowJo 9 (Tree Star) software at the University of Connecticut Flow Cytometry and Confocal Microscopy Facility.

Live imaging and degranulation

384-well plates were coated with human I-CAM as described above in the migration assay section. Daudi cells were stained with calcein-AM (1 µL in media) at 37º C for 30 minutes then washed two times with T cell media. Daudi and Vγ9Vδ2 T cells were added to the wells in a 3:1 E: T ratio. Treatments were then added as described in the text. Cells were visualized using an Andor confocal microscope (Andor) set up for multi-dimension acquisition and live imaging at the University of Connecticut Flow Cytometry and Confocal Microscopy Facility. Images were taken every 30-60 seconds for 30-240 minutes at 37 ºC.

Statistical analysis

One-way ANOVA was used to calculate significance. Comparisons were done relative to the control or between pairs of conditions. Columns in bar graphs represent the mean ± SEM. An α level of 0.05 was used.

Results

Activation of PKC in Vγ9Vδ2 T cells induces a migration stop signal

As mentioned previously, the signaling pathway of αβ T cells is well characterized, however, the pathways involved in the Vγ9Vδ2 T cell are still being defined. One of the most well-known signaling molecules in the αβ TCR pathway is protein kinase C (PKC). This kinase is activated by the compound phorbol 12-myristate 13-acetate (PMA), ultimately leading to αβ T cell stimulation. Once stimulated, if in the presence of other cells, or in our case, in the presence of human ICAM, normally motile αβ T cells will interact with other cells/ICAM treated plate and instead of continuing to the next cell, they will stop and interact with the opposing cell/ICAM

treated plate for a longer time, in a stable synapse. This stop signal response can be visualized microscopically, which is what I have done here.

Vγ9Vδ2 T cells were added to ICAM coated well and treated with or without 20 ng/mL PMA. These cells were then visualized microscopically. Images were taken every 30-60 seconds for 30-240 minutes and compiled to form videos. Control cells readily moved around, while cells treated with PMA showed diminished motility, and lost polarity as stop signal was induced (Figure 4), indicating that the activation of PKC results in stimulation Vγ9Vδ2 T cells.

Binding of TCR component CD3 by OKT3 in Vγ9Vδ2 T cells induces stop signal

Another frequently stimulator of αβ T cells is the monoclonal antibody OKT3. OKT3 binds to the CD3 portion of the αβ TCR and ultimately stimulates the cell enough to induce stop signal, resulting in decreased motility. It remains unknown whether stimulation of CD3 ultimately leads to stimulation of the Vγ9Vδ2 T cell. Using the same method described above, Vγ9Vδ2 T cells were treated with 1 µg/mL OKT3 and their motility on ICAM-1 coated wells was visualized.

OKT3 treatment resulted in the stimulation and stop signal induction of the Vγ9Vδ2 T cells (Figure 5). These cells were far less motile when compared to control cells. This data indicates that CD3 stimulation results in Vγ9Vδ2 T cell stimulation and induces the stop signal, and may be required for Vγ9Vδ2 T cell stimulation.

Inhibition of Src kinases blocks induction of the migration stop signal in Vγ9Vδ2 T cells

OKT3 treatment of Vγ9Vδ2 T cells strongly induced the stop signal. To further investigate this mechanism of Vγ9Vδ2 T cell stimulation, I wanted to look at Src kinase activity in the Vγ9Vδ2 T cells by using the Src kinase inhibitor PP2. PP2 inhibits most of the Src kinases, which is active just downstream of the T cell receptor in αβ T cell receptor signaling.

Here, we performed live imaging on Vγ9Vδ2 T cells treated with both OKT3 and PP2, both of which act on different proteins within the cell. It was noticed that these cells were more motile than cells treated with OKT3 alone, yet still less motile than untreated control cells (Figure 6). Using Image J and its cell tracking software, the coordinates of each T cell were captured throughout videos of control, OKT3, and OKT3 and PP2 treated cells (Figure 7). The mapping of the cells allows for a clear visualization of the stop signal induction in OKT3 treated Vγ9Vδ2 T cells, and the rescue of motility in cells treated with the Src kinase inhibitor PP2. This indicates that the signaling through the CD3 protein on the Vγ9Vδ2 T cells can be blocked by inhibition of Src kinases, demonstrating that these Src kinases are indeed active in Vγ9Vδ2 T cells, and that they are downstream of CD3 in the Vγ9Vδ2 T cell receptor pathway.

Src kinases are required for the lysis of target cells by Vγ9Vδ2 T cells

The end result of stimulation of a Vγ9Vδ2 T cell may or may not include lysis of the target cell, which indicates a mechanism unto itself. Does this mechanism require Src kinases, or does the lysis of the target cell by Vγ9Vδ2 T cells utilize a different signaling pathway? To investigate this, live imaging was utilized as described above, but added Daudi cells, a Burkitt's lymphoma cell line, used here as target cells, in a 3:1, effector: target (E: T) ratio. Cells were then treated with 0 nM HMBPP, 100 nM HMBPP, or 100 nM HMBPP and 5 μM PP2. Videos were taken every 30 seconds for 1 hour and analyzed using Image J. The number of degranulated cells per video were calculated and a percentage of degranulation was calculated by dividing this number by the total number of Daudi cells per video. It was found that HMBPP increases the percentage of degranulated cells, while treating with HMBPP and PP2 brings this value down drastically, indicating that Src kinases appear to be active in the lysis of target cells by Vγ9Vδ2 T cells (Figure 9).

To further validate these findings, a flow cytometry based lysis assay was performed. This assay involved staining Daudi cells with the membrane stain DiD, these cells were then mixed with purified Vγ9Vδ2 T cells with or without PP2 and/or HMBPP for 4 hours. After 4 hours, they were analyzed by flow cytometry. Here, levels of cell death were examined via FITC-conjugated Annexin V. Using FlowJo software, DiD positive cells were gated and at the percentage of these cells that were also Annexin V positive was calculated. Our results reflected those found in Figure 7, where HMBPP increased the levels of cell lysis by Vγ9Vδ2 T cells, while treatment of HMBPP alongside PP2 significantly decreased levels of lysis. This indicates that Src kinases are required for lysis of target cells, in our case, specifically Daudi cells, by Vγ9Vδ2 T cells.

Lck is required for the lysis of target cells by Vγ9Vδ2 T cells

The findings in Figures 8 and 9 revealed that Src kinases are required for the lysis of target Daudi cells by Vγ9Vδ2 T cells, however which of the Src kinases are actually required, is still a question. PP2 is a pan Src kinase inhibitor, so these results show a requirement of Src kinases in general, but no specific kinase has been identified. Based on αβ T cell signaling, it was hypothesized that the Src kinase Lck would be required for lysis of these target cells by Vγ9Vδ2 T cells. To determine if this kinase is involved, the Lck inhibitor SKI-1 was utilized.

Here, the flow cytometry based lysis assay was performed as described above. DiD stained Daudi cells were then mixed with purified Vγ9Vδ2 T cells and treated with or with 10 μM SKI-1 and/or 100 nM HMBPP. The results very similarly matched those seen in Figure 9, where an increase in lysis when treated with HMBPP alone was observed, followed by a rescue back to control levels when treated with SKI-1 (Figure 10). Taken together, this shows that the Src kinase Lck is required for lysis of target Daudi cells by Vγ9Vδ2 T cells.

Discussion

The signaling pathways of Vγ9Vδ2 T cells are very interesting as they are still yet to be fully characterized. Here, we have elucidated these pathways further, specifically in synapse formation and lysis of target cells, specifically Daudi cells.

The synapse formation of Vγ9Vδ2 T cells is of great importance, as it is here that the signaling cascade is initiated. We were able to identify that both PKC and CD3 are involved in the formation of this synapse. By activating PKC with PMA, Vγ9Vδ2 T cell stop signal induction along ICAM treated wells was visualized. This experiment shows that without the presence of phosphoantigen, the stimulation of PKC alone can induce the stop signal in these Vγ9Vδ2 T cells, thus PKC activation is sufficient for Vγ9Vδ2 T cell stop signal induction. The protein CD3, a known component of both the αβ TCR and the Vγ9Vδ2 TCR was stimulated, using OKT3. This resulted in visualization of stop signal induction in cells treated with OKT3. Again, without phosphoantigen present, stop signal induction was visualized, indicating that CD3 itself is sufficient for Vγ9Vδ2 T cell stop signal induction.

Src kinases were also investigated and the effects of OKT3 stop signal induction was partially blocked by co-treating the cells with PP2. By blocking Src kinase activity, the Vγ9Vδ2 T cell was less likely stop and form a stable synapse, and was more likely to continue migrating along the ICAM coated surface. This suggests that somewhere downstream of CD3 in this signaling pathway, Src kinases are required for this synapse formation, and the cell is unable to do this when the Src kinases have been inhibited. We were able to identify that these Src kinases function downstream from CD3 because inhibition of Src kinases in cells with stimulated CD3 resulted in blocked stop signal formation. If Src kinases were indeed upstream of CD3, inhibiting Src kinases while at the same time activating CD3 would result in stop signal induction, as CD3

is sufficient for stop signal induction. However, it was seen that the cells became more migratory and did not form as many stable synapses. In these studies, little indication was shown in the order of activation of components in the stop signal signaling pathway, but it is likely that CD3 becomes activated first, leading to the activation of PKC or Src kinases further downstream, as seen in αβ T cells.

Vγ9Vδ2 T cells have multiple functions and it is important to identify the pathways involved in each of these individual functions. One of the main functions Vγ9Vδ2 T cells have is to act innately in identifying and lysing target phosphoantigen containing cells. Here, and throughout chapter IV, I identify some of the components of this pathway. We found that Src kinases are also required for degranulation and lysis of target cells, more specifically the Src kinase Lck. Chapter IV further identifies other important proteins that are involved, and the final discussion of this dissertation gives a full description of the known Vγ9Vδ2 signaling pathways as of now.

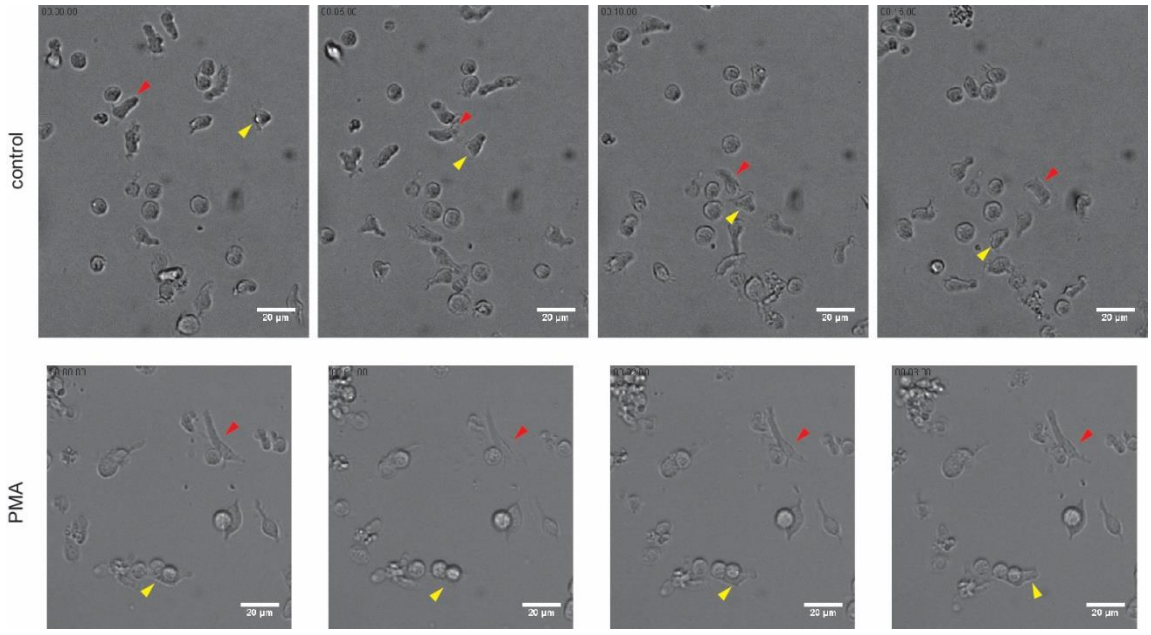

Figure 4. PMA induces Vγ9Vδ2 T cell stop signal.

Live imaging of Vγ9Vδ2 T cells with or without 20 ng/mL PMA. Yellow and red arrows denote two separate cells within the same frame.

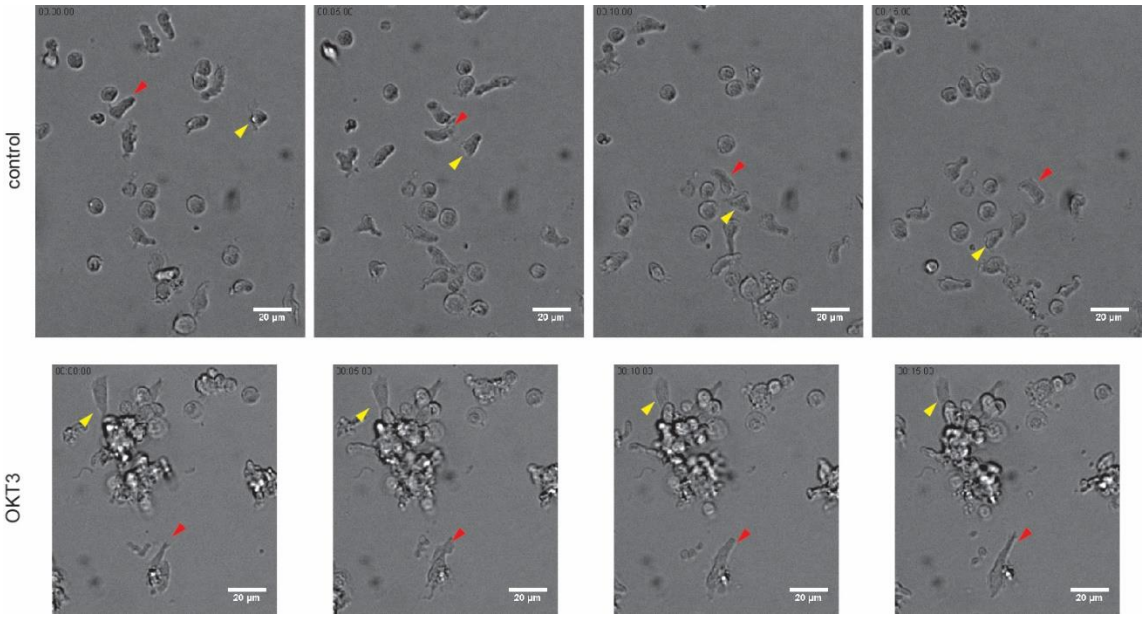

Figure 5. OKT3 induces Vγ9Vδ2 T cell stop signal.

Live imaging of Vγ9Vδ2 T cells with or without 1 µg/mL OKT3. Yellow and red arrows denote two separate cells within the same frame.

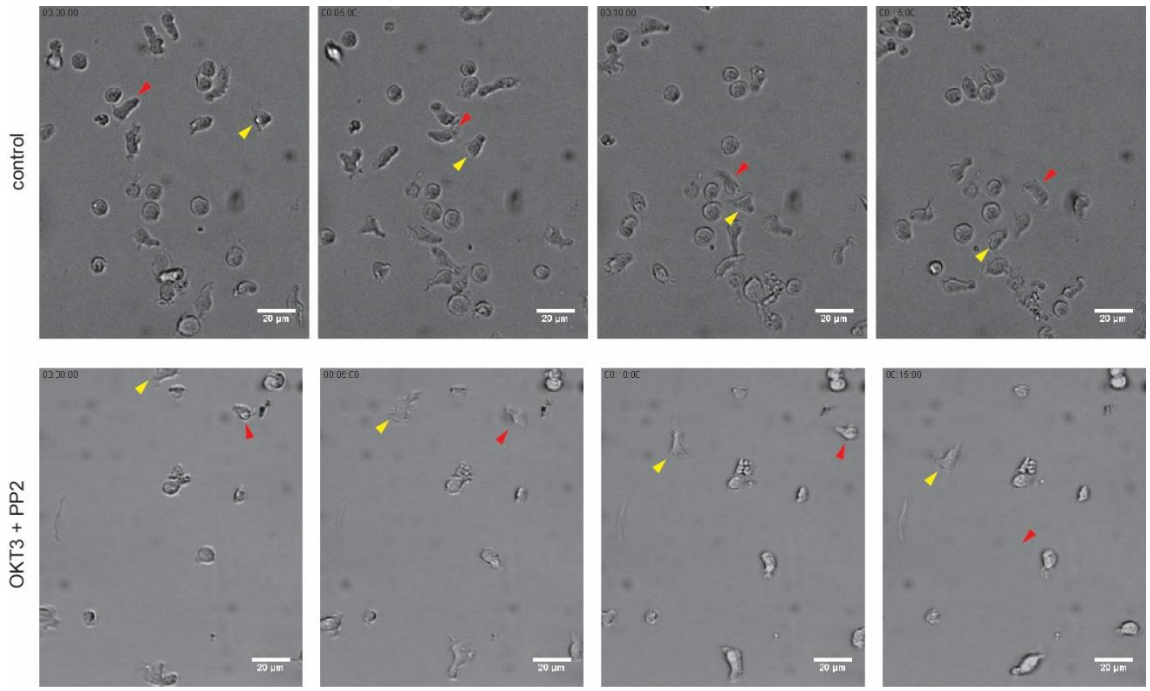

Figure 6. PP2 rescues Vγ9Vδ2 T cell stop signal induced by OKT3.

Live imaging of Vγ9Vδ2 T cells with or without 1 μg/mL OKT3 + 5 μM PP2. Yellow and red arrows denote two separate cells within the same frame.

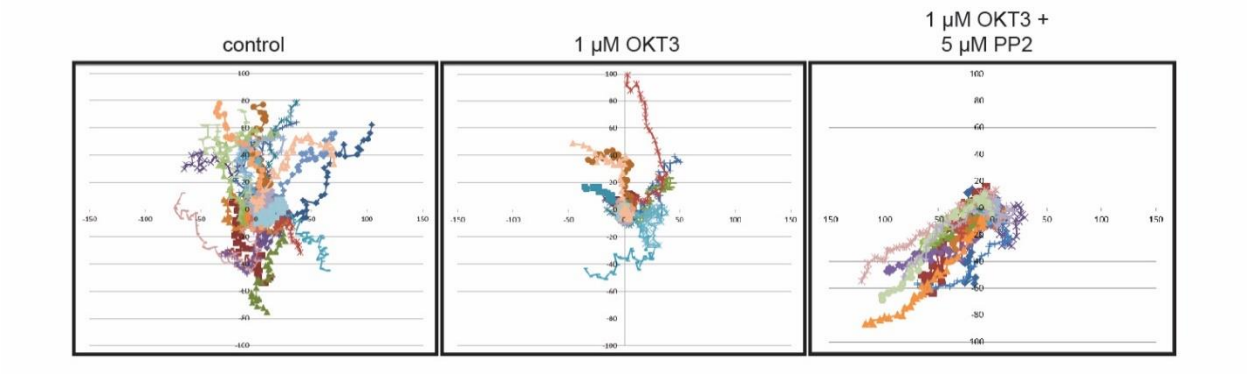

Figure 7. Mapping of OKT3 induced cell stopping and rescue with PP2.

Mapping of cells treated with or without 1 µg/mL OKT3 and 5 µM PP2 from one 60-minute video per treatment (Figures 5 and 6).

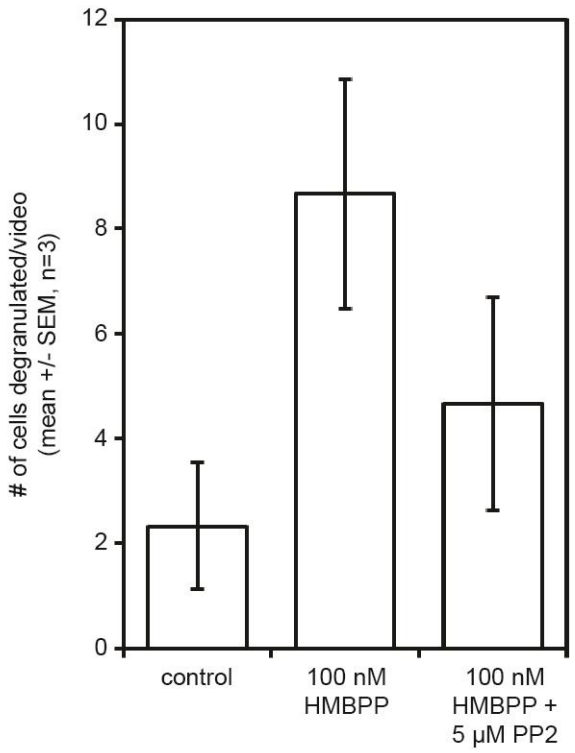

Figure 8. PP2 inhibits degranulation of Vγ9Vδ2 T cells.

Vγ9Vδ2 T cells and Daudi cells were mixed together and treated with or without 100 nM HMBPP and 5 µM PP2. The number of degranulated Vγ9Vδ2 T cells per video were quantified over the course of one hour. n=3.

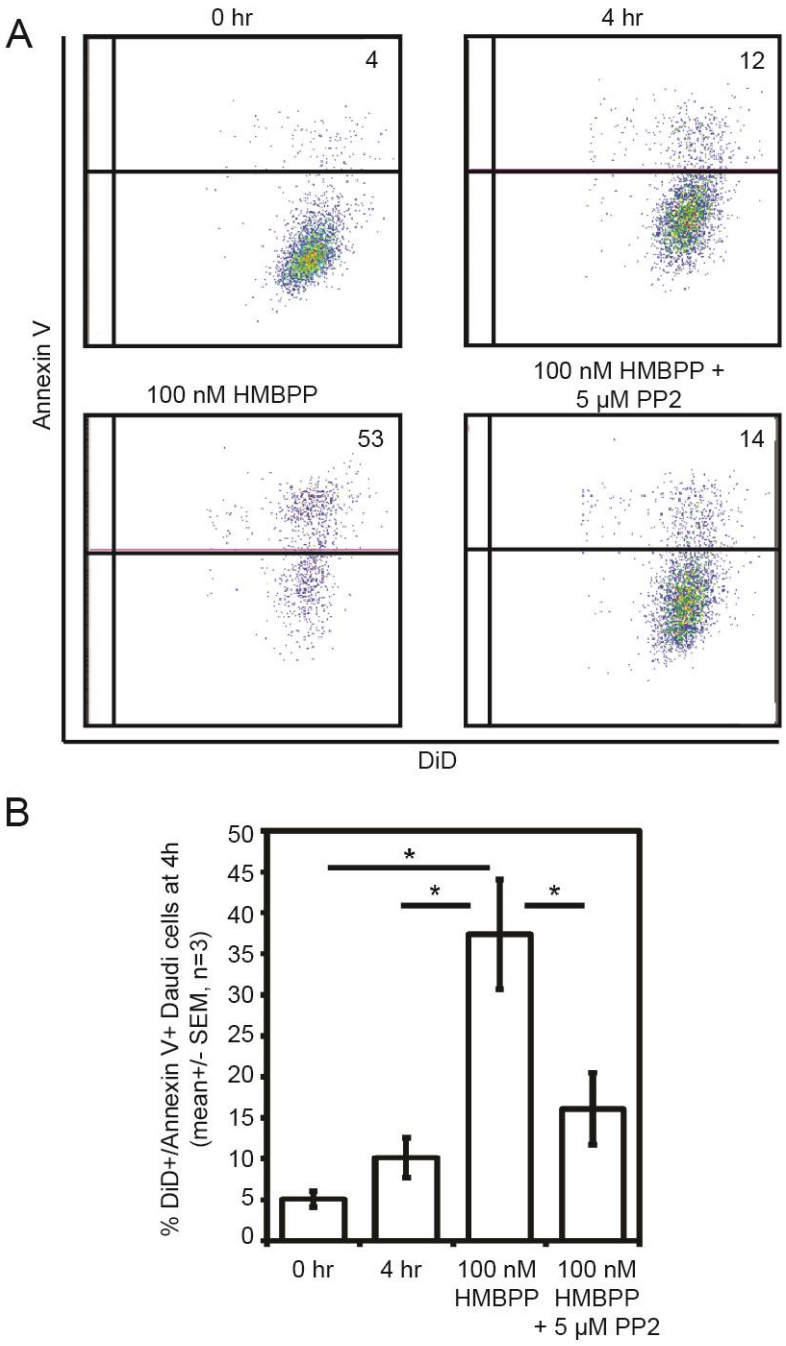

Figure 9. Src kinases are required for the lysis of target cells by Vγ9Vδ2 T cells.

A) Flow analysis of target Daudi cells and effector Vγ9Vδ2 T cells mixed and treated with 100 nM HMBPP with or without 5 μM PP2 for four hours. B) Quantification of panel A. Flow plots are representative of greater than three independent experiments. * significantly different from indicated treatments.

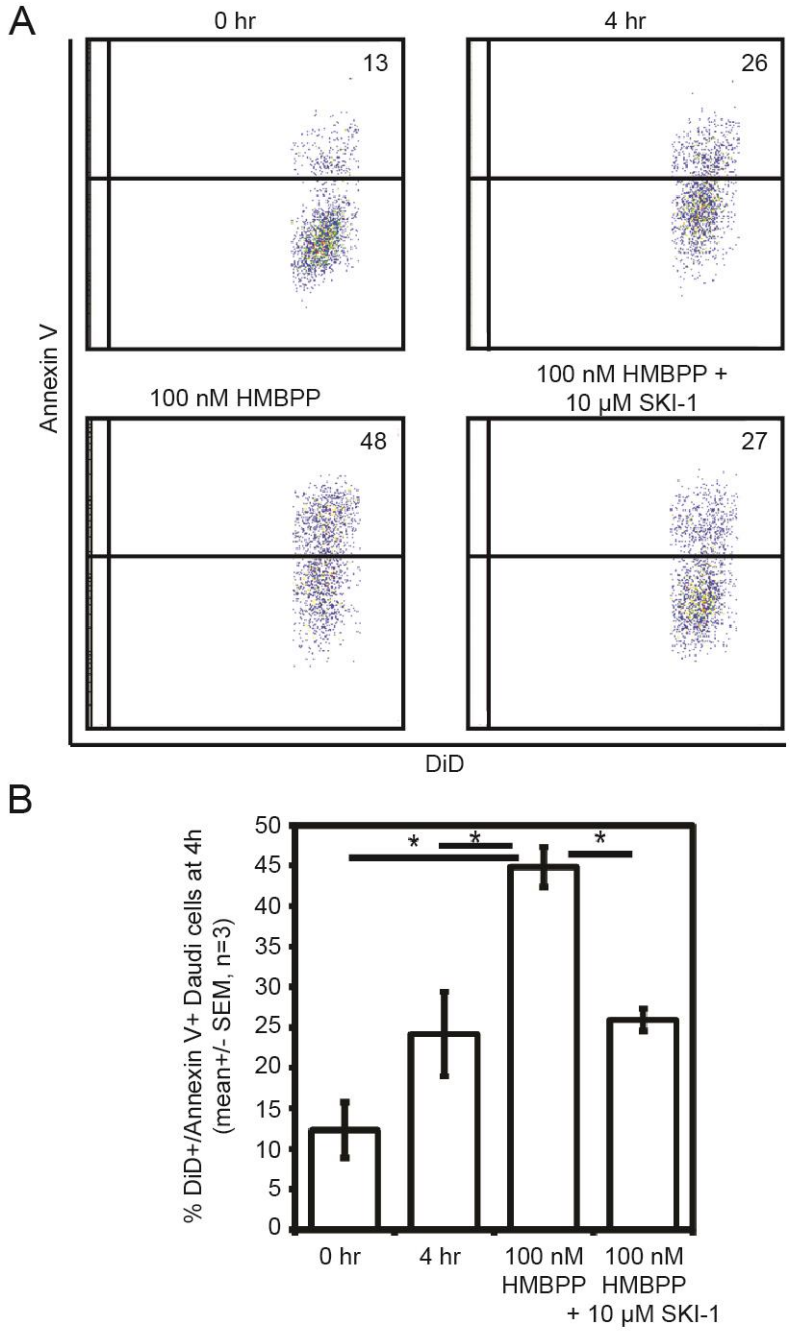

Figure 10. Lck is required for lysis of target cells by Vγ9Vδ2 T cells.

A) Flow analysis of target Daudi cells and effector Vγ9Vδ2 T cells mixed and treated with 100 nM HMBPP with or without 10 µM SKI-1 for four hours. B) Quantification of panel A. Flow plots are representative of greater than three independent experiments. * significantly different from indicated treatments.

CHAPTER III

EVALUATION OF A 7-METHOXYCOUMARIN-3-CARBOXYLIC ACID ESTER DERIVATIVE AS A FLUORESCENT, CELL-CLEAVABLE, PHOSPHONATE PROTECTING GROUP

Abstract

This chapter is adapted from our published work [59]. Cell-cleavable protecting groups often enhance cellular delivery of species that are charged at physiological pH. Although several phosphonate protecting groups have achieved clinical success, it remains difficult to use these prodrugs in live cells to clarify biological mechanisms. Here, we present a novel compound containing a 7-methoxycoumarin-3-carboxylic acid ester as a fluorescent protecting group. This compound is an analogue of (*E*)-4-hydroxy-3-methyl-but-2-enyl diphosphate (HMBPP) and here, we assess cellular uptake and human Vγ9Vδ2 T cell activation. The fluorescent ester displayed low cellular toxicity (IC_{50} > 100 μM) and strong T cell activation (EC_{50} = 0.018 μM) relative to the unprotected anion (EC_{50} = 23 μM). The coumarin-derived analogue allowed no-wash analysis of biological deprotection, which revealed rapid internalization of the prodrug. These results demonstrate that fluorescent groups can be applied both as functional drug delivery tools and useful biological probes of drug uptake.

Introduction

A variety of drugs and other biologically interesting molecules contain phosphate or phosphonate substructures [60]. However, the negative charge that such compounds bear at physiological pH frequently acts as a barrier to cellular entry [61]. As such, development of cell-cleavable protecting groups that increase in vivo absorption is of great interest, with several phosphonate prodrugs recently achieving clinical status [62]. Although cell-cleavable

phosphoester [63] and phosphonamidate [64] protecting groups effectively increase cellular uptake [65], it remains challenging to use these compounds to assess biological mechanism in real time because concentrations of compounds in live cells and their uptake rates cannot be readily assessed.

The small isoprenoid (*E*)-4-hydroxy-3-methyl-but-2-enyl diphosphate (**1**, HMBPP, Figure 11) is a metabolic intermediate found in bacteria and other microorganisms [51]. HMBPP synthesis is required for bacterial growth [66] and also functions as a potent pathogen-associated molecular pattern (PAMP) that stimulates an immune response from human Vγ9Vδ2 T cells [27]. However, the mechanisms of HMBPP immunostimulation are currently a topic of intense debate [67, 68], and novel activators of Vγ9Vδ2 T cells are desirable [69]. Therefore, development of HMBPP analogues that can contribute to an understanding of its immunostimulatory mechanism is warranted [53].

Here, we present a pH-sensitive, fluorescent, cell-cleavable phosphonate protecting group, the oxymethyl ester of 7-meth-oxycoumarin-3-carboxylic acid, to effectively quantify cellular uptake of a phosphonate HMBPP analog. Compounds containing this group display potent activation of Vγ9Vδ2 T cells. Moreover, this reporter might also provide a means by which cellular uptake of a variety of phosphate and phosphonate drugs can be readily assessed with some precision.

Materials and Methods

Biological reagents and supplies

PE-conjugated anti-human CD3 was obtained from eBioscience. Human interleukin 2 was obtained from Miltenyi Biotec. Annexin V-FITC was obtained from BD Biosciences. HMBPP was obtained from Echelon Biosciences. CellQuantiBlue was obtained from BioAssay Systems.

FITC-anti-human gamma delta TCR antibody (5A6.E91) and DiD cell stain was purchased from Thermo Fisher Scientific. Fetal bovine serum and all other tissue culture supplies also were obtained from Thermo Fisher. Polyester backed silica G plates, with UV 256 were obtained from Sorbtech Technologies. Human PBMCs were isolated from blood from Research Blood Components. K562 cells were obtained from ATCC.

Cell culture

K562 cells were cultured in fresh K562 media (RPMI-1640, 10% heat-inactivated Fetalclone III, 1x penicillin/streptomycin). Daudi and RPMI-8226 cells were cultured in fresh Daudi/RPMI media (RPMI-1640, 10% heat-inactivated FBS, 1x penicillin/streptomycin).

Flow cytometry

Total gamma delta TCR was labeled using FITC-anti-human pan gamma delta TCR antibody and CD3 was labeled using PE-conjugated anti-human CD3 as described [51].

Killing assay

The killing assay was performed as described [51] with slight modification. T cells were expanded from PBMCs by stimulation with 0.01 µM HMBPP. Cells were purified by negative selection using a kit for γδ T cells (Miltenyi). K562 cells were stained with DiD (2 minutes in 4 µM DiD in BSA/PBS), quenched by addition of an equal volume of FBS, and washed twice in T cell media. $6x10^3$ K562 cells were mixed with $3x10^4$ T cells and test compounds to a final volume of 100 µL. Mixtures were incubated for 4 hours at 37 degrees then placed on ice for 5 minutes. Annexin V-FITC (3 µL) was added for 15 minutes on ice, then cells were diluted by addition of 200 µL binding buffer (BD) and immediately analyzed by flow cytometry.

Proliferation assay

To assess K562 proliferation, 10^4 cells/well were added to 96-well plates in 100 µL K562 media in the presence of test compounds. Similarly, experiments with Daudi cells were initiated at $5x10^3$ cells/well and RPMI-8226 cells initiated at $6x10^3$ cells/well. The cell concentrations were determined by prior dose response experiments to maximize proliferation rates. Cells were allowed to proliferate for 72 hours. During the last 2 hours, cells were labeled with 10 µL of CellQuantiBlue reagent and scanned with a Victor X5 plate reader.

Quantification of cellular uptake

Compounds were exposed to PBS, K562 cells in PBS, or 50% pooled human plasma in PBS. K562 cells were used at a concentration of 1 million per mL. The fluorescence was detected using a Victor X5 plate reader with excitation at 355 nm and emissions at 405 nm. Compounds were mixed with each biological matrix to a final concentration of 10 µM on ice. A baseline reading was measured. Compounds were incubated for one hour at 37ºC and subsequent readings were taken every 15 minutes.

Statistics

One-way ANOVA was used to calculate statistical significance. Comparisons were done relative to the control. Columns in bar graphs represent the mean +/- standard deviation. An α level of 0.05 was used.

Results

Design of fluorescent prodrug

The initial goal of this synthetic effort was to generate a fluorescent prodrug. This would allow for detection of prodrug uptake into cells via plate reader or potentially even live imaging. We applied the commonly used [62] non-fluorescent pivaloyloxymethyl (POM) [70] protecting

group to both phosphonates [51] and bisphosphonates [71] and observed strong gains in cellular potency, but lacked ways to easily quantify uptake in live cells. Here, we focused on a derivative of the HMBPP analogue (*E*)-4-hydroxy-3-methyl-but-2-enyl phosphonate (Figure 11. **2**, C-HMBP). We viewed C-HMBP as an ideal molecule to use in this regard because: 1) it has strong biological activity in a system that requires intracellular delivery; 2) it displays only weak cellular toxicity; 3) the mechanism(s) of action of its butyrophilin binding partner, BTN3A1, remain unclear; and, 4) POM-protected analogues **3** and **4** (Figure 11) were already available for use as biological controls. Thus, we would be readily able to assess changes in potency/toxicity of the protecting strategy. Furthermore, in contrast to other phosphonates that require full deprotection for biological activity, this compound is biologically active as the monoacid mono methyl ester. Therefore, rates of monohydrolysis of varied protecting strategies can be directly compared in cellular assays without the complexities of dihydrolysis.

The structures of compounds **5-9** can be seen in figure 12. Compound **9** was fluorescent, as expected, and was readily detected with maximum excitation at 355 nm and emission at 405 nm. Therefore, it was examined in a variety of biological experiments to determine if it would function as a prodrug.

Coumarin-derived prodrug acts as an active phosphoantigen

We determined the activity of compound **9** in a functional assay for its ability to stimulate proliferation of primary human Vγ9Vδ2 T cells (Figure 13). Peripheral blood mononuclear cells (PBMCs) were treated with test compounds. In these assays, compound **9** was expected to undergo cellular metabolism, leading to intracellular release of the carboxylic acid **5** and the biologically active compound **8** (Figure 14). Compound **4** was used as a control, because it too would be expected to deliver active compound **8** with similar stoichiometry. Both compounds **4** and **9** did

function as Vγ9Vδ2 T cell agonists, causing a large expansion of the population of cells that express both CD3 and the Vγ9Vδ2 T cell receptor (Figure 13A). This is a key finding, because it demonstrates that the coumarin-derived protecting group can effectively deliver a phosphonate payload, resulting in biological activity.

Coumarin-carboxylate oxymethyl ester protecting group functions as well as POM protecting group

The maximal agonist activity (observed at 1 μM) of compound **9** was not statistically different from that of POM analogue **4** (Figure 13B) in cells from the same donors. Dose-response curves (Figure 13C) determined that compound **9** displays an EC_{50} of 0.018 μM, whereas compound **8** displays an EC_{50} of 23 μM. Therefore, the coumarin-carboxylate oxymethyl ester (CCOM) strategy offered a 1300-fold increase in activity. The potency of compound **9** compares favorably to the EC_{50} value of 0.50 μM that we obtained previously for compound **4** (Table 1), although availability of these primary human cells dictated that the current set of compounds be tested in cells from different donors than those used for earlier compounds. This data shows minimal differences between the CCOM and POM protecting groups of a matched pair of compounds, suggesting that the CCOM protecting group has similar prodrug functionality to that of the well-established and clinically utilized POM protecting group.

Because the previous experiments utilized a three-day exposure time, the assays might not have been sensitive enough to assess subtle differences in the rates of phosphonate release. Therefore, we sought to assess the activity of the novel compounds in a model of T cell-mediated cytotoxicity, which occurred with a shorter exposure of just 2 hours (Figure 13D). K562 cells that were pre-loaded with compounds **4** and **9** were able to trigger Vγ9Vδ2 T cell-mediated killing with similar efficacy.

CCOM protecting group is non-toxic to leukemia cell lines

The ideal prodrug protecting group would be non-toxic. We expected that to be the case for CCOM protection, as the activity of compound **9** in the T cell proliferation assay was similar to that of POM compound **4**. To establish the effects of the CCOM protecting group on cell viability, we evaluated growth inhibition in several cell lines. The carboxylic acid **5** alone was nontoxic to K562, Daudi, RPMI-8226, and Jurkat cells when they were exposed for 72 hours at concentrations up to 100 μM (Table 2). Treatment of K562, Daudi, or Jurkat cells with compounds **4** or **9** displayed no toxicity. Differences were observed between compounds **4** and **9** only in RPMI-8226 cells at 100 μM treatment (Figure 15), much higher than the EC_{50} values for stimulation of Vγ9Vδ2 T cells.

CCOM prodrug loses fluorescence as it is metabolized

We next determined whether compound **9** would be a useful probe with which to determine rates of biological deprotection (Figure 16). Compounds **5** and **9** were readily detected by spectrofluorimetry in aqueous solutions. Importantly, the fluorescence intensity of compound **5**, but not prodrug **9**, was strongly dependent upon the pH of the solution (Figure 16A), correlation with the expected protonation status of the carboxylic acid in compound **5**. In water, the intensity of **5** was less than 10% of its intensity at pH 3 (Figure 16A). Therefore, the CCOM prodrugs would be expected to rapidly lose fluorescence intensity during metabolism at neutral pH, as the carboxylate is released from the prodrug and remains in the deprotonated form.

We then adapted this assay to a 384-well-plate format for use in a plate reader equipped with a 355/40 nm excitation filter and a 405/10 nm emission filter. As expected, the fluorescence intensity of **9** in phosphate-buffered saline (PBS) was much higher than that of **5** in PBS (Figure 16B). Additionally, the fluorescence of compound **5** was further reduced when incubated in human

plasma (Figure 17). The loss of fluorescence in plasma was not due to metabolism of the coumarin, as analysis by thin-layer chromatography (TLC) of plasma extracts under UV light confirmed that this group had not been destroyed, and further spectral analysis did not identify a shift in the excitation or emission spectra. Therefore, the esterase-mediated hydrolysis of **9** could be readily assessed by quantification of the two-step (release followed by quenching) loss of fluorescence following exposure to various biological matrices. Importantly, this measurement could be done directly in a single plate without washing or further assay steps.

In the presence of human plasma, the concentration of compound **9** decreased over time (Figure 16C) with second-order kinetics. The half-life was determined to be 6 minutes in this assay, whereas the half-life of compound **9** in PBS at 37ºC was 26 hours. In order to confirm that the loss of fluorescence of **9** was due to hydrolysis of the CCOM-phosphonate ester and not fluorescence destruction, we extracted the end products and analyzed by TLC (Figure 16D). As expected, compound **9** was fully hydrolyzed to yield the free carboxylic acid in a time-dependent manner. Loss of the prodrug occurred at the same time as the appearance of the free acid. The enzymatic release occurred with a half-life of 7.8 minutes in this assay. The rate of hydrolysis in plasma is similar to some bis-POM compounds [72]. This is an important finding, because it indicates that the presence of a bicyclic aromatic group does not prevent enzymatic hydrolysis of the phosphonate ester, nor does it permit rapid non-enzymatic degradation.

Phosphonate ester prodrugs successfully pass into the cells within hours

We used compound **9** to examine internalization into K562 cells in PBS. No loss of fluorescence was observed in PBS (Figure 16E). Surprisingly, K562 cells could rapidly decrease the extracellular concentration of compound **9** (Figure 16F). This occurred with first-order kinetics and a half-life for 55 minutes. Although our current data cannot rule out the possibility that the

K562 cells secreted an esterase, we believe these findings demonstrate the striking efficacy of phosphonate ester prodrugs to deliver their payload. Within hours, effectively all the drug can pass into the cells.

Discussion

In conclusion, we show biological analysis of the novel fluorescent CCOM phosphoantigen prodrug **9**. These results show that bulky fluorescent systems can be tolerated by cellular esterases without loss of activity or generation of toxicity relative to the commonly used POM protection. The fluorescent prodrug used in these studies loses fluorescence as it crosses into the cell, making it impossible to visualize via microscopy, however compound **9**, as well as other fluorescent prodrugs [73] are useful to detect the speed of cellular uptake in a way that is much faster and requires significantly smaller volumes of cells and materials relative to radiolabeling or HPLC [74] approaches, making them amenable to high-throughput applications. Although our current results are focused on release of the monoacid form, we predict that a parallel strategy could be used to modify phosphonates to release the diacid form of compounds that require full deprotection for biological activity.

Compound	EC_{50}	Fold difference from Compound 8	Reference
2	4000 nM	5.8x	Hsiao et al.
8	23000 nM	--	New
4	520 nM	44x	Hsiao et al.
9	18 nM	1300x	New

Table 1. EC_{50} values for T cell expansion [51].

Compound	K562	RPMI-8226	Daudi	Jurkat
5	>100 µM	>100 µM	>100 µM	>100 µM
2	>100 µM	>100 µM	>100 µM	>100 µM
8	>100 µM	>100 µM	>100 µM	>100 µM
4	>100 µM	>100 µM	>100 µM	>100 µM
9	>100 µM	64 µM	>100 µM	>100 µM

Table 2. 72 hour IC_{50} values in selected cell lines.

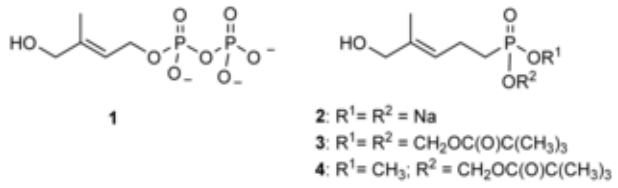

1

2: $R^1 = R^2 = Na$

3: $R^1 = R^2 = CH_2OC(O)C(CH_3)_3$

4: $R^1 = CH_3$; $R^2 = CH_2OC(O)C(CH_3)_3$

Figure 11. HMBPP and some biologically active analogues, compounds 1-4.

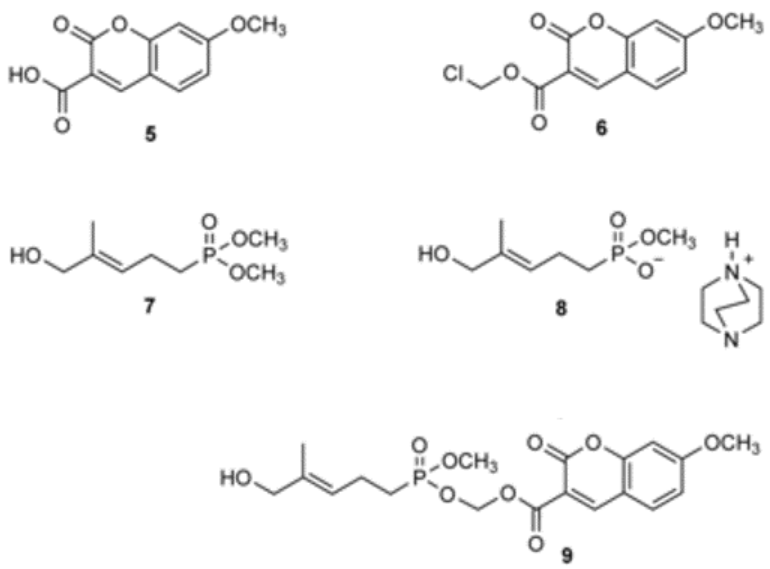

Figure 12. Structures of synthetic phosphoantigens 5-9.

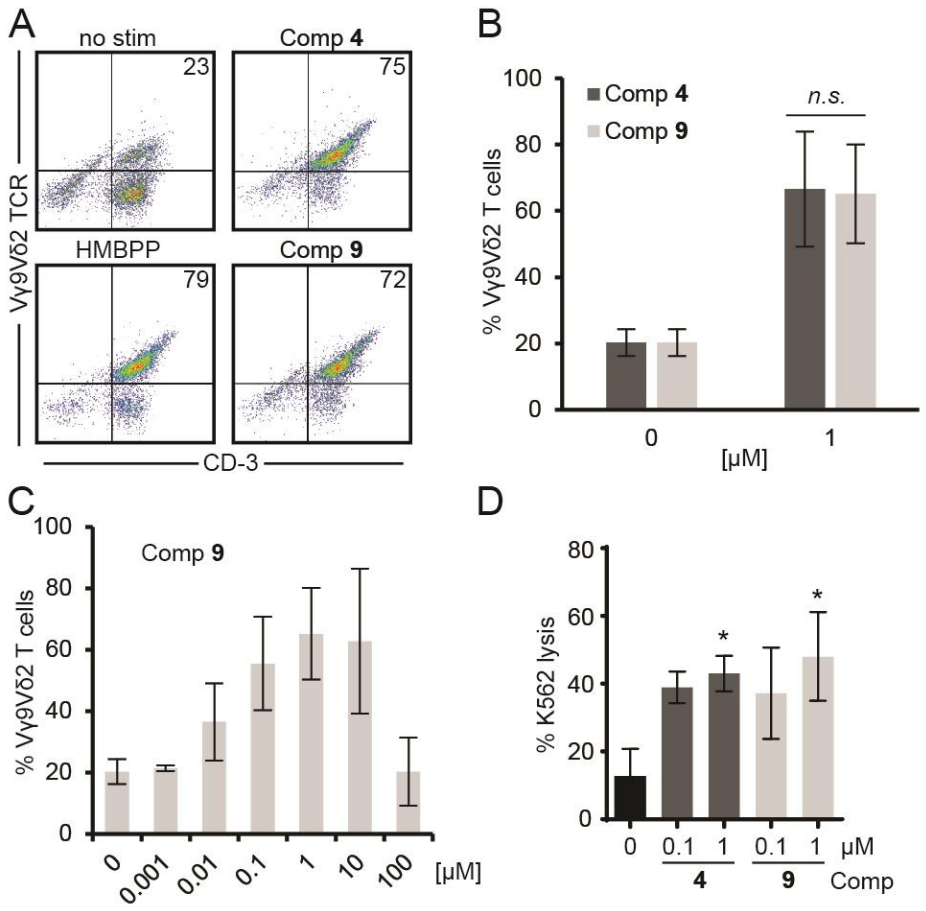

Figure 13. Compound 9 is a potent Vγ9Vδ2 T cell agonist.

A) PBMCs were stimulated with **9**, and phenotyping was performed to quantify the percentages of cells expressing both the Vγ9Vδ2 TCR and the pan T cell marker CD3. Compound **9** was evaluated at a concentration (1 μM) previously shown to be maximal for compound **4**. Data is representative of three independent experiments. B) Quantification of Vγ9Vδ2 T cell proliferation in response to compounds **4** and **9**. C) Dose-response curve for compound **9**. D) Induction of Vγ9Vδ2 T cell-mediated K562 lysis by compounds **4** and **9**. Graphs represent the mean +/- standard deviation, n=3. Statistical significance was determined by ANOVA, *: $p<0.05$.

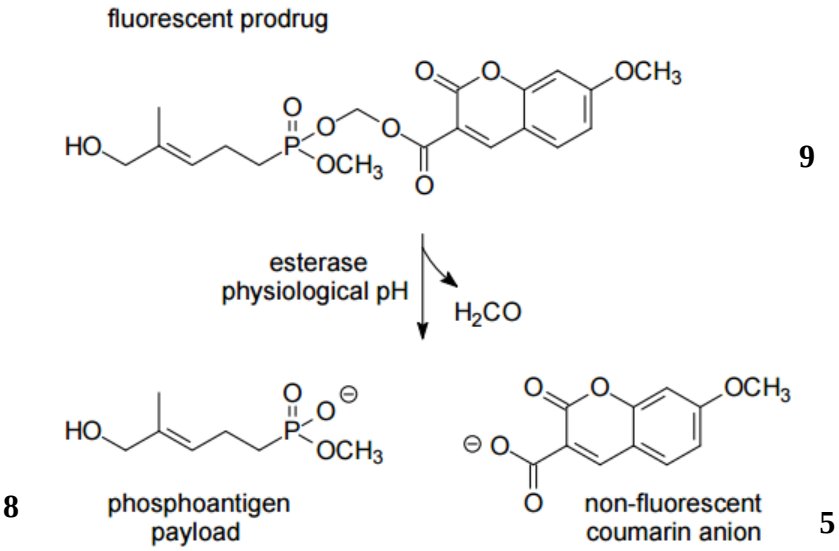

Figure 14. Expected metabolism of compound 9 into the carboxylic acid 5 and the payload 8.

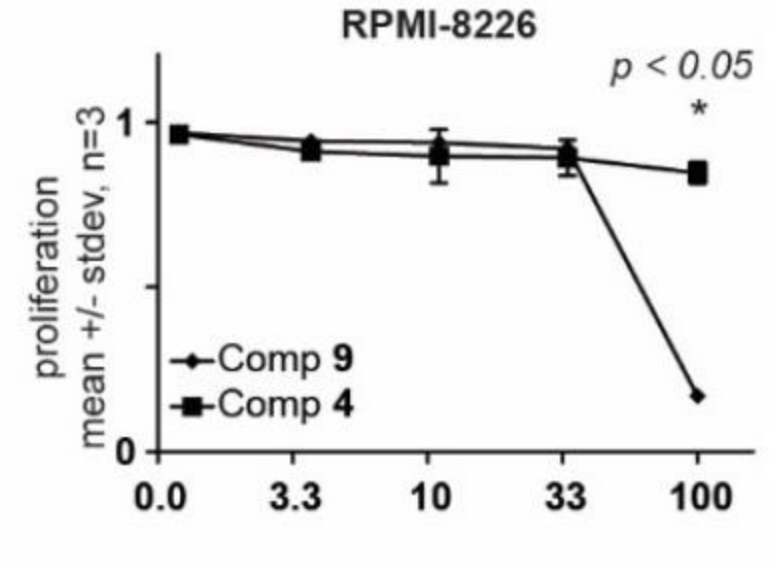

Figure 15. Proliferation of RPMI-8226 cells in the presence of compound 4 or 9.

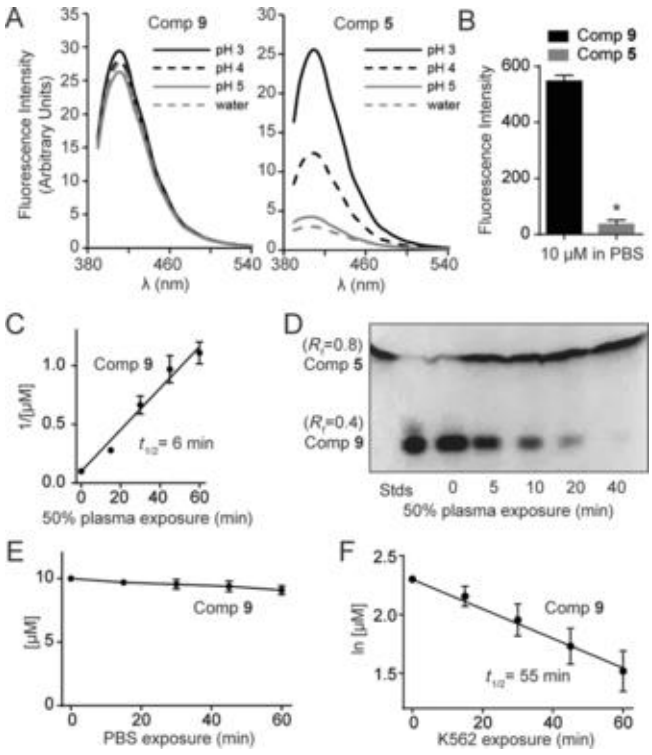

Figure 16.

A) Fluorescence spectra of compounds **5** and **9** in water or citrate buffers at various pH values. B) Intensity of 10 μM compounds **5** and **9** in PBS at pH 7.6. C) Metabolism in plasma was determined by plate reader or D) TLC. E) Stability in PBS. F) Rate of uptake into K562 cells. Graphs in panels (B), (C), (E), and (F) represent the mean +/- standard deviation, n=3. Statistical significance was determined by ANOVA, *: p<0.05.

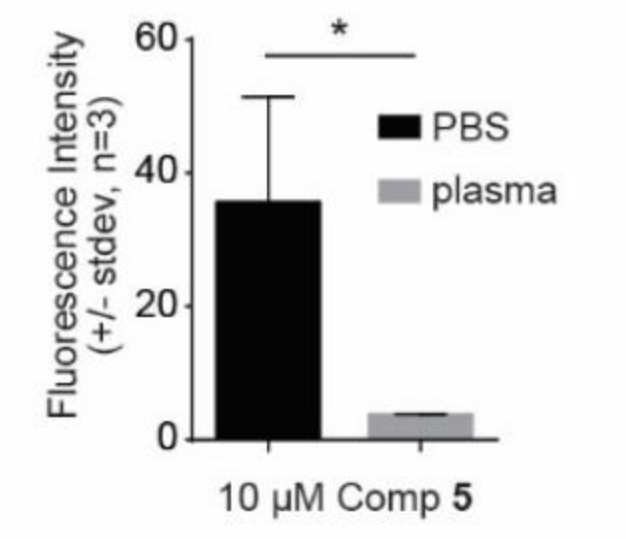

Figure 17. Quantification of compound 5 in PBS in the absence or presence of human plasma.

CHAPTER IV

HMBPP ANALOG PRODRUGS BYPASS ENERGY-DEPENDENT UPTAKE TO PROMOTE EFFICIENT BTN3A1-MEDIATED MALIGNANT CELL LYSIS BY Vγ9Vδ2 T LYMPHOCYTE EFFECTORS

Abstract

This chapter is adapted from our published work [75]. Vγ9Vδ2 effector T cells lyse cells in response to phosphorus-containing small molecules, providing primates a unique route to remove infected or malignant cells. Yet, the triggering mechanisms remain ill-defined. We examined lysis mediated by human Vγ9Vδ2 effector T cells in response to the naturally-occurring (*E*)-4-hydroxy-3-methyl-but-2-enyl diphosphate (HMBPP) or a synthetic cell-permeable prodrug, bis (pivaloyloxymethyl) (*E*)-4-hydroxy-3-methyl-but-2-enyl phosphonate. CD27+/CD45RA- Th1-like effector γδ cells killed K562 target cells though a mechanism that could be enhanced by either compound or TCR antibody and blocked by Src inhibition or butyrophilin 3 isoform 1 (BTN3A1) disruption. Pretreatment at 4°C decreased HMBPP-induced lysis but did not reduce lysis induced by bis (pivaloyloxymethyl) (*E*)-4-hydroxy-3-methyl-but-2-enyl phosphonate. Together, our results show that internalization of HMBPP into target cells is required for BTN3A1-dependent lysis by Vγ9Vδ2 effector T cells. The enhanced activity of the prodrug analog is due to its ability to bypass the pathways required for entry of HMBPP. These findings support an inside-out model of T cell triggering driven by small-molecule induction of BTN3A1.

Introduction

It is essential for organisms to recognize and destroy foreign invaders, and the immune system has evolved a variety of means to do so. In adaptive immunity, T cells can employ the TCR to recognize a tremendous diversity of peptide antigens bound to the MHC. In contrast, innate cells

can utilize pattern-recognition receptors such as the TLRs to detect foreign small molecules known as pathogen-associated molecular patterns. The human Vγ9Vδ2 T cells are unique in that they respond to pathogen-associated small molecules in a way that appears dependent on TCR signaling [76]. The mechanisms controlling this non-traditional activation process are a matter of current interest [68, 77].

Vγ9Vδ2 T cells detect the small molecule (phosphoantigen) (*E*)-4-hydroxy-3-methyl-but-2-enyl diphosphate (HMBPP) [53]. As HMBPP is not produced by mammals, this sensitivity is indicative of a role for Vγ9Vδ2 T cells in pathogen elimination [78]. However, a lower-affinity molecule, isopentenyl diphosphate (IPP), is produced by mammals and can be elevated in malignant cells, suggesting a role for Vγ9Vδ2 T cells in immunosurveillance [32, 79]. Likewise, treatment with bisphosphonate drugs, which activate Vγ9Vδ2 T cells, can reduce risk of certain cancers [80]. If cells contain elevated levels of IPP, as in some cancerous cells, or HMBPP, as in infected cells, they will activate Vγ9Vδ2 T cells to cause a multifaceted immune response [25, 68, 81] including direct target cell lysis. HMBPP or its analogs may be of clinical use as a way to direct Vγ9Vδ2 T cells to attack the malignant cells [82].

A B7 family protein, butyrophilin 3 isoform A1 (BTN3A1), is required for HMBPP to activate Vγ9Vδ2 T cells [36, 42, 83, 84]. There are conflicting x-ray crystallography reports of how this occurs [35, 44]. One suggests a model of extracellular presentation similar to the traditional MHC-peptide-TCR complex [44]. However, another model clearly demonstrates that ligands bind to the intracellular domain of BTN3A1 [35], and our own nuclear magnetic resonance studies support the latter [85]. However, much remains unknown with respect to the mechanisms by which these small molecules work [86]. To address this question through alternative means, we described a cell-permeable prodrug analog of HMBPP, bis (pivaloyloxymethyl) (*E*)-4-hydroxy-3-

methyl-but-2-enyl phosphonate (POM_2-C-HMBP) [62, 85]. In this chapter, we use HMBPP and POM_2-C-HMBP to reveal new information about the mechanisms governing their cellular uptake leading to lysis by Vγ9Vδ2 effectors and the excellent potency of the novel prodrug.

Materials and Methods

Reagents and supplies

RPMI-1640, FBS, nonessential amino acids, pyruvate, penicillin streptomycin, HEPES, BME, HMBPP and FITC-γδ TCR antibody (clone 5A6.E91) were obtained through Fisher Scientific. IL-2 and the MACS γδ T cell negative selection kit were obtained through Miltenyi Biotec. PE-CD3 (UCHT1), allophycocyanin-TNF-α (MAb11), PE-IFN-γ (4S.B3), FITC-IL-2 (MQ1-17H12), allophycocyanin-CD45RA (HI-100), PerCP-eFluor710-CD27 (LG.7F9), FITC-Annexin V, and PerCP-eFluor710-Annexin V were from eBioscience. K562 cells were from American Type Culture Collection, while Research Blood Components (Boston, MA) supplied blood. DiD, calcein AM, pcDNA3.1, and DNA primers were obtained through Life Technologies, while CRISPR/Cas9 repair templates were obtained through Integrated DNA Technologies. Restriction enzymes including XhoI, EcoRV, and NheI were obtained through New England Biolabs. PE-BTN3A1 (CD277) antibody (BT3.1), FITC-CD183 (G025H7), and functional-grade anti-human TCR γ/δ Antibody (B1), and human IFN-γ ELISA MAX deluxe kit were obtained from Biolegend, whereas G418, PP2, and PHA P were obtained from Sigma-Aldrich. Anti-myc (9E10) antibody was purified from hybridoma cells obtained from the Developmental Studies Hybridoma Bank at The University of Iowa. POM_2-C-HMBP was a kind gift of Dr. David Wiemer at the University of Iowa.

Vγ9Vδ2 T cell expansion and purification

Human PBMCs from healthy anonymous donors were isolated from heparinized blood using Lymphoprep (Axis-Shield) within 24 hours of collection. Cells were counted by hemocytometer in the presence of trypan blue, then aliquoted in freezing media (10% DMSO, 20% FBS, 70% media), and stored in liquid nitrogen. PBMCs were resuspended at 1×10^6 cells/mL in fresh T cell media (RPMI 1640, 10% heat-inactivated FBS, 1x HEPES, pyruvate, nonessential amino acids, and BME). Cells were stimulated with 0.01 μM HMBPP or 0.01 μM POM_2-C-HMBP for 3 days and cultured for another 4-18 days after compound removal. Fresh IL-2 (5 ng/mL) was provided every 3 days. After 7-21 days, Vγ9Vδ2 T cells were purified by negative selection. Experiments were performed at least three times using at least two donors.

K562 cell culture

K562 cells were cultured in RPMI 1640, 10% Fetal Clone III Serum (Hyclone), and 1% penicillin/streptomycin and maintained between 0.2 and 1 x 10^6 cells per mL.

Surface staining

For surface-staining experiments (γδ TCR/CD3, CD27/CD45RA, validation of BTN3A1 disruption), cells were washed twice in FACS buffer (2% BSA/PBS), suspended in FACS buffer, and incubated at 4 ºC for 30 minutes with antibodies (2-5 μL in 100 μL). Cells were washed twice in FACS buffer and analyzed using a BD FACSCalibur (BD Biosciences). In dual color experiments, gates were determined using single-stained controls. Data was analyzed with FlowJo 9 (Tree Star) and X software at the University of Connecticut Flow Cytometry and Confocal Microscopy Facility.

Intracellular cytokine staining

Purified expanded Vγ9Vδ2 T cells (4 x 10^6 cells in 1 mL in a 12-well plate) were incubated with PMA (10 ng/mL), ionomycin (1 μM), and brefeldin A solution (1x) according to manufacturer's protocol (BD Biosciences). Cells were incubated 4 hours at 37 ºC, washed in FACS buffer, and fixed by addition of 4% paraformaldehyde for 10 minutes. Cells were washed in FACS buffer, permeabilized by addition of 0.1% saponin, and blocked with anti-CD16/CD32 (Fc Block) for 10 minutes. Cells were stained for 30 minutes with fluorescent antibodies, washed twice, and analyzed. In four-color experiments, gates were drawn using controls deficient in each antibody.

IFN-γ ELISA

K562 cells were suspended in T cell media and were treated with various concentrations of test compounds or PHA as described in the text for 2 hours. K562 cells were washed twice and mixed with T cells at an E: T ratio of 3:1 in 200 μL in duplicate. Mixtures were incubated for 24 hours, following which IFN-γ was assessed by ELISA according to the manufacturer's protocol (BioLegend).

Lysis assay

K562 cells were stained with DiD (2 minutes in 4 μM DiD in BSA/PBS), quenched by addition of an equal volume of FBS, and washed twice in T cell media. K562 cells were treated as described in this chapter. K562 cells were mixed with T cells at an effector: target ratio of 3:1 in 200 μL. Mixtures were incubated for 4 hours at 37 ºC then placed on ice for 5 minutes. FITC- or PerCP-eFluor710-Annexin V (3 μL) was added for 15 minutes on ice, then cells were diluted by addition of 200-300 μL binding buffer (BD Biosciences) and analyzed by flow cytometry. In the multicolor experiments, K562 cells were stained with DiD or calcein-AM (15 minutes, 1 μM in media) and washed. DiD+ cells were exposed to test compounds while calcein+ cells were

untreated. Cells were washed twice in media. Cells were mixed at a 1:1 DiD/calcein ratio, and mixed with Vγ9Vδ2 T cells at an E: T ratio of 3:1 in 200 μL.

Live imaging

ICAM-1 was obtained by protein G Sepharose purification of Chinese hamster ovary cell spent media as described [57, 58]. The 384-well clear bottom plates were coated with 5 μg/μL (ICAM-1) for 60 min. Plates were washed with PBS and blocked with 2% BSA at 37 ºC for 30 minutes. K562 cells pretreated with HMBPP or POM_2-C-HMBP were added and incubated at 37 ºC for 30 minutes. T cells were added to the wells in a 3:1 ratio (E: T). Cells were visualized using an Andor confocal microscope (Andor) set up for multi-dimension acquisition and live imaging. Images were taken every 30-60 seconds for 30-240 minutes at 37 ºC.

Disruption and re-expression of BTN3A1

CRISPR/Cas9 was used to disrupt BTN3A1 according to the method of Ran with slight modification [87]. sgRNAs of the following sequences designed to remove a 45-bp region of genomic DNA containing the BTN3A1 start codon were cloned into pX335-U6-Chimeric_BB-CBh-hSpCas9n (D10A) (Addgene): 5'-AAT GAA AAT GGC AAG TTT CC-3' (sense) and 5'-TAT CAG GAG ATA CTG GAA GG-3' (antisense). To facilitate homology directed repair, cells were cotransfected with a 192-bp single stranded repair template (Integrated DNA Technologies) (5'-GGT CAC CAT ACT TGA GTT AGC TCT AGG GAA GTG GAG GTT TCC ATT TGG AAT TCT ATA GCT TCT TCC AGG TCA TAG TGT CTG CCC ACC CTC GAG GAT ATC CCT GGC CTT CCT TCT GCT CAA CTT TCG TGT CTG CCT TTT GCT TCA GCT CAT GCC TCA CTC AGG TAG GGA ACA ATT CCA CGC TTG-3'). The repair template contained central restriction sites for XhoI and EcoRV to facilitate genotyping. Transfection was performed by electroporation with a gene pulser XCELL (Bio-rad) using 316 V, 500 μF capacitance and 4-

mm conditions. The transfection was performed using 1 x 10^7 cells, 10 µg of each sgDNA plasmid, and 200 pg ssODN in 400 µL volume. At 24 hours post-transfection, single cells were separated by limiting dilution and allowed to grow for 3 to 4 weeks. Genomic DNA from individual clones was isolated by resuspension of the cells from 1 mL culture in buffer (8 mM Tris, 5 mM EDTA, 200 mM NaCl, and 0.2% SDS [pH 8.0]) containing 200 µg/mL proteinase K (Fisher) followed by heating at 55 ºC for 1 hour, isopropanol precipitation, 70% ethanol wash, and resuspension in water. Genotyping was performed by PCR of genomic DNA with the following primers: 5'- GTG AAG ACA CTG AAG GAC AGA A-3' and 5'-CAG GTT TGG GAA GGA GTC AA-3'. The amplicon was 336 bp for the wild-type (WT) BTN3A1 and 303 bp for the expected mutant. The mutant DNA was further assessed by test digest with XhoI and EcoRV. Sanger sequencing was performed.

In BTN3A1-deficient cells, BTN3A1 was reintroduced by transfection and selection. BTN3A1 was cloned into pcDNA3.1 (Life Technologies) using the following primers from Life Technologies: forward primer into NheI site of pcDNA3.1 5'-GCT ATC GCT AGC ATG AAA ATG GCA AGT TTC-3', reverse primer into XhoI site of pcDNA3.1 including myc tag and stop codon 5'-GCT ATC CTC GAG TCA CAG ATC CTC TTC TGA GAT GAG TTT TTG TTC CGC TGG ACA AAT AGT CAG and validated by Sanger sequencing. The plasmid (10 µg) was electroporated using the above conditions and selected with G418.

Statistical analysis

One-way ANOVA was used to calculate significance. Comparisons were done relative to the control or between pairs of conditions. Columns in bar graphs represent the mean ± SEM. An α level of 0.05 was used. Dose-response curves were analyzed using nonlinear regression

(log[agonist] versus response) in GraphPad Prism (GraphPad) to generate EC_{50} values and confidence intervals.

Results

Stimulation with HMBPP or POM_2-C-HMBP generates effector Vγ9Vδ2 T cells with a Th1 phenotype

Human blood contains Vγ9Vδ2 T cells that express subpopulations reminiscent of naïve and memory T cells [88]. We first assessed the phenotypes of Vγ9Vδ2 T cells following exposure to HMBPP or POM_2-C-HMBP (Figure 18A). HMBPP was used in this study as it is the most potent naturally-occurring Vγ9Vδ2 T cell agonist, with activity that is 4 to 5 orders of magnitude greater than any other known natural molecule [27]. POM_2-C-HMBP was used because we predicted it would rapidly deliver the BTN3A1 B30.2 ligand C-HMBP to the cytoplasmic binding site by passive transmembrane diffusion (Figure 18A) [85]. PBMCs were treated with either HMBPP or POM_2-C-HMBP, cultured, and assessed for proliferation, Th1/Th2 polarization, and naïve/memory phenotype. Treatment with the compounds and IL-2 caused an increase in the proportion of γδ TCR+/CD3+ cells, which were isolated to >97% purity (shown for HMBPP in Figure 18B, 18C).

We assessed the polarization by intracellular cytokine staining (Figure 18D). Cells were labeled with antibodies to TNF-α, IFN-γ, IL-2, and IL-10. Few IL-10 positive cells were observed (not shown). In contrast, the majority of the expanded cells were positive for both TNF-α and IFN-γ. A subset of these cells expressed IL-2, whereas another subset was positive only for IFN-γ (Figure 18E). No differences in cytokine production were observed in cells that were expanded by HMBPP versus POM_2-C-HMBP. The pattern of cytokine production is consistent with a Th1

phenotype, and the cells were of sufficient quality to produce multiple cytokines regardless of the stimulatory compound used for initial expansion.

We assessed both compounds for their ability to generate effector cells by staining for CD27 and CD45RA. Unstimulated Vγ9Vδ2 TCR+/CD3+ cells were largely CD27+ with a range of CD45RA expression (Figure 18F). Following stimulation, a strong majority of the cells became CD45RA-. Therefore, most of the cells used in this study were Vγ9Vδ2 TCR+/CD3+/CD27+/CD45RA-, consistent with an antigen experienced effector memory phenotype. Again, no differences were observed after exposure to HMBPP versus POM_2-C-HMBP. Thus, regardless of whether the initial stimulation was performed with HMBPP or POM_2-C-HMBP, the resultant Vγ9Vδ2 effector cells are of consistent phenotype.

Effector Vγ9Vδ2 T cells kill target cells in a Src-dependent manner

To measure the lytic capabilities of the effector T cells, we used a flow cytometric method [89] based on Annexin V staining of the target cells that allows tracking of both the killing of the target cells and the effectors (Figure 19). We mixed DiD+ K562 cells with the effectors for 4 hours in the continuous presence of HMBPP with or without the Src kinase inhibitor PP2. As expected, treatment with HMBPP induced T cell mediated killing of the K562 cells (Figure 19A, 19B). This effect was blocked by PP2. Therefore, inducible Vγ9Vδ2 T cell-mediated killing is dependent on Src kinase activation.

Short-term preloading of target cells enhances specificity while reducing background Vγ9Vδ2 effector autolysis

During these studies, we observed that a number of effector T cells became Annexin V positive. We directly tested for T cell autolysis under these conditions (Figure 19C). In the absence of K562 cells, the continuous presence of HMBPP significantly increased the number of Annexin

V-positive T cells. To avoid this unwanted autolysis, we preloaded the K562 target cells alone for 2 hours, washed, and introduced them to the effectors for 4 hours. This preloading strategy resulted in lower baseline levels of target cell lysis in the absence of stimulation, typically to the 5-20% range, and reduced the amount of T cell autolysis, allowing for a clearer measurement of inducible cell lysis. Figure 19D shows the gating scheme of the lysis assays used throughout this paper, in which DiD+ K562 target cells were analyzed for Annexin V binding.

Activity of the effector cells for lysis of the target cells could be increased by pretreatment of the target cells with HMBPP or POM_2-C-HMBP in a dose-dependent manner (Figure 19E). Pretreatment of the target cells with the compounds resulted in a more specific response by the effector cells than did cotreatment for target cell lysis because it reduced the amount of T cell autolysis. Furthermore, preloading with POM_2-C-HMBP (EC_{50} = 1.2 nM) was more effective at promoting lysis than was preloading with HMBPP (EC_{50} = 19 nM) (Figure 19E). Preloading the target cells with POM_2-C-HMBP was also more effective at promoting IFN-γ secretion than was preloading with HMBPP, in which EC_{50} values of 22 nM for POM_2-C-HMBP and 590 nM for HMBPP were observed (Figure 19F). To directly monitor the efficacy of the prodrug strategy, we also measured IFN-γ production in response to the active metabolite of POM_2-C-HMBP, C-HMBP which showed a much larger EC_{50} value of 32 μM (1500-fold difference) (Figure 20). The superior activity of the neutral compound versus the charged compound during short incubations supports a model in which target cell internalization is critical for inducible T cell-mediated killing and cytokine production by effector Vγ9Vδ2 T cells.

BTN3A1 disruption in target cells

BTN3A1 is necessary for prenyl diphosphates to induce proliferation of Vγ9Vδ2 T cells [43] and HMBPP and its analogs interact with the intracellular domain of BTN3A1 [35, 85], but

it is not yet clear whether BTN3A1 functions in a similar capacity in experienced cytotoxic effector cells during cytolysis. To clarify the role of BTN3A1 in target cells, we created K562 cell lines deficient of functional BTN3A1 using CRISPR/Cas9 (Figure 21A). All cell lines were analyzed by PCR to determine if the desired BTN3A1 mutation was produced. Of 35 clones, a range of indel mutations was observed, and clones 17, 18 and 26 were identified as knockouts (Figure 21B) as judged by the successful deletion of the start codon and insertion of a restriction site as intended by the single stranded DNA repair template. To validate loss of BTN3A1, we assessed surface levels of BTN3A1 in WT, clone 4 (WT clone), and knockout clones 17, 18 and 26 by flow cytometry. A significant decrease in the fluorescence intensity of BTN3A1 staining was seen in knockout cell lines when compared with WT K562 cells and clone 4 (Figure 21C). Surface levels of CD183 were analyzed by flow cytometry as a control and collectively show no reduction in surface expression levels (Figure 21D).

BTN3A1 in target cells is required for lysis induced by HMBPP or POM_2-C-HMBP

To evaluate whether BTN3A1 is required for inducible target cell lysis by Vγ9Vδ2 T cells, we performed lysis assays with the three clones of BTN3A1-disrupted cells. One WT clone (clone 4) and parental WT K562 cells were both used as controls. Cells were pretreated for 2 hours with HMBPP or POM_2-C-HMBP and then exposed to Vγ9Vδ2 effector cells. In the absence of ligand, all three BTN3A1-deficient clones showed no change in lysis when compared to WT K562 cells and the WT clone 4 (Figure 22A). However, when the BTN3A1-deficient cells were treated with HMBPP or POM_2-C-HMBP, inducible lysis was significantly decreased relative to WT cells (Figure 22A-C).

To show that the change in cell lysis induced by the small molecules was due to lack of BTN3A1, we generated a BTN3A1-myc construct and electroporated it in to the CRISPR/Cas9

clone 26, producing a stable rescue cell line by selection in G418. Clone 26 cells expressing exogenous BTN3A1 showed a significant increase in lysis compared to clone 26 (Figure 22D, 22E). Together, loss of target cell BTN3A1 expression reduces the ability of both HMBPP and POM_2-C-HMBP to trigger activation of Vγ9Vδ2 effector cells.

As further validation of the role of BTN3A1 in activation of Vγ9Vδ2 effector cells and the functionality of our CRISPR mutants, we loaded WT K562 cells or BTN3A1-deficient clones 17, 18 and 26 with various concentrations of C-HMBP and assessed their ability to stimulate production of IFN-γ (Figure 23). As expected, preloaded WT K562 cells stimulated IFN-γ in a dose-dependent manner (Figure 23A). All three of the BTN3A1-deficient clones were unable to trigger IFN-γ production. WT K562 cells that had been pre-exposed to PHA for 2 hours also triggered a dose-dependent increase in IFN-γ production (Figure 23B). However, the effect of PHA on IFN production was only mildly reduced by loss of BTN3A1.

BTN3A1 in target cells is dispensable for lysis induced by TCR antibody

To determine whether these BTN3A1-deficient cells were still susceptible to killing by Vγ9Vδ2 effector cells, we then examined the ability of a γδ TCR antibody to induce their lysis (Figure 22F, 22G). T cells were pre-incubated with the antibody then mixed with target cells. In WT K562 cells, the TCR antibody was sufficient to induce the T cells to kill the K562 cells. In contrast to the inducible lysis stimulated by HMBPP, the loss of BTN3A1 function had no effect on inducible lysis stimulated by the TCR antibody. Thus, BTN3A1 is required for lysis induced by phosphorous compounds, but loss of BTN3A1 does not affect the ability of the target cells to be lysed when stimulated by TCR crosslinking.

HMBPP, but not POM_2-C-HMBP, uses an energy-dependent uptake pathway to enter target cells, which is required for inducible Vγ9Vδ2 T cell mediated lysis

Based on the more potent activity of the charge-neutral POM_2-C-HMBP compared to the negatively charged HMBPP (Figure 19E, 19F), we hypothesized that these target cells use an active uptake process to internalize HMBPP. To further investigate this possibility we pretreated K562 cells with HMBPP or POM_2-C-HMBP at either 37 ºC or 4 ºC for 2 hours, as incubation of cells at low temperatures inhibits energy-dependent uptake mechanisms [90]. After preincubation, we mixed the target cells with the effectors and assessed their lysis (Figure 24A). HMBPP-treated cells exhibited a significant decrease in inducible lysis when preloaded at 4 ºC in comparison to those treated at 37 ºC, whereas POM_2-C-HMBP treated cells did not lose activity when loaded at the lower temperature (Figure 24B). Thus, energy-dependent cellular entry is required for the activity of HMBPP.

These findings are also evident from live-cell imaging experiments (Figure 24C, 24D). The K562 cells were exposed to compounds as described above, plated onto ICAM-1 to allow for traction [57, 58, 91] and exposed to the effectors. Cells that had been loaded with POM_2-C-HMBP were lysed by the T cells, while untreated cells were scanned but not killed (Figure 24C). Again, pretreatment at 4 ºC blocked the ability of HMBPP but not POM_2-C-HMBP to trigger T cell mediated lysis (Figure 24D), and POM_2-C-HMBP demonstrated enhanced potency relative to HMBPP.

To further investigate these effects, we used flow cytometry to generate dose-response curves for both compounds at both temperatures. Lysis induced by HMBPP was significantly reduced by loading at 4ºC relative to 37ºC, whereas the activity of POM_2-C-HMBP was unchanged (Figure 24E, 24F, Table 3). The charged molecule C-HMBP was also analyzed in the same manner

and showed a similar pattern to that of HMBPP (Figure 25A). These data show that the activity of both HMBPP and C-HMBP are decreased at 4ºC, indicating an energy-dependent uptake mechanism is required for their activity, but not that of POM_2-C-HMBP. Together, these data oppose the model of extracellular ligand binding.

Inducible lysis by Vγ9Vδ2 T cells is selective for loaded target cells

It was not clear whether the effectors were sensitive enough to kill only cells that contain HMBPP and not HMBPP-deficient neighboring cells. Therefore, we assessed the ability of Vγ9Vδ2 T cells to lyse a mixture of K562 cells in which only some cells were loaded (Figure 26). We labeled K562 cells with one of two fluorescent probes (DiD and calcein). DiD+ cells were then loaded with either HMBPP or POM_2-C-HMBP for 2 hours, washed, and exposed to effectors. In this mixed population, some constitutive lysis was observed, which was consistent regardless of the label. Treatment with HMBPP or POM_2-C-HMBP increased the fraction of lysed cells. Vγ9Vδ2 T cells effectively lysed the targets that contained either HMBPP or POM_2-C-HMBP while ignoring the non-loaded cells in the mixture (Figure 26A, 26B).

POM_2-C-HMBP remains active within target cells, whereas HMBPP is quickly metabolized

Once HMBPP is internalized, the target cells are susceptible to lysis by the Vγ9Vδ2 T effectors. However, it is not clear how long target cells retain this susceptibility. We tested this by preloading target cells with 100 nM HMBPP or 100 nM POM_2-C-HMBP for 2 hours and then resting the target cells for 0 (no rest), 12, or 24 hours. After this time, the target cells were mixed with Vγ9Vδ2 effector T cells for 4 hours and analyzed by flow cytometry as described above. Results shown in Figure 27A and 27B reveal that the effect of HMBPP is lost within 12 hours, while POM_2-C-HMBP remains fully active at 12 hours and 24 hours post loading.

To further investigate these findings, we extended our experiment to include additional time points. The activity gained by pretreatment with 100 nM HMBPP was again lost between 6 and 12 hours (Figure 27C), whereas the activity of 100 nM POM_2-C-HMBP is lost only after 48 hours (Figure 27D). Even at 10 nM (Figure 27E), POM_2-C-HMBP remains active for longer than 100 nM HMBPP. This analysis was also done using C-HMBP at 10 μM (Figure 25B), which lost its activity between 12 and 24 hours, similar to that of 10 nM POM_2-C-HMBP. Thus, target cells are capable of HMBPP destruction or removal in the absence of T cell-mediated cytolysis. POM_2-C-HMBP and C-HMBP, appear to avoid this metabolic fate, presumably due in part to the metabolic stability of the phosphonate bond relative to the analogous phosphate linkage of HMBPP. Therefore, cellular response is controlled by a balance of uptake and degradation (Figure 28).

Discussion

In this study, we use HMBPP and a cell-cleavable prodrug analog, POM_2-C-HMBP, to clarify the mechanisms of Vγ9Vδ2 TCR triggering during target cell lysis and the role of cellular internalization in this process. We demonstrate that an energy-dependent uptake mechanism is required for charged phosphorus compounds to use BTN3A1 to trigger Vγ9Vδ2 mediated cell lysis. This uptake mechanism can be readily bypassed by the charge-neutral POM_2-C-HMBP, leading to a dramatic increase in BTN3A1-mediated killing and cytokine production relative to the charged compound HMBPP.

Exposure of PBMCs to either compound generates effector cells that produce IFN-γ, TNF-α, and IL-2. This is similar to the indirect-acting zoledronate [92]. These effectors can kill K562 target cells in a way that is enhanced by addition of either phosphorus compound. The inducible lysis is dependent upon Src kinase activity, as it can be blocked by cotreatment with PP2, which

presumably inhibits the T cell-specific Src isoforms Lck and/or Fyn in this model. Given that K562 cells do not express MHC [40, 93, 94], the process is MHC independent. Inducible lysis is dependent upon the presence of BTN3A1, as disruption of this gene by CRISPR/Cas9 blocks the ligand-induced lysis while re-expression of BTN3A1 rescues the effect. Likewise, disruption of BTN3A1 fully abrogates the ability of phosphoantigens, but not PHA, to stimulate cytokine production by Vγ9Vδ2 T effectors. However, BTN3A1 disruption does not affect lysis induced by TCR antibody, so it is likely that the function of BTN3A1 is specific to HMBPP and its analogs. The sensitivity to lysis induced by HMBPP is selective enough that it can kill only the loaded cells within a mixed population, but it is transient, disappearing in 6-12 hours after exposure.

We also determined that entry of charged ligands but not the neutral prodrug decreases at low temperatures, which supports a role for a type of energy-dependent uptake, likely endocytosis and internalization in the activity of HMBPP. This finding is consistent with a model in that, given the pKa values of HMBPP, diffusion into the cytoplasm is strongly enhanced as the molecule becomes protonated during acidification of endocytic vesicles, similar to that previously described with respect to cellular entry of bisphosphonate drugs [95]. Vγ9Vδ2 T cells recognize cells containing these molecules bound to the BTN3A1 B30.2 domain and form an MHC-independent immunological synapse with the target cell that leads to the activation of the Vγ9Vδ2 T cell. This active uptake mechanism would not be necessary for Vγ9Vδ2 T cells to sense metabolites produced by intracellular pathogens, which can readily access the binding site. However, internalization is likely critical when Vγ9Vδ2 effector cells respond to distantly affected cells in the absence of contact, such as has been reported in *Plasmodium* infection [96] and response to tumor-derived IPP [97].

There are only two naturally-occurring compounds that are currently known to activate BTN3A1 directly: HMBPP and IPP, the former of which clearly has the stronger binding [85]. Therefore, BTN3A1 can be described as a receptor for HMBPP, with IPP and the synthetic compounds being analogs of HMBPP that also bind the receptor. Use of HMBPP and its analogs provides clarity over use of zoledronate and the other bisphosphonates, which, although they are clinically used agents, act indirectly and display a multitude of cellular effects resulting from depletion of isoprenoids and sterols, including cell toxicity. The direct acting BTN3A1 ligands HMBPP and POM_2-C-HMBP display markedly increased therapeutic indices relative to zoledronate [85]. Furthermore, as we show in the current study, POM_2-C-HMBP offers several differences over HMBPP: it retains the ability to generate high quality Th1 effector cells, it shows faster cell uptake that is independent of endocytosis, and it sensitizes cells for a longer time. It is not yet clear whether these differences would result in therapeutic benefit.

Although it has been recognized that HMBPP and its analogs activate T cells that express the Vγ9Vδ2 TCR [40], the mechanisms have remained enigmatic [68, 77]. Investigators have tried to fit these small molecules into traditional models of TCR stimulation triggered by peptide antigens. In part, this is because the TCR extracellular domain [98] and downstream signaling is required for HMBPP activity [99], which our findings with PP2 and the TCR antibody support. At the same time, HMBPP activity has been reported to be independent of MHC [44], which is consistent with our findings because K562 cells do not express MHC. The apparent discordance of these results has led others to search for an antigen presenting protein that is functionally analogous to MHC and could serve to present HMBPP directly to the Vγ9Vδ2 TCR on the cell surface, which is exemplified by the models put forth initially by Wang et al. [43] and Morita et al. [40, 43] and subsequently by Vavassori et al. [44].

However, now that the importance of the internal B30.2 domain of BTN3A1 in HMBPP activity has been identified [35, 43, 68, 85, 100], it has become apparent that Vγ9Vδ2 T cell activation does not fit the traditional models. The earlier studies that suggested external presentation [40] were likely confounded by use of high ligand concentrations which allowed for transmembrane diffusion and BTN3A1 activation even in lightly fixed cells. Because BTN3A1 is a B7 family protein, it is possible that HMBPP functions through inducible BTN3A1-mediated co-stimulation (Figure 28). Unfortunately, this implies that the term "phosphoantigen" may be a confusing misnomer as HMBPP and its analogs are not actually stimulatory MHC-TCR ligands (i.e. antigens). Instead, they are ligands which control the function of a B7 family member. Thus, these nonpeptide antigens, which activate Vγ9Vδ2 T cells, may be better classified as pathogen-associated molecular patterns that bind to a type of pattern recognition receptor, the B30.2 domain of BTN3A1.

The outstanding unknown is the identity of the extracellular binding partners of BTN3A1 and the Vγ9Vδ2 TCR. Specifically, models in which zero, one, or two extracellular ligands are unknown can be envisioned. Although the TCRγ J region has been reported to be required for detection of prenyl diphosphates [98], direct extracellular binding between the TCR and BTN3A1 has not been observed [35]. However, these studies did not exclude the possibility of multimeric complex of BTN3A1 directly binding to the TCR (i.e., the direct triggering model, Figure 28). In contrast, if the traditional two-signal aggregation/conformational change mechanisms are true [43], then both proteins would require an extracellular ligand on the opposing cell. This model of TCR binding with BTN3A1 costimulation is supported by studies that show additional factors on chromosome 6 influence phosphoantigen detection [101]. However, existing data does not appear to exclude a kinetic segregation model as described in other T cell types [102]. If this model were

true, the Vγ9Vδ2 TCR would be required only as a signaling platform, with the TCRγ J region required but not used for binding the opposing cell. T cell activation would occur not through extracellular ligand binding to an MHC-like complex, but rather though inducible costimulation leading to synapse formation and steric exclusion of inhibitory proteins. In fact, CD45 exclusion has from the Vγ9Vδ2 synapse already has been observed [2, 103]. Identification of the extracellular binding partner(s), if any exist, will further elucidate the mechanisms underlying this unique cross-membrane signaling event.

	EC_{50} 37º (95% CI)	EC_{50} 4º (95% CI)	Fold change
HMBPP	0.042 (0.017-0.10)	1.1 (0.57-2.3)	27
POM_2-C-HMBP	0.0041 (0.0017-0.010)	0.01 (0.0017-0.034)	1.5
C-HMBP	2.1 (0.55-8.0)	48 (41-57)	22

Table 3. Phosphorus compound EC50 values at 37˚C and 4ºC. [1]

[1] EC_{50} values determined by dose response lysis assays at both 37˚C and 4˚C. 95% confidence intervals are shown in parenthesis. All values are in µM concentration. n=3.

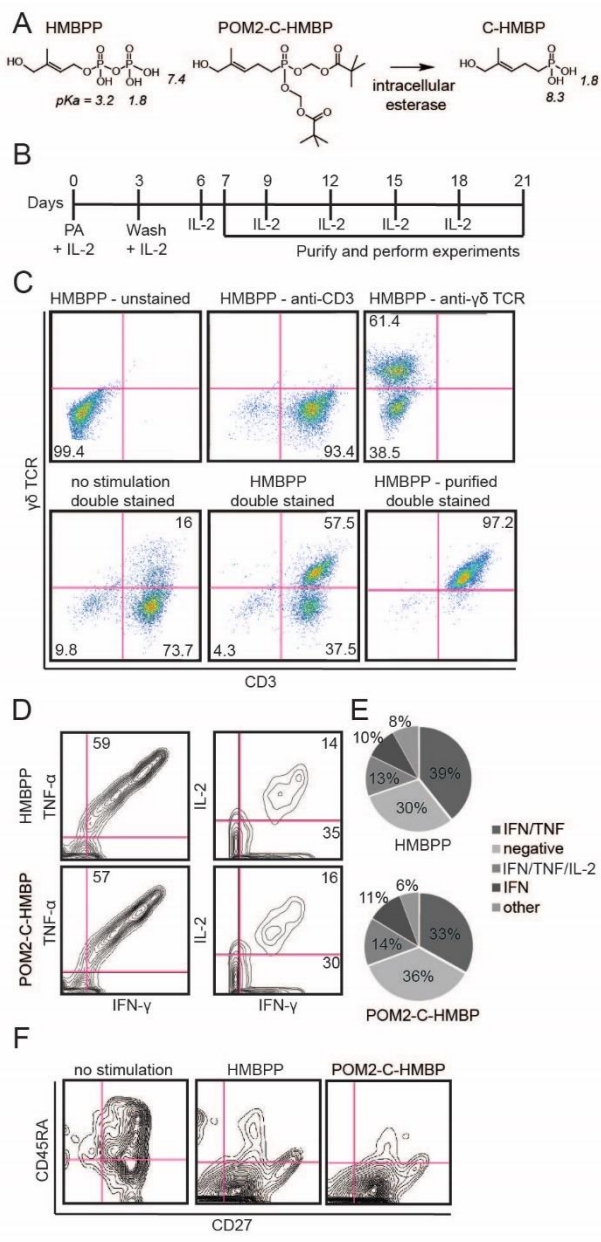

Figure 18. HMBPP and POM2-C-HMBP stimulate expansion of Th1 polarized effector Vγ9Vδ2 T cells.

A) Chemical structures of compounds used in this study. The pKa of each acidic hydrogen atom (as determined by Marvin software) is given in italics. B) Timeline showing HMBPP (10 nM) and IL-2 stimulation as well as experimental window used to expand effector T cells from PBMC. C) Vγ9Vδ2 T cell expansion analysis by flow cytometry of cell populations before and after purification by negative selection. D) Intracellular cytokine staining of IL-2, IFN-γ, and TNF-α in effector T cells as assessed by flow cytometry. E) Quantification of cytokine production by effector cell populations. Values represent the mean of three independent experiments, no significant differences were observed. F) Effector cell memory phenotype as assessed by flow cytometric

staining for CD45RA and CD27. Flow plots in all panels are representative of greater than three independent experiments.

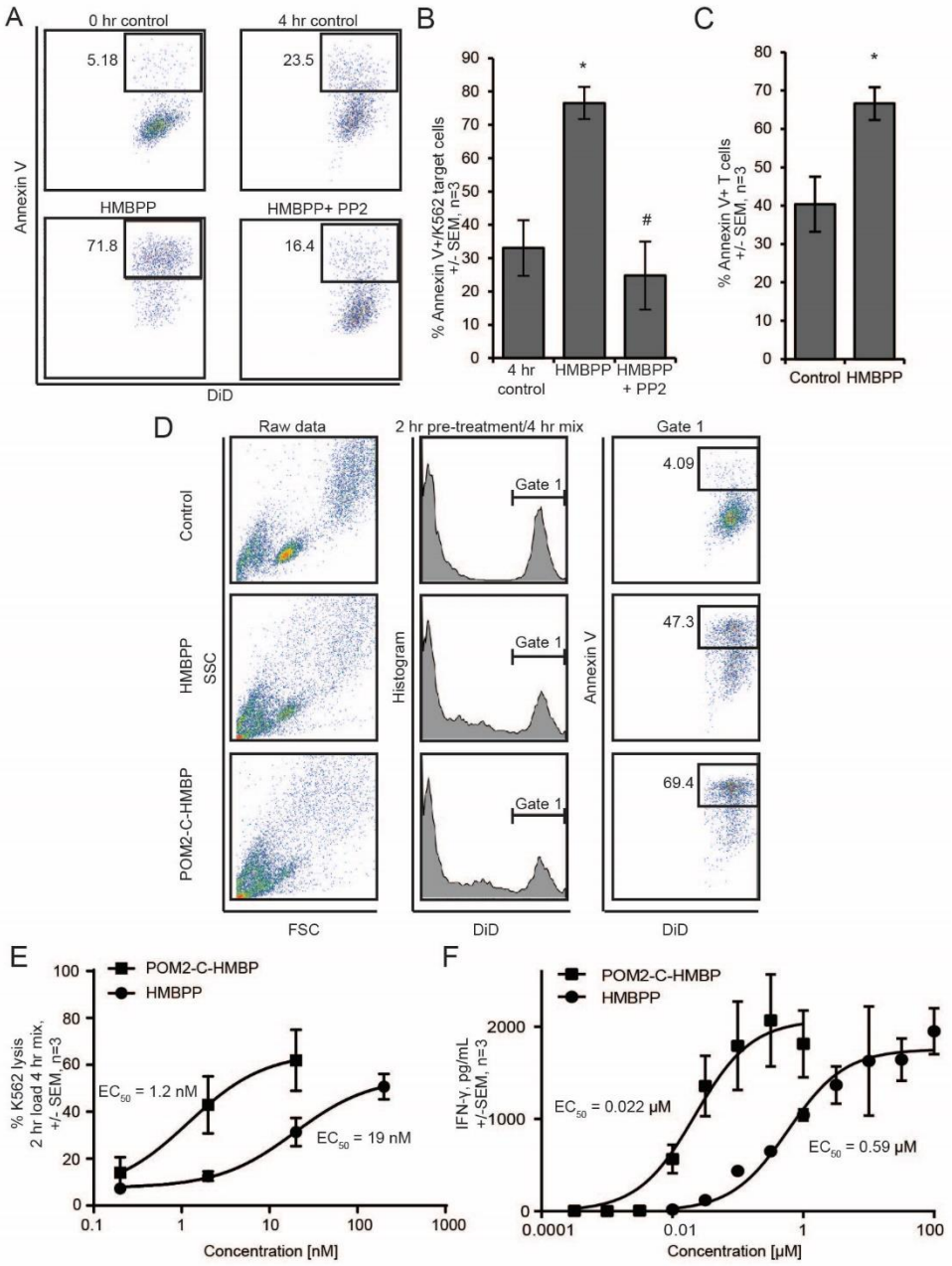

Figure 19. Target cell lysis by Vγ9Vδ2 effector T cells requires activity of Src kinases and is enhanced by POM$_2$-C-HMBP during short-term pretreatment.

A) Target and effectors cells were mixed and simultaneously exposed to 100 nM HMBPP with or without 10 µM PP2 for four hours. B) Quantification of panel A. C) Effector T cells demonstrate autolysis in the continued presence of HMBPP. D) K562 cell population gating scheme for 2-hour pretreatment of K562 cells with phosphorus compounds (100 nM), followed by 4-hour incubation with effector cells. E) Dose-response quantification of 2-hour pretreatment lysis assays for both HMBPP and POM$_2$-C-HMBP with EC_{50} values. F) Dose-response quantification of IFN-γ

secretion following a 2-hour phosphorus compound pretreatment and 24-hour incubation with effector cells. Flow plots are representative of greater than three independent experiments. * significantly different from control; # significantly different from treatment.

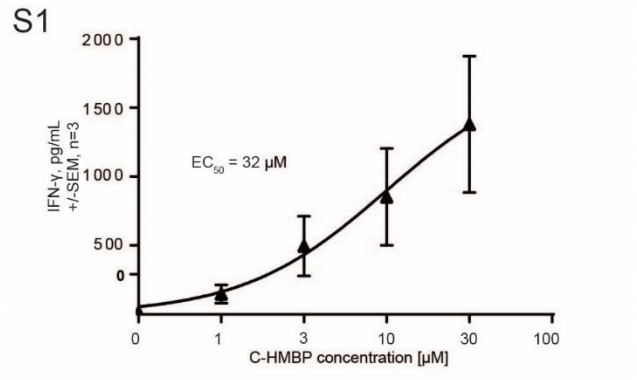

Figure 20. IFN-γ secretion induced by C-HMBP.

Quantification of IFN-γ following 2-hour C-HMBP pretreatment and 24-hour incubation with effector γδ cells.

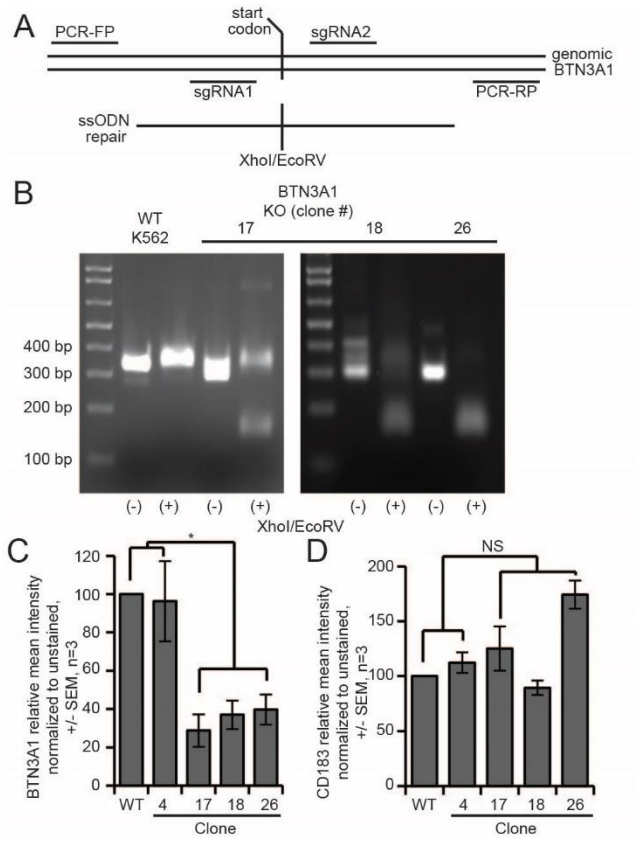

Figure 21. Disruption of BTN3A1 expression in target cells.

A) Schematic of design for knockout utilizing CRISPR/Cas9. The start codon was excised from genomic DNA using paired single strand breaks and replaced with a dual restriction site using an ssODN repair template to facilitate genotyping of clones. B) PCR genotyping of wild-type K562 cells and three BTN3A1 CRISPR/Cas9 knockout clones that displayed the desired genotype. C) Quantification of BTN3A1 surface expression in WT, clone 4 and three BTN3A1 CRISPR/Cas9 knockout clones, as analyzed by flow cytometry. D) Quantification of surface expression of CD183 in WT, clone 4 and three BTN3A1 CRISPR/Cas9 knockout clones, as analyzed by flow cytometry.

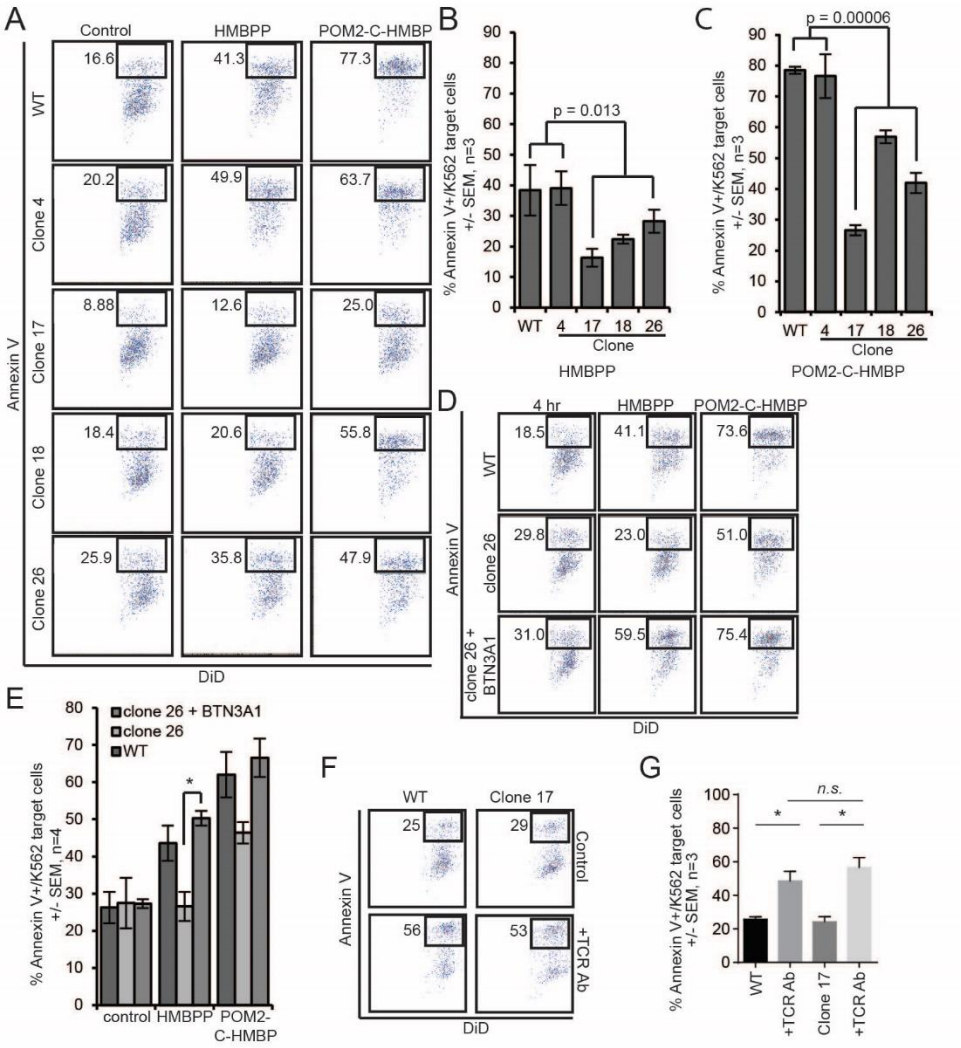

Figure 22. Disruption of BTN3A1 expression in target cells reduces their lysis by Vγ9Vδ2 effector T cells in response to direct-acing ligands.

A) Lysis assay results of WT, BTN3A1 WT clone 4, and BTN3A1-deficient clones 17, 18, and 26. K562 cells were preloaded for 2 hours with 100 nM HMBPP or 100 nM POM2-C-HMBP. B and C) Quantification of lysis assays shown in panel A. D) Lysis assay results of WT, clone 26, and clone 26 + BTN3A1 K562 cells pretreated for 2 hours with 100 nM test compound at 37ºC followed by a 4 hour coincubation with effector cells. E) Quantification of lysis assay described in D, where there is a significant rescue of lysis in clone 26 when expressing myc-tagged BTN3A1. F) Flow diagrams of K562 cell lysis induced by pretreatment of T effector cells with TCR antibody. G) Quantification of panel F. Flow plots are representative of greater than three independent experiments. ***** significance between treatments or groups identified.

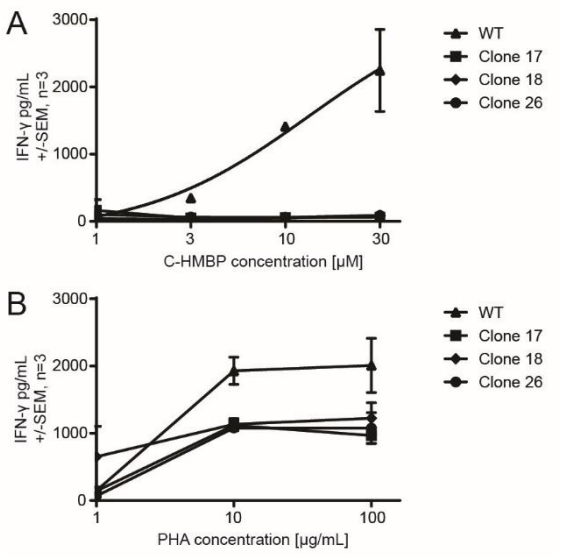

Figure 23. IFNγ secretion induced by C-HMBP is abrogated by depletion of BTN3A1.

WT K562 cells or BTN3A1 deficient K562 clones 17, 18 and 26 were preloaded for 2 hours with the indicated concentrations of C-HMBP (Panel A) or PHA-P (Panel B). Loaded cells were washed and exposed to effector Vγ9Vδ2 T cells for 24 hours, then IFN-γ was determined by ELISA.

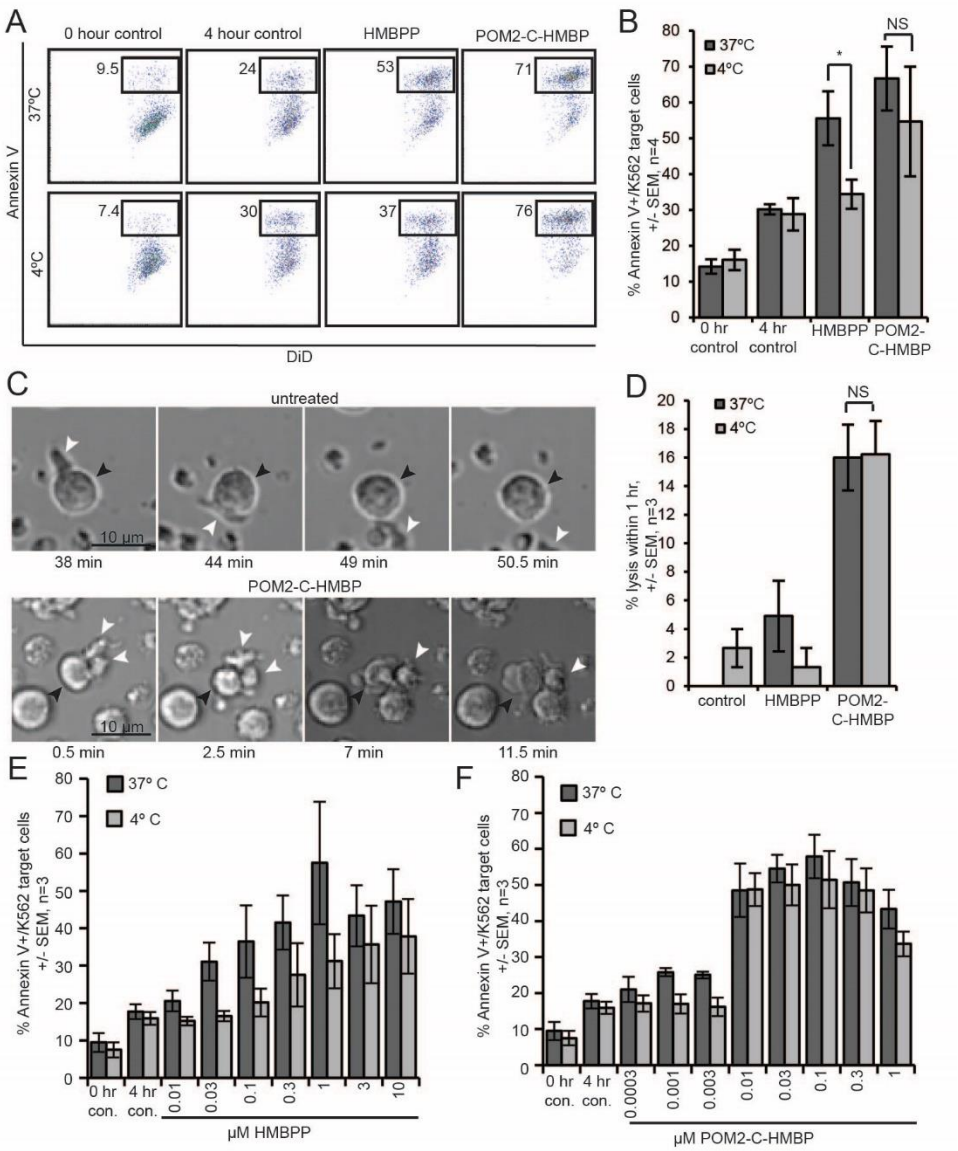

Figure 24. HMBPP, but not POM2-C-HMBP, uses energy dependent uptake to enter target cells.

A) Flow cytometry plots of lysis assays where K562 cells were pretreated with test compound (100 nM) for 2 hours at either 37 ºC or 4 ºC, followed by 4-hour incubation with effector cells. B) Quantification of lysis assays described in panel A. Percent lysis was found by the percentage of Annexin V/K562 target cells for each of the treatments, 0-hour control, 4-hour control, 100 nM HMBPP, and 100 nM POM_2-C-HMBP at both 37ºC and 4ºC. C) Live imaging of K562 cells untreated or pretreated with 100 nM POM_2-C-HMBP at 37ºC. White arrowheads indicate effector Vγ9Vδ2 T cells; black arrow heads indicate target K562 cells. D) Quantification of imaging analysis, percent lysis was determined by the number of cells lysed within 1 hour, divided by the total number of K562 cells in the visual field multiplied by 100. E) HMBPP dose-response lysis assay at 37ºC and 4ºC. F) POM_2-C-HMBP dose response lysis assay at 37ºC and 4ºC. Flow plots

are representative of greater than three independent experiments. ***** significance between treatments or groups identified.

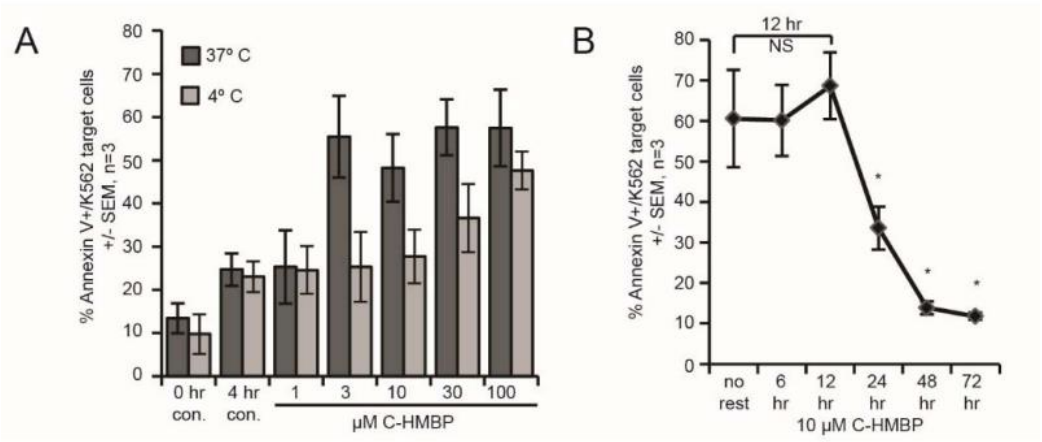

Figure 25. Lysis assays with C-HMBP.

A) C-HMBP requires energy dependent uptake to enter target cells. C-HMBP dose response lysis assay at 37ºC and 4ºC. B) Metabolism of C-HMBP. Time course lysis assay of K562 cells pre-treated for 2 hours with 10 µM C-HMBP. K562 cells were rested for 0 hours (no rest), 6 hours, 12 hours, 24 hours, 48 hours or 72 hours. Once rested, cells were incubated with effector cells for 4 hours. *, significant compared to no rest.

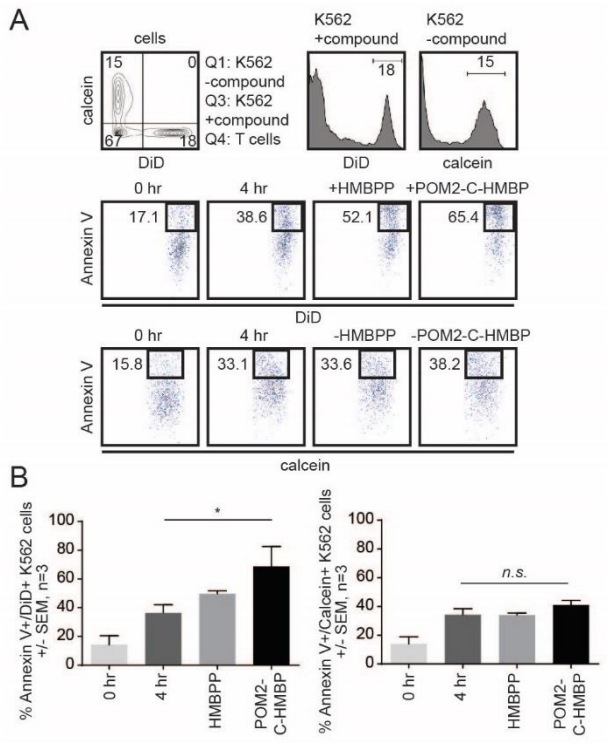

Figure 26. Vγ9Vδ2 T cells specifically target cells containing phosphorus compounds.

A) Cells were stained with either DiD or calcein. DiD+ cells were pre-treated for 2 hours with HMBPP (100 nM) or POM_2-C-HMBP (100 nM), then mixed with effector cells for 4 hours. B) Quantification of panel A. Flow plots are representative of three independent experiments. ***** significance of treatments or groups identified compared to control.

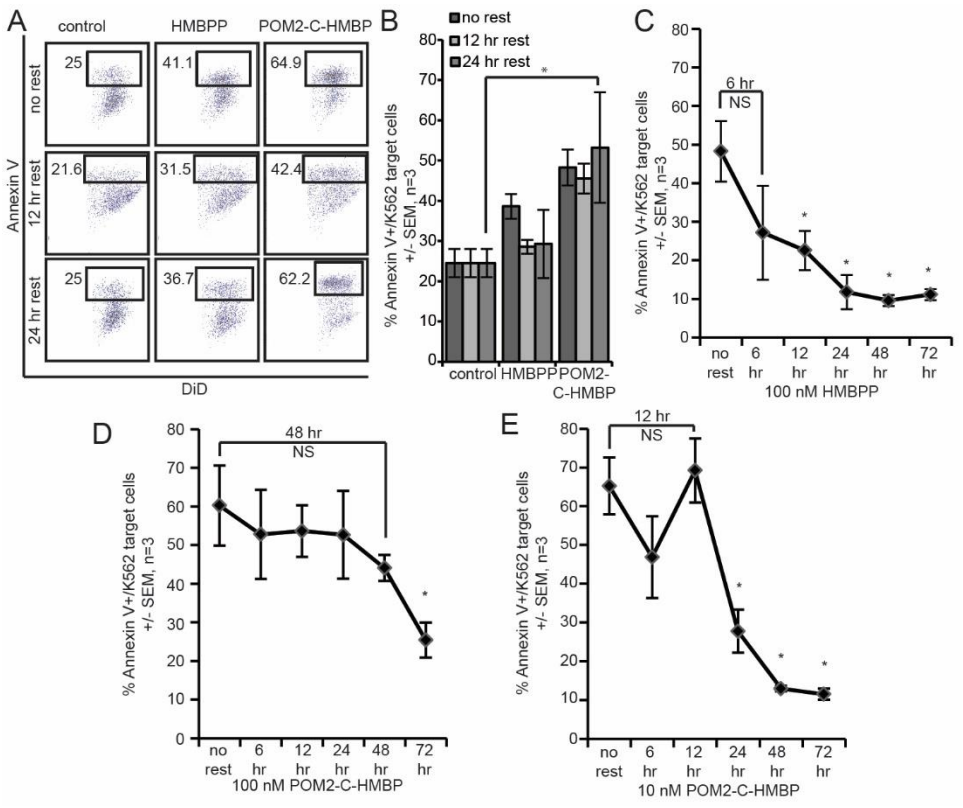

Figure 27. HMBPP, but not POM2-C-HMBP, is rapidly metabolized.

A) Flow cytometry data of lysis assays where K562 cells were pretreated with compound (100 nM) for 2 hours at 37 ºC, followed by a 0- (no rest), 12- or 24- hour resting period. Once rested, cells were incubated with effector cells for 4 hours. B) Quantification of lysis assay described in panel A. *****, significance between treatments or groups identified. C) Time-course lysis assay of K562 cells pretreated for 2 hours with 100 nM HMBPP. K562 cells were rested for 0 (no rest), 6, 12, 24, 48, or 72 hours. Once rested, cells were incubated with effector cells for 4 hours. ***** significant compared to no rest. D) Time-course lysis assay of K562 cells pre-treated for 2 hours with 100 nM POM_2-C-HMBP, as described in C. ***** significant compared to no rest. E) Time-course lysis assay of K562 cells pre-treated for 2 hours with 10 nM POM_2-C-HMBP, as described in C. ***** significant compared to no rest. Flow plots are representative of greater than three independent experiments.

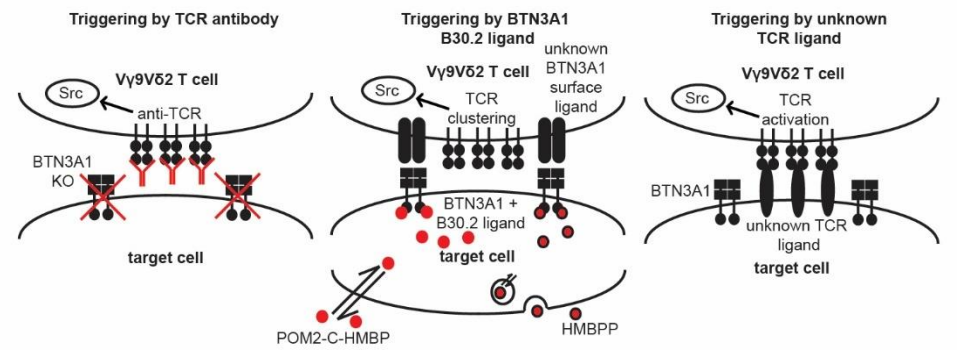

Figure 28. Hypothetical models of BTN3A1-mediated T cell activation.

Phosphoantigens such as HMBPP are internalized by an energy-dependent process, which can be bypassed by POM_2-C-HMBP. Both BTN3A1 and the Vγ9Vδ2 TCR are required for T cell activation in response to these phosphoantigens. It is unknown how BTN3A1 activation may trigger a T cell response but this could occur either through direct TCR engagement or a costimulatory process.

CHAPTER V

ANALYSIS OF HYDROXYL MODIFIED HMBPP ANALOGS ON THE STIMULATION AND ACTIVATION OF Vγ9Vδ2 T CELLS

Abstract

Cells containing small, charge-negative phosphorous compounds known as phosphoantigens are recognized by Vγ9Vδ2 T cells. This recognition results in the stimulation and/or activation of these cells, leading to proliferation of Vγ9Vδ2 T cells or lysis of target cells. Previously, we have analyzed the molecule bis (pivaloyloxymethyl) (E)-4-hydroxy-3-methyl-but-2-enyl phosphonate (POM_2-C-HMBP), an analog of the naturally occurring phosphoantigen (E)-4-hydroxy-3-methyl-but-2-enyl diphosphate (HMBPP). Using both POM_2-C-HMBP and HMBPP, we have shown that POM_2-C-HMBP functions as an active phosphoantigen with greater potency and a longer period of activation, in comparison to HMBPP. Here, we have tested several novel HMBPP analogs with modifications to the allylic hydroxyl group, an area in which modifications have only now been investigated. We have compared the effects of these new compounds on proliferation of Vγ9Vδ2 T cells and lysis of target cells to those of POM_2-C-HMBP and HMBPP. We show that some compounds in which the hydroxyl group is modified stimulate proliferation of Vγ9Vδ2 T cells and Vγ9Vδ2 T cell mediated lysis with nanomolar potency. This demonstrates an opportunity for future phosphoantigen prodrugs to be modified in this location.

Introduction

It is estimated that about 36 percent of people will be diagnosed with cancer at some point in their life (National Cancer Institute). It is one of the most common diseases in the world and the discovery and development of new treatments and cures are imperative. Searching for a treatment with few or no side effects is crucial, as a majority of currently used treatments have devastating

side effects. Currently, the most common treatments for cancer are surgery, and chemo- and radiation-therapies. However, more recently there has been an increase in immunotherapy, where the patient's immune system is utilized to fight the cancer. Here, we present new compounds that will work as immunotherapeutics to stimulate and activate a specific type of T cell, the Vγ9Vδ2 T cells.

γδ T cells make up 1-15% of peripheral blood lymphocytes in humans [104], of which the specific subset of Vγ9Vδ2 T cells is even smaller. Though few in number, these cells are essential for helping the human body fight off microbial infections as well as some cancerous cells [23, 32]. Vγ9Vδ2 T cells recognize and kill target cells containing compounds known as phosphoantigens. Phosphoantigens are naturally occurring products of the mevalonate pathway, and have a multitude of different ways by which they can exist within the target cell. They can be present natively within the target cell (in the case of mammalian IPP), they can be present due to microbial infections (in the case of microbial HMBPP), they can be upregulated by bisphosphonate drugs, such as zoledronate, and lastly they can be administered and taken up into the cell via endocytosis or in prodrug form [75].

These phosphorus containing molecules have the capacity to activate Vγ9Vδ2 T cells by binding to the intracellular B30.2 region of the protein butyrophilin subfamily 3 member A1 (BTN3A1) within the target cell [36, 51]. However, which structural components of the molecule are actually required for the binding of the phosphoantigen to BTN3A1 is still unknown. HMBPP, a phosphoantigen produced by microorganisms, and IPP, a phosphoantigen produced by mammalian cells, are both naturally occurring and are diphosphate molecules. Recently, we and others have shown that phosphonate molecules can activate Vγ9Vδ2 T cells with similar efficacy [51, 59, 75].

Throughout this document, we have investigated a series of novel phosphoantigen compounds, some acting as Vγ9Vδ2 T cell activators better than others. It is important to identify modifications to these HMBPP analogs that result in more a more potent EC_{50} in expansion and Vγ9Vδ2 T cell induced lysis. Cell permeability of these compounds appears to be of great importance, but other variables to consider include cellular/extracellular metabolism as well as phosphorylation.

In this chapter, we describe the phosphoantigenic activity of several novel compounds. We also investigated the effects of these compounds on target cell viability, allowing us to identify drugs that may or may not be toxic to K562 (human myeloid leukemia) cells in addition to their activity as phosphoantigens. Together these results allow us to identify some structural components which allow phosphoantigens to function, while other functional groups inhibit phosphoantigen function. By determining these features, it brings us closer to designing phosphoantigens that stimulate and activate Vγ9Vδ2 T cells while also avoiding the drastic side effects of current chemotherapy drugs.

Materials and Methods

Reagents and supplies

RPMI-1640, FBS, NEAA, pyruvate, penicillin streptomycin, HEPES, BME, HMBPP and FITC-γδ TCR antibody (clone 5A6.E91) were obtained through Fisher Scientific. IL-2 and the MACS γδ T cell negative selection kit was obtained through Miltenyi. K562 cells were from ATCC while Research Blood Components (Boston, MA) supplied blood. CytoTox 96 ® Non-Radioactive Cytotoxicity Assay was obtained through Promega. CellQuantiBlue was obtained from BioAssay Systems.

Vγ9Vδ2 T cell expansion and purification

Human PBMCs from healthy anonymous donors were isolated from heparinized blood using Lymphoprep (Axis-Shield) within 24 hours of collection. Cells were counted by hemocytometer in the presence of trypan blue then aliquoted in freezing media (10% DMSO, 20% FBS, 70% media) and stored in liquid nitrogen. PBMC were resuspended at 1×10^6 cells/mL in fresh T cell media (RPMI-1640, 10% heat-inactivated FBS, 1x HEPES, pyruvate, NEAA, and BME). Cells were stimulated with 0.01 μM HMBPP or 0.01 μM POM_2-C-HMBP for 3 days and cultured for another 4-18 days after compound removal. Fresh IL-2 (5 ng/mL) was provided every 3 days. After 7-21 days, Vγ9Vδ2 T cells were purified by negative selection. Experiments were performed at least three times using at least two donors.

K562 cell culture

K562 cells were cultured in RPMI-1640, 10% Fetal Clone III Serum (Hyclone) and 1% penicillin streptomycin and maintained between 0.2 and 1 x 10^6 cells per mL.

Cytotoxicity/proliferation assay

Isolated Vγ9Vδ2 T cells or K562 cells were split to $5x10^4$ cells/mL. 100 μL of cells were added to each well in a 96 well plate. Cells were then treated with the compounds described in text for 72 hours. After 72 hours 10 μL CellQuanti-Blue reagent was added to each well and incubated for 2 hours at 37˚C at which point plates were read using a VICTOR plate reader. Analysis was done using GraphPad Prism.

Lysis assay

K562 cells were treated as described in text in T cell media. K562 cells were mixed with T cells at an effector: target ratio of 3:1 in a total of 200 μL. Plate was spun for 3 minutes at 600 rcf. Mixtures were then incubated for 4 hours at 37 ºC. Plate was spun again for 3 minutes at 600

rcf. 50 µL of supernatant from each well was placed in a new flat bottom 96 well plate. 50 µL of the reconstituted substrate mix from CytoTox 96 assay was added to each well and incubated in the dark for 30 minutes. 50 µL of CytoTox 96 stop solution was added to all wells. Plate was read immediately after at 490 nm on VICTOR plate reader to determine lysis of target cells.

Statistical Analysis

One-way ANOVA was used to calculate significance. Comparisons were done relative to the control or between pairs of conditions. Columns in bar graphs represent the mean ± SEM. An α level of 0.05 was used.

Results

Synthetic phosphoantigens successfully stimulate Vγ9Vδ2 T cells to proliferate.

One of the first responses of a stimulated Vγ9Vδ2 T cell is proliferation. Upon synapse formation with target cells containing phosphoantigens, the Vγ9Vδ2 T cell will begin to proliferate and differentiate into an effector Vγ9Vδ2 T cell. Here, we tested the ability of our novel compounds (Figure 29) to induce proliferation in Vγ9Vδ2 T cells by treating hPBMCs with each compound for 3 days. After 3 days, the compounds were washed off and cells were left to proliferate for a total of 14 days, receiving a treatment of IL-2 every 3 days. After 2 weeks, the resulting cells were analyzed by flow cytometry, specifically looking for γδ T cells, which would be both γδ TCR and CD3 positive (Figure 30A). From this data, a dose response curve was produced for each compound (Figure 30B), where compounds **15**, **16** and **14** were most active with EC_{50} values of 4.6, 34 and 4.7 nM respectively (Table 4).

Synthetic phosphoantigens activate Vγ9Vδ2 T cells to target and lyse target cells.

When Vγ9Vδ2 T cells have been stimulated to proliferate, they also begin differentiating. These differentiated T cells can then be further activated by cells containing phosphoantigens to

react with an assortment of other Vγ9Vδ2 T cell responses. One such response in the ability of Vγ9Vδ2 T cells to recognize and lyse these phosphoantigen containing cells. We wanted to test the ability of our novel phosphoantigens to activate Vγ9Vδ2 T cells to lyse target K562 cells. Here, we pre-treated K562 cells with several doses of each compound for 2 hours. Pretreated K562 cells were mixed with Vγ9Vδ2 T cells for 24 hours at which point a Cyto Tox 96 assay was performed to determine lysis of target cells (Figure 31). Compounds **15**, **16** and **14** showed the most activity with EC_{50} values of 12, 15 and 3.9 nM respectively (Table 5). However, compounds **11** and **12** also showed some activity with EC_{50} values of 1.0 and 1.7 μM respectively, while both compounds **10** and **13** appeared to be inactive in this assay (Table 5).

*Compounds **15** and **16** show cytotoxicity of K562 cells at high concentrations.*

As previously discussed, we determined the ability of our synthetic phosphoantigens to stimulate Vγ9Vδ2 T cells to expand and differentiate into effector Vγ9Vδ2 T cells, we also investigated the ability of these phosphoantigens to activate Vγ9Vδ2 T cells to lyse and kill target cells; however, it is imperative that we also investigate the cytotoxicity of these compounds on target cells which we have previously treated. We investigated this by running a CellQuanti-Blue assay after treating K562 cells with various concentrations of each compound for 72 hours. The only compounds to show cytotoxicity were **15** and **16**, which showed cytotoxicity, but only at the highest concentration of 100 μM (Figure 32).

Discussion

These studies have allowed us to investigate the structural components of active phosphoantigens in the activation in Vγ9Vδ2 T cells more thoroughly. By testing novel HMBPP analogs, we have found that modifying these phosphoantigens at the allylic hydroxyl group, can still produce active phosphoantigens. This is important, as the interaction of the active

phosphoantigen and the B30.2 domain binding pocket may be limited. The binding pocket of BTN3A1 only allow for specific molecules, by altering these phosphoantigens at the hydroxyl group, we were able to show that this modification still allows for phosphoantigen binding and ultimately activation of the Vγ9Vδ2 T cell.

In these studies, the HMBPP analogs modified at the epsilon hydroxyl group were also synthesized as prodrugs by the addition of a protecting MOCCA group or one/two protecting POM groups at the phosphoester position. If the future of these drugs is in cancer immunotherapy, it is advantageous to synthesize them in prodrug form. These protecting groups help to make the phosphoantigen more cell permeable, and will ultimately help in the design of a cell specific phosphoantigen prodrug. Once the prodrug is metabolized into an active phosphoantigen, the phosphoantigen gains a negative charge, ultimately helping to keep the drug inside the cell [62, 105].

All 3 of these compounds, compounds **14**, **15**, and **16** were found to be promising phosphoantigen prodrugs in these studies. Each of them showed successful expansion of Vγ9Vδ2 T cells, as well as the ability to stimulate Vγ9Vδ2 T cells to lyse phosphoantigen treated target cells. In order to investigate the effects of these phosphoantigen prodrugs as potential cancer immunotherapeutics, it is important to determine if they will be able to expand Vγ9Vδ2 T cells inside the body. The next step is to continue these studies *in vivo*, chapter VI investigates compound **15** and others in *in vivo* mouse studies.

Compound	EC_{50} (μM)
10	Inactive
11	Inactive
12	~10.
13	Inactive
14	0.0047
15	0.0046
16	0.034

Table 4. Vγ9Vδ2 T cell expansion EC_{50} values of phosphoantigen compounds.

Compound	EC_{50} (μM)
10	23
11	1.0
12	1.6
13	Inactive
14	0.0039
15	0.0012
16	0.015

Table 5. Lysis assay EC_{50} values of phosphoantigen compounds.

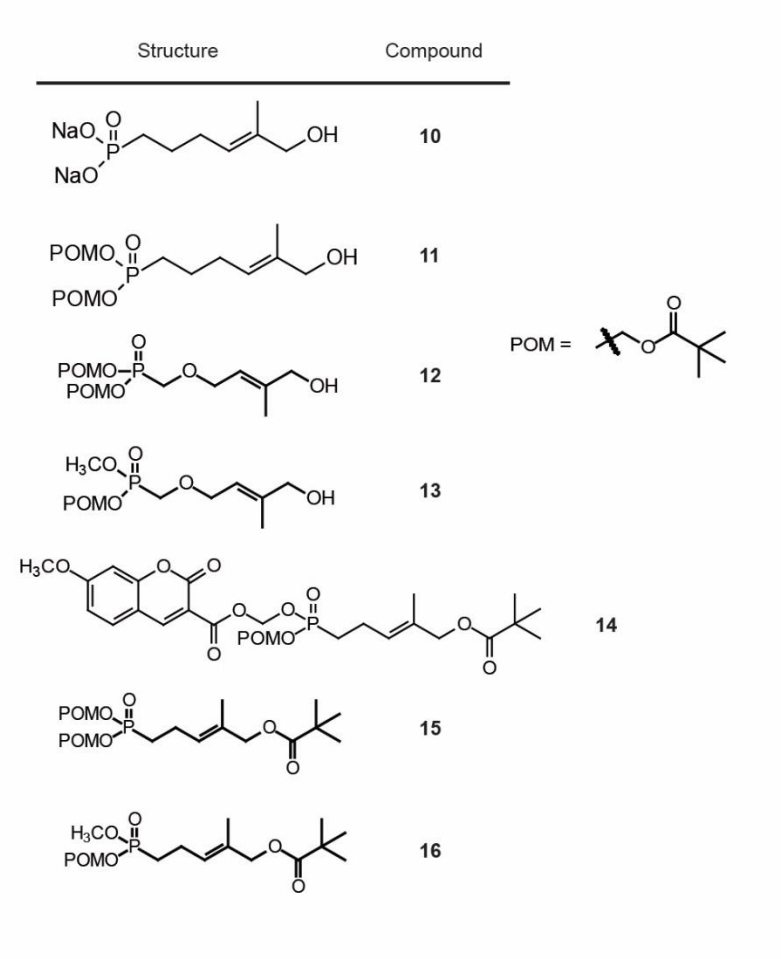

Figure 29. Structures of compounds 10, 11, 12, 13, 14, 15, and 16.

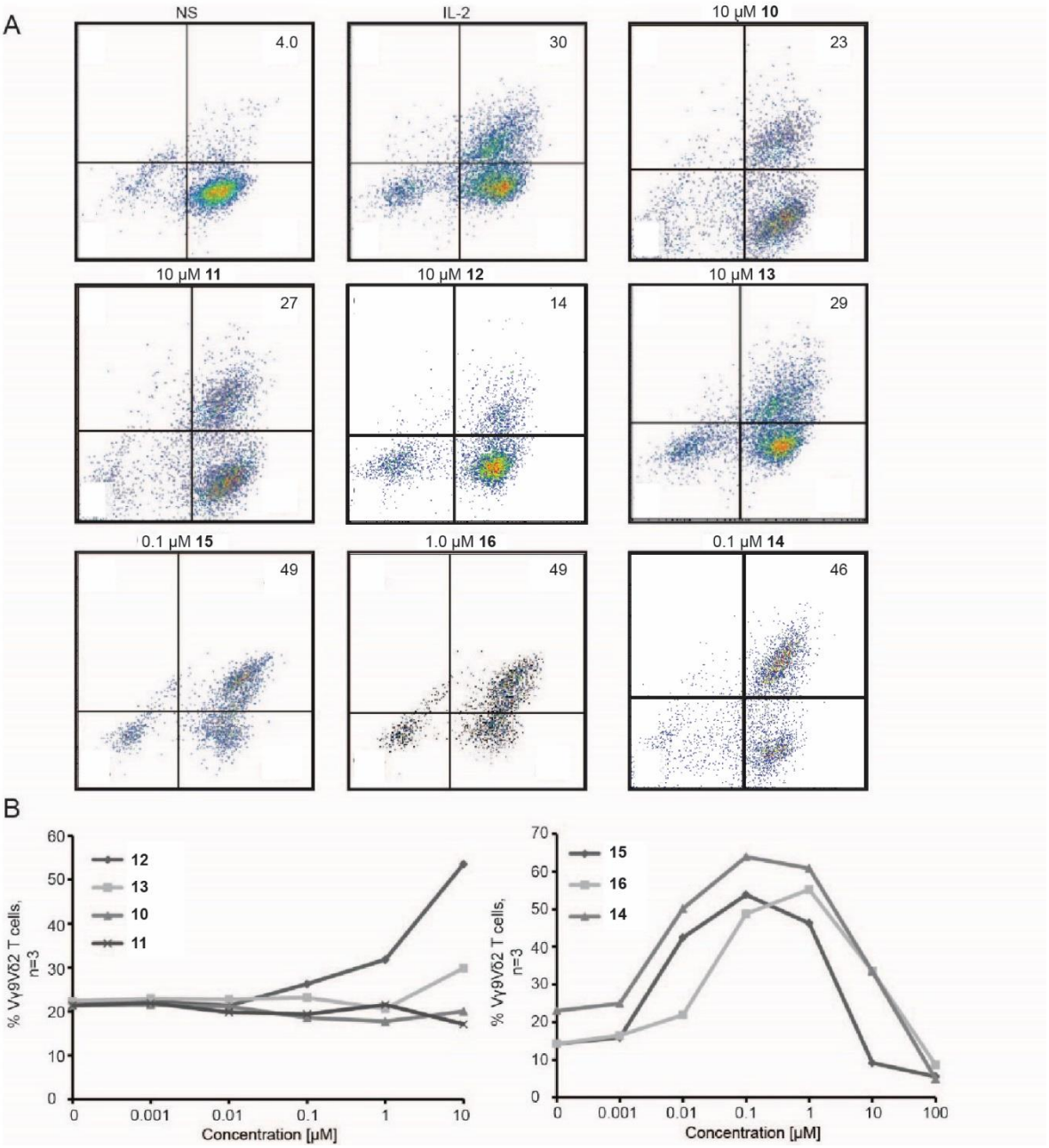

Figure 30. Synthetic phosphoantigens successfully stimulate Vγ9Vδ2 T cells to proliferate.

A) Flow data of 14-day expansion of hPBMCs after 72-hour treatment with synthetic phosphoantigens, percentage Vγ9Vδ2 T cells seen in quadrant I. B) Quantification of panel A). Flow plots are representative of greater than three independent experiments. n=3

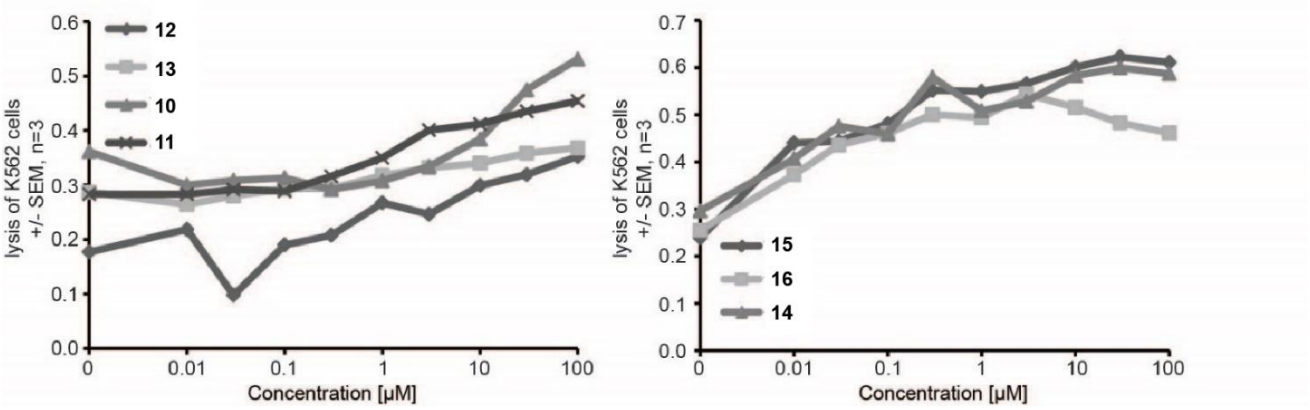

Figure 31. Synthetic phosphoantigens activate Vγ9Vδ2 T cells to target and lyse target cells.

Dose-response quantification of 2-hour pretreatment Cyto Tox 96 lysis assays for compounds **10**-**16**. K562 cells were mixed with expanded Vγ9Vδ2 T cells for 24 hours at 37º C. n=3.

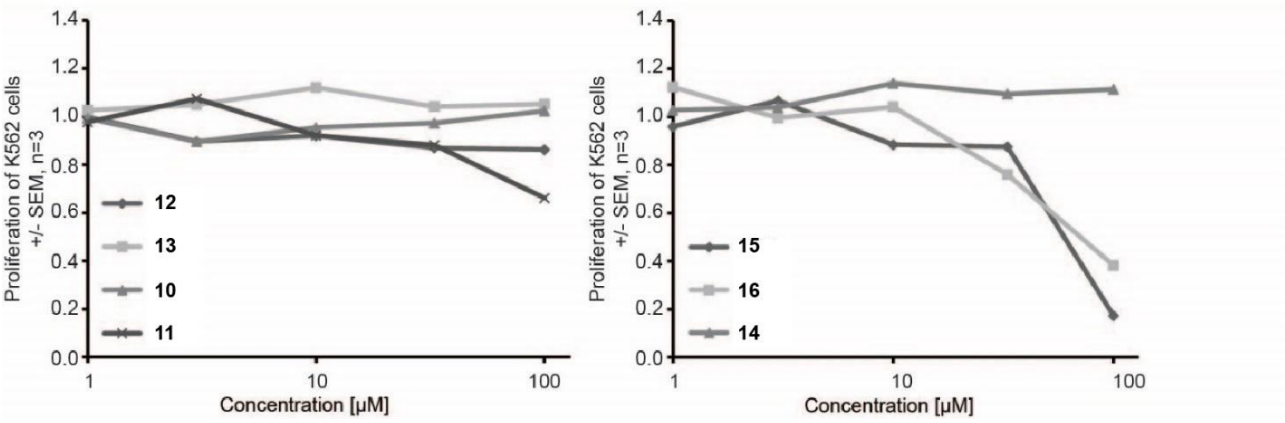

Figure 32. Compounds 15 and 16 show cytotoxicity of K562 cells at high concentrations.

Dose-response quantification for cytotoxicity/cellular metabolism using CellQuanti-Blue for compounds **10**-**16**. K562 cells treated with phosphoantigens for 72 hours at 37º C. n=3.

CHAPTER VI

EVALUATION OF NOVEL PHOSPHOANTIGENS *IN VIVO*

Introduction

Cancer is a leading cause of death around the world, and its incidence is rising, with an estimated 14 million new cases every year. These statistics are expected to increase to 22 million new cases per year within the next 20 years (National Cancer Institute). It is thereby imperative for scientists to explore and discover new and effective treatments.

Among the most promising of cancer treatments is cancer immunotherapy, where the patient's immune system is stimulated to produce an immune response in order to treat the cancer. Over the past 15 years, Vγ9Vδ2 T cells have been increasingly studied in the field of cancer immunotherapy [32, 106-111]. There are two main categories of Vγ9Vδ2 T cell immunotherapy investigated thus far: *in vivo* stimulation of Vγ9Vδ2 T cells, in which the cells of the patient are stimulated without removal from the patient, or *ex vivo* stimulation of Vγ9Vδ2 T cells, in which the Vγ9Vδ2 T cells are removed and expanded outside the patient and ultimately returned to the patient's circulation.

Research investigating the *in vivo* stimulation of Vγ9Vδ2 T cells most notably uses FDA approved aminobisphosphonates to increase amount of naturally occurring IPP within the cell, ultimately leading to an increase in the number and activity of Vγ9Vδ2 T cells Although these aminobisphosphonates were not FDA approved for Vγ9Vδ2 T cell immunotherapy, this use was discovered as a side effect to the original use: treatment of osteoporosis, rheumatoid arthritis, and cancer metastasis [33]. Once it was discovered that these aminobisphosphonates were able to expand Vγ9Vδ2 T cells *in vivo*, this strategy for Vγ9Vδ2 T cell immunotherapy became increasingly well studied. Many groups have used aminobisphosphonates and IL-2 together in

treating lymphoma and myeloma [108], acute myeloid leukemia [112], renal cell cancer [112, 113], prostate cancer [34, 114], and breast cancer [34, 115]. *Fewer* studies include novel direct phosphoantigenic compounds although there has been some research on BrHPP. BrHPP, when treated with IL-2 has been investigated in solid tumors of the kidney, colon, esophagus, ovaries, breast, and stomach/intestines [116]. Interestingly, an area of great therapeutic potential resides in the research of phosphoantigen prodrugs, like the ones described throughout chapters 3-5. These prodrugs, and others like them, have yet to be investigated *in vivo*. The phosphoantigens POM_2-C-HMBP, **9, 15, 17**, and **18** were shown to be active in our *ex vivo* experiments using donor human peripheral blood mononuclear cells (hPBMCs) and various blood cancer cell lines. To further investigate their efficacy as potential cancer immunotherapeutics, we have begun testing these compounds *in vivo* in a humanized mouse model.

To test the ability of these novel compounds to stimulate Vγ9Vδ2 T cells *in vivo* we had to determine a model system. Since Vγ9Vδ2 T cells are only found in humans and primates, studies in normal mice are not possible. Preclinical in vivo studies of Vγ9Vδ2 T cells are usually conducted in either primates or humanized mice. As testing in primates is beyond our ability, we focused our studies on developing a humanized mouse model to do *in vivo* testing. Here, we produced a humanized mouse model utilizing recombination activating gene 2 (RAG-2) deficient mice, liposomal clodronate, and hPBMCs. We have also show that the novel compounds POM_2-C-HMBP, **9**, **15**, **17**, and **18** show minimal toxicity when injected subcutaneously at doses below 10 mg/kg.

Materials and Methods

Reagents

RPMI-1640, FBS, nonessential amino acids, pyruvate, penicillin streptomycin, HEPES, BME, Bovine serum albumin (BSA), 10% neutral buffered formalin solution, and FITC-γδ TCR antibody (clone 5A6.E91) were obtained through Fisher Scientific and PE-CD3 (UCHT1) was from eBioscience. APC-CD68 (clone FA-11) was from Biolegend and Isothesia isoflurane was obtained through Henry Schein. Blood was obtained through Research Blood Components (Boston, MA) and liposomal clodronate was obtained through Encapsula NanoSciences. POM_2-C-HMBP, compounds **9**, **15**, **17**, and **18** were kind gifts of Dr. David Wiemer at the University of Iowa.

Mice

Homozygous RAG-2 and IL-2 deficient mice, strain C;129S4-Rag2tm1.1Flv Il2rgtm1.1Flv/J, were distributed by Jackson Labs (Mount Desert Island, ME). Mice were housed in the University of Connecticut Animal Care Services facility under IACUC protocol A16-020. Breeding pairs were set up between 6 and 12 weeks of age and were allowed to continue to breed until approximately 6 months of age. Litters were weaned at approximately 21 days and separated into new cages by sex, with no more than 5 animals per cage.

Subcutaneous injections of novel phosphoantigen compounds

Novel phosphoantigen compounds were prepared at a concentration of 1 mg/kg and 10 mg/kg. For each phosphoantigen: one mouse was first injected with the 1 mg/kg dose subcutaneously by scruffing the mouse behind the ears and legs and injected behind the head at the scruff site. Mouse was observed over the course of two days, if no observable changes occurred, i.e. lesion of the injection site, lethargy, loss of fur or whiskers, increased anxiety, or

death, then another injection of the same dose was administered. At the time of the second dose, a second animal was injected at low dose, in the same manner as described above. Provided both mice looked healthy after initial injections of the low dose, and remained healthy for following doses, the same procedure was followed for higher dose injections. n=2 for each dose of each compound.

Tissue harvest and fixation

Mice injected with phosphoantigen compounds were sacrificed after injections were completed. Kidney, liver, and spleen were isolated from each mouse treated with the 10 mg/kg doses. These tissues were then fixed in 10% neutral buffered formalin solution, at a ratio of 10 mL per 1 gram tissue. Tissues were then placed at 4º C until toxicology studies could be performed.

Liposomal clodronate injections

Liposomal clodronate was acquired through Encapsula NanoSciences and administered intravenously (IV) via retroorbital injection (RO). Mice were anesthetized using isoflurane and 150 µL of clodrosome was injected per 25 g mouse. After 24 hours, mice were either sacrificed and splenocytes were harvested, or mice were injected with human peripheral blood mononuclear cells (PBMCs) as described below. If PBMCs were injected, mice were sacrificed 48 hours after injection of clodrosome and splenocytes were harvested directly after.

Human PBMC isolation

Blood was obtained from healthy anonymous donors through Research Blood Components. Within 24 hours of collection, Lymphoprep (Axis-Shield) was used to isolate human PBMCs (hPBMCs) from heparinized blood. Cells were aliquoted in freezing media (10% DMSO, 20% FBS, 70% media) and stored in liquid nitrogen.

hPBMC injections

Approximately 30 million hPBMCs (per mouse) were thawed in fresh T cell media (RPMI 1640, 10% heat-inactivated FBS, 1x HEPES, pyruvate, nonessential amino acids, and BME), washed with phosphate-buffered saline (PBS) and resuspended in 150 µL PBS. This 150 µL was aspirated into a 1 mL syringe with a 27-gauge needle. Mice were anesthetized using isoflurane and hPBMCs were injected via RO injection. Assuming an approximate 50 µL dead space, approximately 100 µL was injected per mouse, for a total of 20 million cells per mouse.

Harvest of splenocytes and cell staining

Mice were sacrificed using carbon dioxide followed by confirmation by cervical dislocation. Once sacrificed, the spleen of the mouse was removed and placed into 500 µL T cell media on ice. Splenocytes were isolated by homogenization using 40 µm nylon cell strainers and T cell media. Once collected, splenocytes were counted, then washed with FACS buffer (2% BSA in PBS), resuspended in FACS buffer and placed on ice. Cells were then stained with anti-mouse CD69, anti-human CD3, and/or anti-human γδ TCR antibodies, 3 µL antibody per 100 µL cells in FACs buffer. Cells were placed at 4º C for 30 minutes, washed twice with FACS buffer and resuspended in 400 µL FACS buffer. 75 µL 16% paraformaldehyde (PFA) was added to fix cells. Cells were analyzed by flow cytometry using a BD Fortessa.

Results

POM_2-C-HMBP is non-toxic in vivo upon repeated doses of 10 mg/kg

The novel phosphoantigen prodrug, POM_2-C-HMBP, has been tested thoroughly as seen in Hsiao et al [51], and here in chapter IV [75]. It has been shown to have great potency and stimulates and activates Vγ9Vδ2 T cells to proliferate, produce cytokines and lyse target cells. As such, this compound was first to test *in vivo*.

The mouse line we would be using as our humanized mouse model was used to first test the effects of POM_2-C-HMBP *in vivo*. One mouse was treated at a dosage of 1 mg compound per 1 kg mouse. This dose was repeated in a second mouse and a third and fourth mouse were treated with a dose of 10 mg/kg. Each mouse underwent a series of injections 3 times per week, for a total of 3 weeks, as shown in Figure 33. All mice survived the treatments to completion and no significant change in weight was found as compared to control mice injected with PBS (Figure 34). Throughout the mouse treatments, mice were monitored for any other changes aside from weight. These included lesions, specifically at the injection site, lethargy, and anxiety. Throughout the study, no changes in those listed were observed in any of the mice treated with POM_2-C-HMBP.

*Compound **4** is not toxic in vivo*

Compounds **4**, **9**, and **17** (Table 6) are expected to be metabolized into the same active phosphoantigen. The ability of compound **4** to function as an active phosphoantigen was characterized in cell culture throughout chapter III. We showed that compound **4** expanded Vγ9Vδ2 T cells with an EC_{50} value of 0.5 μM, and had the ability to activate Vγ9Vδ2 T cells to lyse target cells. We also found that it was non-toxic to several leukemia cell lines. To that end, we found it important to investigate this compound further *in vivo*.

Here, we utilized the same assay as described above and shown in Figure 33. Compound **4** was administered subcutaneously in both low (5 mg/kg) and high doses (10 mg/kg). In animals treated with low doses, we saw a slight increase in weight, although this weight increase wasn't as much as what was seen in control mice, the mice were still gaining weight. Mice treated with high doses of compound **4** saw a decrease in weight (Figure 35). This decrease in weight was not accompanied by any other symptoms such as lethargy, anxiety, or lesions at the injection site. That

being said, it would be interesting to look at the effects of compound **4** on expanding Vγ9Vδ2 T cells *in vivo*.

*Compound **9** is not toxic in vivo*

Throughout chapter III, compound **9** (Table 6) was evaluated for its ability to expand the Vγ9Vδ2 T cell population in hPBMCs, its ability to stimulate lysis of target cells by Vγ9Vδ2 T cells. It proved to be a very promising phosphoantigen prodrug, as it stimulated Vγ9Vδ2 T cells to expand and stimulated lysis by Vγ9Vδ2 T cells, and had an EC_{50} of 18 nM with little to no cellular toxicity. Thus, here we decided to investigate the effects of compound **9** *in vivo*.

Compound **9** was administered subcutaneously in mice as described above and shown in Figure 33. Low doses (5 mg/kg) of compound **9** resulted in a slight increase in weight, this increase was not as much as what was seen in control mice, but importantly, these mice did not lose weight. However, mice treated with the higher dose of compound **9** did show a decrease in weight (Figure 36). All mice survived all nine doses and did not show any other symptoms, i.e. anxiety, lethargy, or lesions. As all mice survived, it would be interesting to further examine the effects of compound **9** on the expansion of Vγ9Vδ2 T cells *in vivo*.

*Compound **15** is not toxic in vivo*

Throughout chapter V compound **15** (Table 6) was analyzed for toxicity in K562 cells as well as the ability to activate Vγ9Vδ2 T cells. Proliferation of K562 cells was not inhibited by compound **15**, except at very high doses, 100 µM and above. When treated with this compound, K562 cells were able to activate Vγ9Vδ2 T cells ultimately leading to the lysis of the K562 cell. As this compound showed great promise as a potential therapeutic phosphoantigen, we wanted to test the toxicity of compound **15** *in vivo*.

Our *in vivo* toxicity screen, as shown in Figure 33, was performed. We found that mice treated with low doses (5 mg/kg) of compound **15** showed similar change in weight as compared to the control mice, however mice treated with the high dose (10 mg/kg) of compound **15** showed a decrease in weight over the course of the treatments (Figure 37). This change in weight did not coincide with any other symptoms that would have been visible, i.e. lethargy, anxiety or lesions at the injection site. All mice survived the duration of all 9 doses. We believe that compound **15** would be a promising compound to use in continuing *in vivo* studies.

*Compound **17** is not toxic in vivo*

Although compound **17** (Table 6) has yet to be fully characterized as an active phosphoantigen in cell culture, its structure predicts that it should be metabolized by cells into the same active phosphoantigen as both compounds **4** and **9** (Table 6). Both compounds have been shown to be active phosphoantigens, where the only difference is their protecting groups, which would ultimately be removed. Although little has been shown, preliminary studies have determined compound **17** does expand Vγ9Vδ2 T cells with an EC_{50} value of approximately 100 nM (data not shown). Here, we have further investigated the toxicity of this compound *in vivo*.

Compound **17** was investigated via our *in vivo* toxicity screen, as described above and in Figure 33. We did not see any major difference in mice treated with low doses (5 mg/kg) of compound **17** when compared to control animals. However, when treated with the higher dose (10 mg/kg) of compound **17**, mice lost weight (Figure 38). This weight loss did not appear to be physically detrimental to the mice, and did not occur alongside any other symptoms such as anxiety, lethargy, or skin lesions. To this extent, it would be worthwhile to further investigate the effects of this compound on *in vivo* expansion of Vγ9Vδ2 T cells.

Development of a humanized mouse model

Vγ9Vδ2 T cells are not produced by mice, meaning we were unable to directly study Vγ9Vδ2 T cells in mice, however we were able to develop a mouse model in which we could inject hPBMCs to humanize the mice. The humanized mouse model we developed was based off previous Vγ9Vδ2 T cell transplant studies which showed successful transfer of Vγ9Vδ2 T cells or hPBMCs into mice [117, 118] or, in one case, stimulation of Vγ9Vδ2 T cells by phosphoantigens in macaques [119]. To do this, we utilized a RAG-2 knockout mouse line. This protein, RAG-2, is essential for VDJ recombination in both T and B cells, when knocked out, the mouse produces neither of these cells, resulting in an immunocompromised mouse. Although the mouse has no B cells or T cells and is immunocompromised, the mouse still produces macrophages, which, unless removed, would kill the human cells we introduce. To address this problem, we treated the mouse intravenously with liposomal clodronate, which would be taken up by macrophages, ultimately killing them within 24 hours. We tested this by IV injecting either PBS or 1 of 2 doses of the liposomal clodronate into mice, 150 µL/25 g mouse and 300 µL/25 g mouse, waiting 24 hours, then harvesting the spleen, isolating splenocytes and staining them for CD68 (Figure 39A). CD68 is a glycoprotein found on macrophages and monocytes, here we used it as a macrophage marker and thus allowed us to compare levels of CD68 in mice treated with 2 doses of liposomal clodronate or PBS. Both doses of liposomal clodronate worked to deplete the macrophage population in the mice (Figure 39B). Killing the host macrophages allowed us to replace the immune system of the mouse with that of a human by injecting human immune cells, specifically hPBMCs.

We next wanted to make sure these hPBMCs were surviving once injected into the host. In order to do this, we wanted to retrieve the injected hPBMCs from the mouse after 24 hours. In

order to do this, we injected 2 mice with liposomal clodronate at a dose of 150 µL/25 g mouse via IV and 2 mice with PBS via IV on day 1 and waited 24 hours. We then injected 2 of our initial 4 mice with approximately 20 million hPBMCs per mouse, one previously treated with PBS and one previously treated with clodrosomes on day 1, via IV on day 2. Day 3 we sacrificed the animals and harvested the spleens. The splenocytes were then stained for CD3, part of the TCR, and γδ TCR (Figure 39C). We expected to see very few, if any γδ TCR positive cells, but since these preliminary experiments will ultimately lead up to the investigation of the expansion of Vγ9Vδ2 T cells *in vivo*, we wanted to set the experiment up as such. We found a small population of CD3 positive cells in mice treated with both liposomal clodronate and hPBMCs that we did not see in mice treated with PBS and hPBMCs (Figure 39D). Based off this data we believe that this model system is working and the lab will continue to the next step of expanding hPBMCs with the novel phosphoantigen compounds **4**, **9**, **15**, and **17** *in vivo*.

Discussion

In this chapter, we have tested several novel phosphoantigen prodrugs for toxicity *in vivo* using mice. The four novel phosphoantigen prodrugs utilized in this study, compounds **4**, **9**, **15**, and **17**, have been shown to expand Vγ9Vδ2 T cells in cell culture from hPBMCs, thus making them good candidates for further testing *in vivo*. Since expansion of Vγ9Vδ2 T cells shows great promise as a method of cancer immunotherapy, it is important to find compounds that can stimulate this expansion both in cell culture and *in vivo*.

To get to the point at which we can begin expanding Vγ9Vδ2 T cells *in vivo*, it is important to test potential compounds for toxicity *in vivo*. It is not uncommon for compounds to be so toxic that when subcutaneously injected, then result in lesions or even death. Here, we found that throughout the 9 treatments at both high and low concentrations, all the mice treated survived.

However, mice treated at higher doses did lose some weight, but were otherwise fine, i.e. no lethargy, visible anxiety, or lesions. Based off this data, it will be interesting to see the continued studies on all 4 compounds and their ability to expand Vγ9Vδ2 T cells *in vivo*.

To truly test these compounds in their ability to expand Vγ9Vδ2 T cells *in vivo*, a proper model system must be set up. Vγ9Vδ2 T cell expansion studies become difficult at this point, as most organisms do not produce this specific type of T cell. Vγ9Vδ2 T cells are only found in primates and humans, ultimately restricting our ability to investigate these cells *in vivo*. To investigate the immunotherapeutic effects of our novel phosphoantigen prodrugs, we have developed a humanized mouse model. Here, we were able to create a model utilizing Rag-2 and IL-2 deficient mice, these mice do not produce T cells or B cells and thereby are immunocompromised. This is of critical importance as it allows us to IV inject human PBMCs without worrying about an immune response from the host T cells or B cells. However, these mice are still able to produce macrophages, which can also illicit an immune response. To avoid destruction of donor hPBMCs in the host, we found it beneficial to inject the mice with clodronate liposomes. These liposomes were phagocytosed by mouse macrophages, resulting in the death of these cells. After 24 hours, mice were injected with donor hPBMCs, which were identified in the spleen of the host 24 hours later. This leads us to believe that this model will function well in investigating the expansion of compounds **4**, **9**, **15**, and **17** in Vγ9Vδ2 T cells *in vivo*.

If these compounds successfully expand Vγ9Vδ2 T cells *in vivo*, there is good potential for their use as cancer immunotherapy agents. Further studies are required before this can be determined. It would also be interesting to investigate the effects of these compounds in directly stimulating the Vγ9Vδ2 T cells to target cancerous cells *in vivo*.

Compound name/number	Compound structure
POM_2-C-HMBP	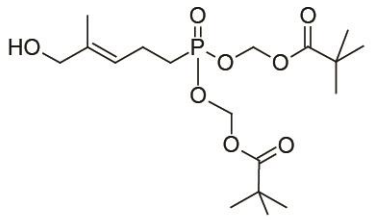
4	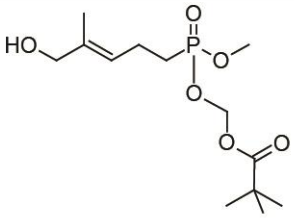
9	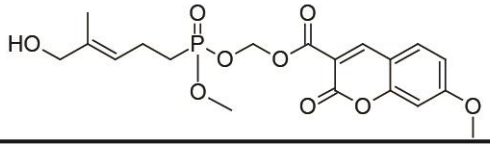
15	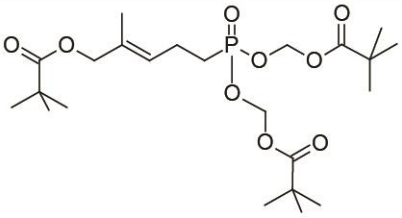
17	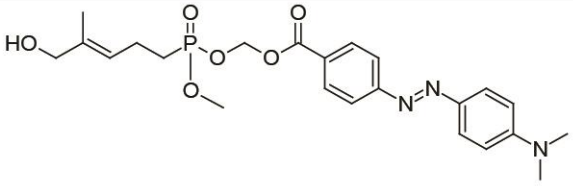

Table 6. Compounds used *in vivo*.

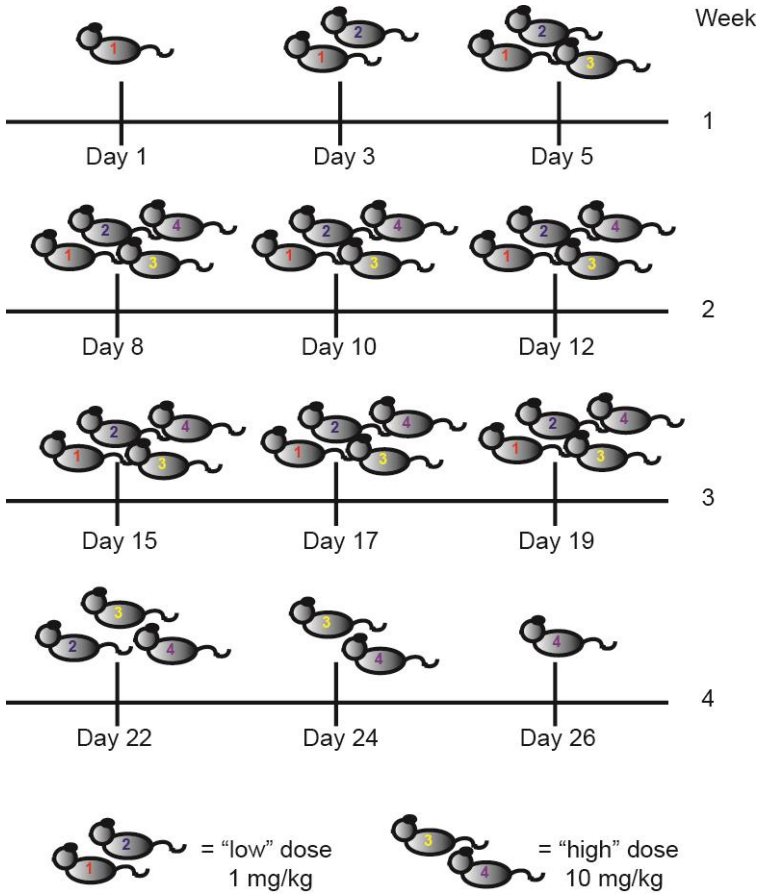

Figure 33. Dosing schedule for novel phosphoantigen toxicity screen in mice.

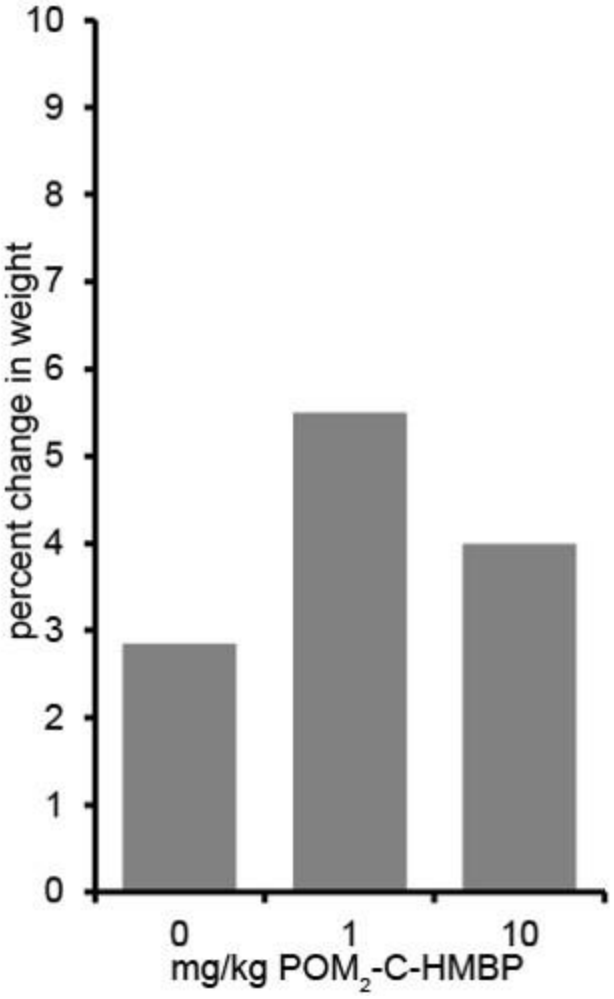

Figure 34. Dosing of mice with POM_2-C-HMBP

Mice were dosed with 0, 1, or 10 mg/kg POM_2-C-HMBP 3 times a week for a total of 3 weeks, or 9 injections. Data is shown in percent change in weight. n=2. *note, all weight was gained, if weight was lost, it would be shown as a negative percent change in weight.

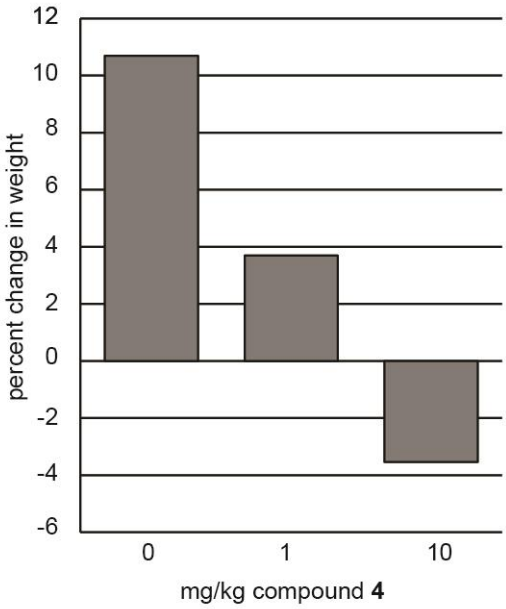

Figure 35. Dosing of mice with compound 4

Mice were dosed with 0, 1, or 10 mg/kg compound **4** 3 times a week for a total of 3 weeks, or 9 injections. Data is shown in percent change in weight. n=2

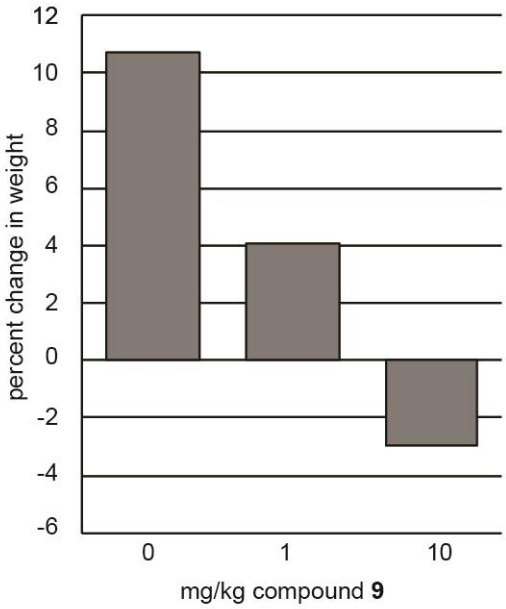

Figure 36. Dosing of mice with compound 9

Mice were dosed with 0, 1, or 10 mg/kg compound **9** 3 times a week for a total of 3 weeks, or 9 injections. Data is shown in percent change in weight. n=2.

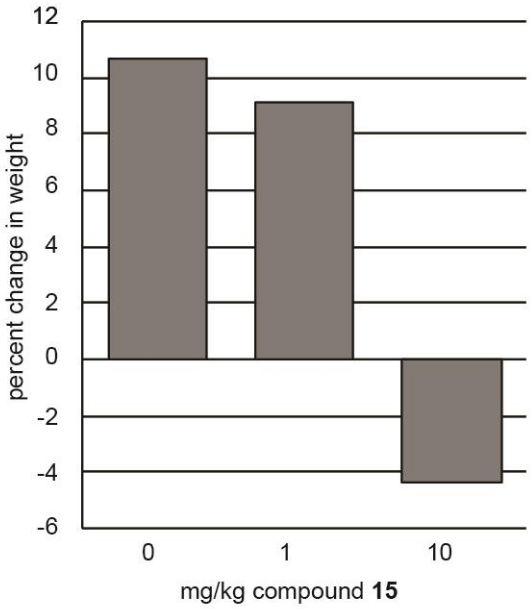

Figure 37. Dosing of mice with compound 15

Mice were dosed with 0, 1, or 10 mg/kg compound **15** 3 times a week for a total of 3 weeks, or 9 injections. Data is shown in percent change in weight. n=2.

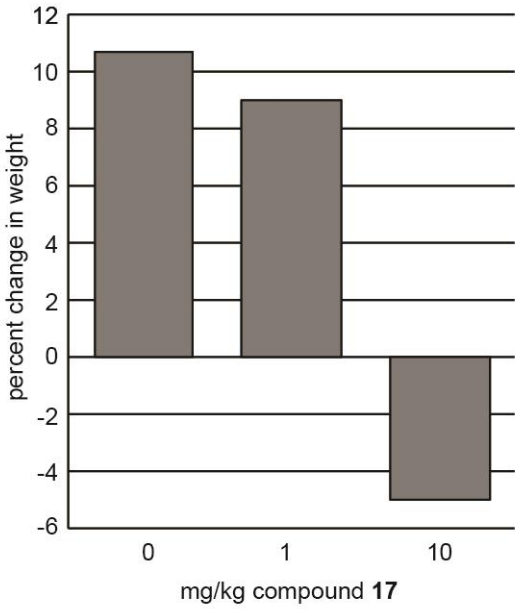

Figure 38. Dosing of mice with compound 17

Mice were dosed with 0, 1, or 10 mg/kg compound **17** 3 times a week for a total of 3 weeks, or 9 injections. Data is shown in percent change in weight. n=2

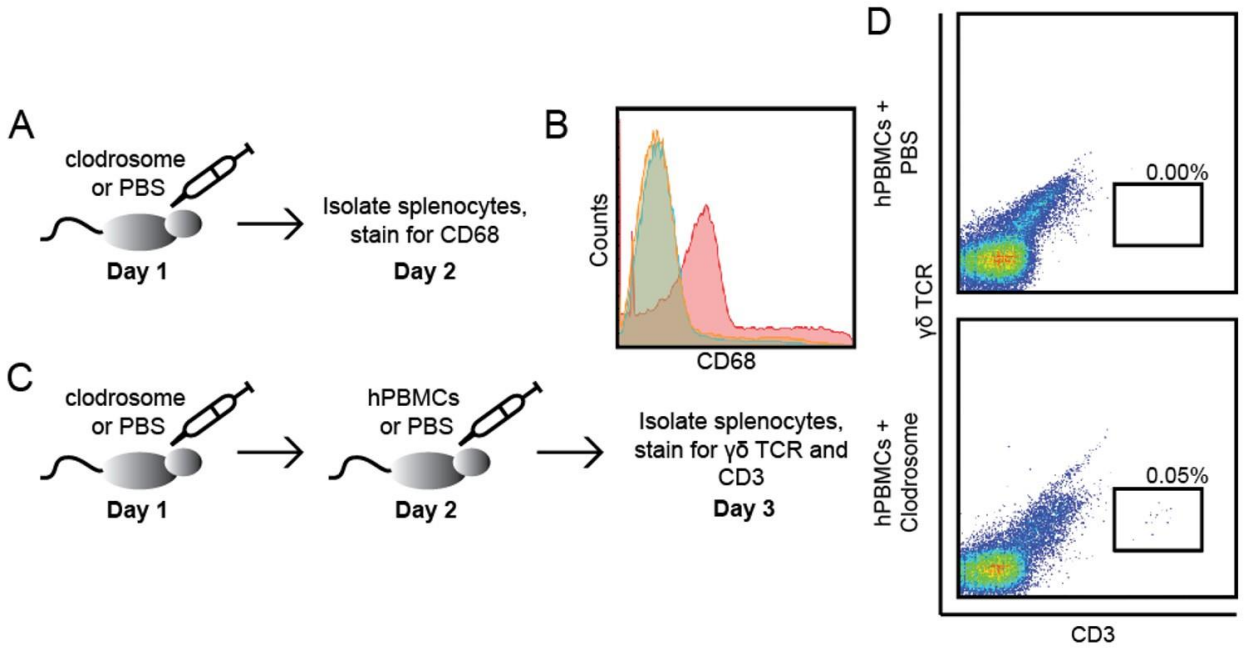

Figure 39. Isolating hPBMCs from humanized mice

A) Schematic of clodrosome injection and splenocyte harvest. B) Flow cytometry data of CD68 expression in mouse splenocytes of mice treated with no clodrosome (red), 150 µL clodrosome in 25 g mouse (green), and 300 µL clodrosome in 25 g mouse (orange). C) Schematic of clodrosome and hPBMC injection and splenocyte harvest. D) Flow cytometry data of hPBMCs collected from mouse splenocytes as described in C. Flow plots are representative of greater than three independent experiments. n=3

CHAPTER VII

CONCLUSION

Signaling pathways leading to Vγ9Vδ2 T cell activation

Throughout chapters II and IV, we investigate mechanisms underlying signaling and activation of Vγ9Vδ2 T cells. In chapter II, our work investigating the pathways of Vγ9Vδ2 T cell signaling is presented. Here, we specifically looked at the signaling involved in the migration and stop signal of Vγ9Vδ2 T cells. By utilizing live imaging techniques, we were able to visualize Vγ9Vδ2 T cells migrating along an ICAM-1 treated well. We were then able to identify the involvement of both PKC and CD3 in the cell migration stop signal. When activated, PKC induced stop signal, as did stimulation of CD3.

The remainder of chapter II was focused on the mechanism of signaling leading to the lysis of target cells. Here, we used a fluorescence based lysis assay and showed that we were able to induce lysis of target cells by treating them with phosphoantigen. We then found that Src kinases are involved in lysis of target cells by Vγ9Vδ2 T cells. Inhibition of Src kinases led to a decrease in percentage of lysis back to normal levels. With a similar experiment, we identified the specific Src kinase, Lck, which is involved. My graduate career began with the data shown in Chapter II, shortly after these experiments were done, Decaup et al [45] found a series of phosphorylated proteins that were involved, at which point my project switched gears to investigating mechanisms occurring on the target cell side of the synapse, as seen in chapter IV.

Chapter IV began by presenting our work in characterizing the phenotype of the Vγ9Vδ2 T cells produced and utilized throughout the entirety of this dissertation. We found that these cells, once expanded ultimately become Th1 memory Vγ9Vδ2 T cells. This was important in

understanding which cytokines these cells produce, as well as determining if these Vγ9Vδ2 T cells gain a memory phenotype.

Chapter IV then delves into the investigation of the requirement of BTN3A1 in the lysis of target cells as well as cytokine production by Vγ9Vδ2 T cells. It was known that Vγ9Vδ2 T cells can be stimulated and activated via phosphoantigens, and these phosphoantigens have been shown to interact with the protein BTN3A1 intracellularly [51, 84]. However, if BTN3A1 was required for these responses, was still unknown. We found that when knocking out BTN3A1 in our target K562 cells, we saw a significant decrease in lysis of target cells by Vγ9Vδ2 T cells, as well as a significant decrease in cytokine production. Furthermore, lysis of target cells was rescued when the cells were rescued by cells electroporated with a BTN3A1 construct. When Vγ9Vδ2 T cells were treated with a Vγ9Vδ2 TCR stimulating antibody, lysis was still observed in BTN3A1 knockout cells. This shows that BTN3A1 is required for phosphoantigen mediated lysis by Vγ9Vδ2 T cells, but is not required for TCR mediated lysis by Vγ9Vδ2 T cells.

If phosphoantigens interact intracellularly as previously mentioned, exogenous phosphoantigens must enter the target cell in some way. Chapter IV then focuses on the mechanism by which Vγ9Vδ2 T cells take up exogenous phosphoantigens. We did a series of experiments at 4ºC or 37ºC, where the cells treated at 4ºC would have a decrease in any energy-dependent transport. We found that exogenous charge negative phosphoantigens enter the cells via an energy-dependent mechanism, while charge neutral phosphoantigen prodrugs freely enter the cells.

Chapter IV continues further with a study in which we treated one set of cells with phosphoantigen, while we left one set untreated, we then mixed both sets together with Vγ9Vδ2 T cells to investigate the ability of Vγ9Vδ2 T cells to specifically target cells exposed to phosphoantigen for lysis. We found that the Vγ9Vδ2 T cells identified and lysed the target cells

specifically treated with phosphoantigen while leaving the untreated cells alone. This indicates that Vγ9Vδ2 T cells recognize phosphoantigen treated cells even when mixed in a pool of untreated cells. This indicates that healthy cells in the vicinity of treated/infected/cancerous cells are safe from lysis.

I concluded chapter IV with a time course study to investigate how long both HMBPP or the charge neutral phosphoantigen prodrug POM_2-C-HMBP remain active within the target cell. Target K562 cells were treated with either HMBPP or POM_2-C-HMBP for 2 hours and were then mixed immediately with Vγ9Vδ2 T cells, or left in culture for a period of time (6, 12, 24, 48, or 72 hours) before being added to Vγ9Vδ2 T cells. Levels of lysis were analyzed and we found that HMBPP was rapidly metabolized, while the phosphoantigen prodrug POM_2-C-HMBP was not.

These two chapters, II and IV, helped us understand some of the underlying mechanisms of activation at the Vγ9Vδ2 T cell as well as some of the underlying mechanisms within the target K562 cell leading to cytokine production or lysis by the Vγ9Vδ2 T cell.

Analysis of novel phosphoantigens and their prodrugs

Chapters III and V focus on the testing of novel phosphoantigen prodrugs in tissue culture. In chapter III my work on testing of a coumarin-derived, fluorescent phosphoantigen prodrug, compound **9** is shown. After testing compound **9** alongside its POM counterpart, compound **4**, we found that the coumarin-carboxylate oxymethyl ester protecting group functions as well as the POM protecting group in expansion of Vγ9Vδ2 T cells, activation of Vγ9Vδ2 T cells to lyse target cells, and in toxicity screens in leukemia cell lines. This fluorescent group also lost fluorescence when metabolized, allowing us to analyze uptake of the coumarin-derived prodrug into cells. We found that compound **9** had a half-life of 55 minutes, indicating that within hours, virtually all the drug can pass into the cells.

Chapter V focuses on a series of novel phosphoantigen prodrugs, compounds **10**-**16**. These compounds are tested for the ability to stimulate Vγ9Vδ2 T cells to proliferate, the ability to induce lysis of target cells, and for target cell toxicity. We found that compounds **10**-**13**, compounds that have been elongated, were unable to expand Vγ9Vδ2 T cells, stimulated lysis of target cells by Vγ9Vδ2 T cells with higher EC_{50} values of 1 μM or more, and did not show cytotoxicity in K562 cells. Compounds **14**, **15**, and **16**, compounds that have been acylated, were able to expand Vγ9Vδ2 T cells, as well as induce lysis of target cells by Vγ9Vδ2 T cells with EC_{50} values of 0.015 μM or lower, and were toxic to K562 cells at 100 μM. Chapter V shows that potential phosphoantigen compounds with elongated alkyl chains do not function as active phosphoantigens, while phosphoantigen prodrugs that have been acylated function well as active phosphoantigens. Compounds **14**, **15**, and **16** are phosphoantigen prodrugs that need to be further studied.

Development of an in vivo model for phosphoantigen tolerability and activity

My research is concluded in chapter VI, where we investigate the toxicity of a selection of novel phosphoantigen prodrugs described throughout chapters III-V. Current immunotherapeutic studies using Vγ9Vδ2 T cells have primarily utilized the indirect phosphoantigen zoledronate. Although FDA approved, continuous exposure to zoledronate has been shown to be toxic to Vγ9Vδ2 T cells [120]. To avoid this, Nada et al have shown that pulsing Vγ9Vδ2 T cells with zoledronate improved quantity and quality of Vγ9Vδ2 T cells when compared to Vγ9Vδ2 T cells that were continuously exposed to zoledronate [121]. As an indirect phosphoantigen, zoledronate may not be the best immunotherapeutic option in Vγ9Vδ2 T cell stimulation. Indirect phosphoantigens function by blocking farnesyl diphosphate synthase (FDPS), ultimately leading to increased levels of IPP, the direct phosphoantigen [120]. This means that zoledronate and other

indirect phosphoantigens increase the risk of off target effects through the inhibition of FDPS, which is not ideal. Phosphoantigen prodrugs avoid this, as they are primary phosphoantigens, giving them an advantage over the more commonly used zoledronate. Our research here tested POM_2-C-HMBP and compounds **4**, **9**, **15**, and a new compound, **17** *in vivo* for toxicity via subcutaneous injections at both a high (10 mg/kg) and low dose (1 mg/kg). POM_2-C-HMBP did not show any toxicity throughout the 9 treatments at both high and low doses, while compounds **4**, **9**, **15**, and **17** did not show toxicity at low doses, but were slightly toxic at high doses, resulting in an overall decrease in weight after the 9 doses. As all the compounds were not toxic at the low dose, these compounds may be good options to test *in vivo* Vγ9Vδ2 T cell expansion experiments with.

To perform *in vivo* Vγ9Vδ2 T cell expansion experiments, a proper model must first be in place. Throughout the second section of chapter VI, I describe a humanized mouse model that we developed for these experiments, as well as other future Vγ9Vδ2 T cell experiments. This model has been shown to sustain human PBMCs that have been IV injected, and will be essential for future *in vivo* Vγ9Vδ2 T cell experiments.

Future of Vγ9Vδ2 T Cell Research and Immunotherapies

Vγ9Vδ2 T cell research remains in its infancy. This dissertation has furthered the field in several ways 1) several signaling molecules have been identified as involved in both stop signal induction and activation of lysis, 2) Vγ9Vδ2 T cells expanded as described here have a memory Th1 phenotype, 3) BTN3A1 is required for lysis of target cells and production of cytokines, but not required for TCR stimulated lysis, 4) exogenous phosphoantigens are brought into the cell via an energy-dependent mechanism, 5) several novel phosphoantigen prodrugs have been developed that show strong potency when tested in cell culture, and 6) several of the prodrugs have been

tested for toxicity *in vivo* in mice and show little toxicity. Though this is a significant increase in information within the field, there is still much to be investigated, especially in terms of the immunotherapeutic potential.

Basic research on Vγ9Vδ2 T cells is still very important. The signaling pathways involved in all Vγ9Vδ2 T cell responses (i.e. NK cell stimulation, cytokine production, lysis of target cells, etc.) still need to be fully uncovered, not only what signaling molecules are involved, but also, where in the signaling pathway are they located. This is important because, as scientists, we cannot assume that Vγ9Vδ2 T cells will utilize the same signaling pathways as αβ T cells, but instead this needs to be shown. As it is likely, and research thus far does indicate that these pathways are very similar, see chapter II and Decaup et al [45], it may not be at the top of the list of things to investigate.

The interaction between phosphoantigen and BTN3A1 is an area of interest currently. It is now well established that phosphoantigens bind at the B30.2 domain [51, 84]. More recently, BTN3A1 has been shown to dimerize and upon phosphoantigen binding, undergo a conformational change [37]. Shippy et al have indicated this to be a negative cooperativity event, hypothesizing that Vγ9Vδ2 T cells would only become active if the binding pockets of both dimerized BTN3A1 proteins have bound phosphoantigen [122]. The conformational change of the BTN3A1 dimer would then lead to activation of the Vγ9Vδ2 T cell. However, the immediate downstream effects of this conformational change are still unknown and are an area of interest. It is entirely possible that this conformational change occurs when the target cell and the Vγ9Vδ2 T cell are interacting, leading to a direct effect on the Vγ9Vδ2 T cell.

Another important area of investigation is this interaction occurring between the Vγ9Vδ2 T cell and the target cell. The molecules interacting directly at the synapse have yet to be identified.

We have suggested three potential models here in Chapter IV (Figure 28), any of which are possible. Once these interactions have been identified, it will open yet another door for potential immunotherapeutics for cancer, but also for autoimmune diseases involving Vγ9Vδ2 T cells, such as rheumatoid arthritis.

Vγ9Vδ2 T cell immunotherapy is an area of research that will continue in the Wiemer Lab as my research concludes. The phosphoantigen prodrugs that have been described here can be further investigated, as well as others to come. These investigations include further studies in cell culture, specifically in cell lines and primary cells that have yet to be tested, but could potentially be targets for Vγ9Vδ2 T cells. These may include non-blood cancers, as Vγ9Vδ2 T cells can migrate out of the peripheral blood into the tissue. Non-blood cancers could be used in mice as well, and would allow for more specific *in vivo* testing of the phosphoantigen prodrugs, as they would be administered directly to the tumor.

In vivo testing of the 5 phosphoantigen prodrugs tested in chapter VI will continue in the Wiemer Lab. These experiments will include testing expansion of Vγ9Vδ2 T cells *in vivo* in the humanized mouse model developed and described in chapter VI, as well as testing the effects of the phosphoantigen prodrugs in treating humanized mice with blood cancers. These experiments will continue with future phosphoantigen prodrugs as well.

Things to consider in the development of future phosphoantigen prodrugs will be the addition of specific protecting groups or linkers that may allow the prodrugs to be either 1) only taken in by cancerous cells or 2) only metabolized by cancerous cells. If either one of these can be done, this would allow phosphoantigen prodrugs to be administered systemically, yet the cancerous cells would be the only cells to have active exogenous phosphoantigen present, ultimately activating the Vγ9Vδ2 T cells to target and lyse them.

Ultimately, the field of Vγ9Vδ2 T cell research still has a great deal to uncover, and unearthing the full mechanism leading to stimulation and activation of these cells will be essential in the production of immunotherapeutics for both cancer and autoimmune diseases. These cells, thought to be nothing of importance for many years, have recently been found to be very important in bacterial infection, immune surveillance of cancer cells, and inflammation. It is essential that we as scientists investigate these fascinating cells, Vγ9Vδ2 T cells, in their entirety.

REFERENCES

1. Davis, D.M. and M.L. Dustin, *What is the importance of the immunological synapse?* Trends Immunol, 2004. **25**(6): p. 323-7.

2. Favier, B., et al., *Uncoupling between immunological synapse formation and functional outcome in human gamma delta T lymphocytes.* J Immunol, 2003. **171**(10): p. 5027-33.

3. Grakoui, A., et al., *The immunological synapse: a molecular machine controlling T cell activation.* Science, 1999. **285**(5425): p. 221-7.

4. Huppa, J.B. and M.M. Davis, *T-cell-antigen recognition and the immunological synapse.* Nat Rev Immunol, 2003. **3**(12): p. 973-83.

5. Neefjes, J., et al., *Towards a systems understanding of MHC class I and MHC class II antigen presentation.* Nat Rev Immunol, 2011. **11**(12): p. 823-36.

6. Salomon, B. and J.A. Bluestone, *Complexities of CD28/B7: CTLA-4 costimulatory pathways in autoimmunity and transplantation.* Annu Rev Immunol, 2001. **19**: p. 225-52.

7. Harding, F.A., et al., *CD28-mediated signalling co-stimulates murine T cells and prevents induction of anergy in T-cell clones.* Nature, 1992. **356**(6370): p. 607-9.

8. Jenkins, M.K., et al., *CD28 delivers a costimulatory signal involved in antigen-specific IL-2 production by human T cells.* J Immunol, 1991. **147**(8): p. 2461-6.

9. Dustin, M.L., *The immunological synapse.* Cancer Immunol Res, 2014. **2**(11): p. 1023-33.

10. Stinchcombe, J.C., et al., *The immunological synapse of CTL contains a secretory domain and membrane bridges.* Immunity, 2001. **15**(5): p. 751-61.

11. Das, V., et al., *Activation-induced polarized recycling targets T cell antigen receptors to the immunological synapse; involvement of SNARE complexes.* Immunity, 2004. **20**(5): p. 577-88.

12. Ramsay, A.G., et al., *Chronic lymphocytic leukemia T cells show impaired immunological synapse formation that can be reversed with an immunomodulating drug.* J Clin Invest, 2008. **118**(7): p. 2427-37.

13. Kearney, C.J., et al., *The Role of the immunological Synapse Formed by Cytotoxic Lymphocytes in Immunodeficiency and Anti-Tumor immunity.* Crit Rev Immunol, 2015. **35**(4): p. 325-47.

14. Thedrez, A., et al., *Self/non-self discrimination by human gammadelta T cells: simple solutions for a complex issue?* Immunol Rev, 2007. **215**: p. 123-35.

15. De Rosa, S.C., et al., *Ontogeny of gamma delta T cells in humans.* J Immunol, 2004. **172**(3): p. 1637-45.

16. Adams, E.J., S. Gu, and A.M. Luoma, *Human gamma delta T cells: Evolution and ligand recognition.* Cell Immunol, 2015.

17. Xu, B., et al., *Crystal structure of a gammadelta T-cell receptor specific for the human MHC class I homolog MICA.* Proc Natl Acad Sci U S A, 2011. **108**(6): p. 2414-9.

18. Spada, F.M., et al., *Self-recognition of CD1 by gamma/delta T cells: implications for innate immunity.* J Exp Med, 2000. **191**(6): p. 937-48.

19. Bai, L., et al., *The majority of CD1d-sulfatide-specific T cells in human blood use a semiinvariant Vdelta1 TCR.* Eur J Immunol, 2012. **42**(9): p. 2505-10.

20. Vincent, M.S., et al., *Lyme arthritis synovial gamma delta T cells respond to Borrelia burgdorferi lipoproteins and lipidated hexapeptides.* J Immunol, 1998. **161**(10): p. 5762-71.

21. Kong, Y., et al., *The NKG2D ligand ULBP4 binds to TCRgamma9/delta2 and induces cytotoxicity to tumor cells through both TCRgammadelta and NKG2D.* Blood, 2009. **114**(2): p. 310-7.

22. Willcox, C.R., et al., *Cytomegalovirus and tumor stress surveillance by binding of a human gammadelta T cell antigen receptor to endothelial protein C receptor.* Nat Immunol, 2012. **13**(9): p. 872-9.

23. Constant, P., et al., *Stimulation of human gamma delta T cells by nonpeptidic mycobacterial ligands.* Science, 1994. **264**(5156): p. 267-70.

24. Mookerjee-Basu, J., et al., *F1-adenosine triphosphatase displays properties characteristic of an antigen presentation molecule for Vgamma9Vdelta2 T cells.* J Immunol, 2010. **184**(12): p. 6920-8.

25. Vantourout, P. and A. Hayday, *Six-of-the-best: unique contributions of gammadelta T cells to immunology.* Nat Rev Immunol, 2013. **13**(2): p. 88-100.

26. Kalyan, S. and D. Kabelitz, *Defining the nature of human gammadelta T cells: a biographical sketch of the highly empathetic.* Cell Mol Immunol, 2013. **10**(1): p. 21-9.

27. Morita, C.T., et al., *Nonpeptide antigens, presentation mechanisms, and immunological memory of human Vgamma2Vdelta2 T cells: discriminating friend from foe through the recognition of prenyl pyrophosphate antigens.* Immunol Rev, 2007. **215**: p. 59-76.

28. Kabelitz, D., et al., *Human Vdelta2 versus non-Vdelta2 gammadelta T cells in antitumor immunity.* Oncoimmunology, 2013. **2**(3): p. e23304.

29. Tanaka, Y., et al., *Natural and synthetic non-peptide antigens recognized by human gamma delta T cells.* Nature, 1995. **375**(6527): p. 155-8.

30. Fournie, J.J. and M. Bonneville, *Stimulation of gamma delta T cells by phosphoantigens.* Res Immunol, 1996. **147**(5): p. 338-47.

31. Coscia, M., et al., *Dysfunctional Vgamma9Vdelta2 T cells are negative prognosticators and markers of dysregulated mevalonate pathway activity in chronic lymphocytic leukemia cells.* Blood, 2012. **120**(16): p. 3271-9.

32. Gober, H.J., et al., *Human T cell receptor gammadelta cells recognize endogenous mevalonate metabolites in tumor cells.* J Exp Med, 2003. **197**(2): p. 163-8.

33. Kunzmann, V., E. Bauer, and M. Wilhelm, *Gamma/delta T-cell stimulation by pamidronate.* N Engl J Med, 1999. **340**(9): p. 737-8.

34. Dieli, F., et al., *Induction of gammadelta T-lymphocyte effector functions by bisphosphonate zoledronic acid in cancer patients in vivo.* Blood, 2003. **102**(6): p. 2310-1.

35. Sandstrom, A., et al., *The intracellular B30.2 domain of butyrophilin 3A1 binds phosphoantigens to mediate activation of human Vgamma9Vdelta2 T cells.* Immunity, 2014. **40**(4): p. 490-500.

36. Palakodeti, A., et al., *The molecular basis for modulation of human Vgamma9Vdelta2 T cell responses by CD277/butyrophilin-3 (BTN3A)-specific antibodies.* J Biol Chem, 2012. **287**(39): p. 32780-90.

37. Sebestyen, Z., et al., *RhoB Mediates Phosphoantigen Recognition by Vgamma9Vdelta2 T Cell Receptor.* Cell Rep, 2016. **15**(9): p. 1973-85.

38. Abeler-Dorner, L., et al., *Butyrophilins: an emerging family of immune regulators.* Trends Immunol, 2012. **33**(1): p. 34-41.

39. Arnett, H.A. and J.L. Viney, *Immune modulation by butyrophilins.* Nat Rev Immunol, 2014. **14**(8): p. 559-69.

40. Morita, C.T., et al., *Direct presentation of nonpeptide prenyl pyrophosphate antigens to human gamma delta T cells.* Immunity, 1995. **3**(4): p. 495-507.

41. Brandes, M., K. Willimann, and B. Moser, *Professional antigen-presentation function by human gammadelta T Cells.* Science, 2005. **309**(5732): p. 264-8.

42. Harly, C., et al., *Key implication of CD277/butyrophilin-3 (BTN3A) in cellular stress sensing by a major human gammadelta T-cell subset.* Blood, 2012. **120**(11): p. 2269-79.

43. Wang, H., et al., *Butyrophilin 3A1 plays an essential role in prenyl pyrophosphate stimulation of human Vgamma2Vdelta2 T cells.* J Immunol, 2013. **191**(3): p. 1029-42.

44. Vavassori, S., et al., *Butyrophilin 3A1 binds phosphorylated antigens and stimulates human gammadelta T cells.* Nat Immunol, 2013. **14**(9): p. 908-16.

45. Decaup, E., et al., *Phosphoantigens and butyrophilin 3A1 induce similar intracellular activation signaling in human TCRVgamma9(+) gammadelta T lymphocytes.* Immunol Lett, 2014. **161**(1): p. 133-7.

46. Nedellec, S., M. Bonneville, and E. Scotet, *Human Vgamma9Vdelta2 T cells: from signals to functions.* Semin Immunol, 2010. **22**(4): p. 199-206.

47. Vermijlen, D., et al., *Distinct cytokine-driven responses of activated blood gammadelta T cells: insights into unconventional T cell pleiotropy.* J Immunol, 2007. **178**(7): p. 4304-14.

48. Gagliani, N. and S. Huber, *Balancing pro- and anti-inflammatory CD4+ T helper cells in the intestine*. Autoimmune Diseases - Contributing Factors, Specific Cases of Autoimmune Diseases, and Stem Cell and Other Therapies. 2012.

49. Lertworapreecha, M., et al., *Cytotoxic function of gamma delta (gamma/delta) T cells against pamidronate-treated cervical cancer cells.* Indian J Exp Biol, 2013. **51**(8): p. 597-605.

50. Fisher, J., et al., *Neuroblastoma killing properties of V-delta 2 and V-delta2 negative gamma delta T cells following expansion by artificial antigen presenting cells.* Clin Cancer Res, 2014.

51. Hsiao, C.H., et al., *Synthesis of a Phosphoantigen Prodrug that Potently Activates Vgamma9Vdelta2 T-Lymphocytes.* Chem Biol, 2014.

52. Giang, I., E.L. Boland, and G.M. Poon, *Prodrug applications for targeted cancer therapy.* AAPS J, 2014. **16**(5): p. 899-913.

53. Wiemer, D.F. and A.J. Wiemer, *Opportunities and challenges in development of phosphoantigens as Vgamma9Vdelta2 T cell agonists.* Biochem Pharmacol, 2014. **89**(3): p. 301-12.

54. Paul, S. and B.C. Schaefer, *A new look at T cell receptor signaling to nuclear factor-kappaB.* Trends Immunol, 2013. **34**(6): p. 269-81.

55. Pollizzi, K.N. and J.D. Powell, *Integrating canonical and metabolic signalling programmes in the regulation of T cell responses.* Nat Rev Immunol, 2014. **14**(7): p. 435-46.

56. Dustin, M.L., *T-cell activation through immunological synapses and kinapses.* Immunol Rev, 2008. **221**: p. 77-89.

57. Wernimont, S.A., et al., *Contact-dependent T cell activation and T cell stopping require talin1*. J Immunol, 2011. **187**(12): p. 6256-67.

58. Wiemer, A.J., S. Wernimont, and A. Huttenlocher, *Live imaging of LFA-1-dependent T-cell motility and stop signals.* Methods Mol Biol, 2012. **757**: p. 191-204.

59. Wiemer, A.J., et al., *Evaluation of a 7-Methoxycoumarin-3-carboxylic Acid Ester Derivative as a Fluorescent, Cell-Cleavable, Phosphonate Protecting Group.* Chembiochem, 2016. **17**(1): p. 52-5.

60. Westheimer, F.H., *Why nature chose phosphates.* Science, 1987. **235**(4793): p. 1173-8.

61. Kornberg, R.D., M.G. McNamee, and H.M. McConnell, *Measurement of transmembrane potentials in phospholipid vesicles.* Proc Natl Acad Sci U S A, 1972. **69**(6): p. 1508-13.

62. Wiemer, A.J. and D.F. Wiemer, *Prodrugs of phosphonates and phosphates: crossing the membrane barrier.* Top Curr Chem, 2015. **360**: p. 115-60.

63. Lee, W.A. and J.C. Martin, *Perspectives on the development of acyclic nucleotide analogs as antiviral drugs.* Antiviral Res, 2006. **71**(2-3): p. 254-9.

64. Pertusati, F., M. Serpi, and C. McGuigan, *Medicinal chemistry of nucleoside phosphonate prodrugs for antiviral therapy.* Antivir Chem Chemother, 2012. **22**(5): p. 181-203.

65. Jessen, H.J., et al., *Bioreversible protection of nucleoside diphosphates.* Angew Chem Int Ed Engl, 2008. **47**(45): p. 8719-22.

66. Gerdes, S.Y., et al., *Experimental determination and system level analysis of essential genes in Escherichia coli MG1655.* J Bacteriol, 2003. **185**(19): p. 5673-84.

67. Karunakaran, M.M. and T. Herrmann, *The Vgamma9Vdelta2 T Cell Antigen Receptor and Butyrophilin-3 A1: Models of Interaction, the Possibility of Co-Evolution, and the Case of Dendritic Epidermal T Cells.* Front Immunol, 2014. **5**: p. 648.

68. Harly, C., C.M. Peigne, and E. Scotet, *Molecules and Mechanisms Implicated in the Peculiar Antigenic Activation Process of Human Vgamma9Vdelta2 T Cells.* Front Immunol, 2014. **5**: p. 657.

69. Zhang, Y., et al., *Lipophilic pyridinium bisphosphonates: potent gammadelta T cell stimulators.* Angew Chem Int Ed Engl, 2010. **49**(6): p. 1136-8.

70. Wiemer, D.F. and N.J. Leonard, *Site of N-amination of adenine and alkyladenines.* J Org Chem, 1974. **39**(23): p. 3438-40.

71. Wiemer, A.J., et al., *Pivaloyloxymethyl-modified isoprenoid bisphosphonates display enhanced inhibition of cellular geranylgeranylation.* Bioorg Med Chem, 2008. **16**(7): p. 3652-60.

72. Farquhar, D., et al., *Synthesis and antitumor evaluation of bis[(pivaloyloxy)methyl] 2'-deoxy-5-fluorouridine 5'-monophosphate (FdUMP): a strategy to introduce nucleotides into cells.* J Med Chem, 1994. **37**(23): p. 3902-9.

73. Kashemirov, B.A., et al., *Fluorescently labeled risedronate and related analogues: "magic linker" synthesis.* Bioconjug Chem, 2008. **19**(12): p. 2308-10.

74. Eisenberg, E.J., G.X. He, and W.A. Lee, *Metabolism of GS-7340, a novel phenyl monophosphoramidate intracellular prodrug of PMPA, in blood.* Nucleosides Nucleotides Nucleic Acids, 2001. **20**(4-7): p. 1091-8.

75. Kilcollins, A.M., et al., *HMBPP Analog Prodrugs Bypass Energy-Dependent Uptake To Promote Efficient BTN3A1-Mediated Malignant Cell Lysis by Vgamma9Vdelta2 T Lymphocyte Effectors.* J Immunol, 2016. **197**(2): p. 419-28.

76. Wrobel, P., et al., *Lysis of a broad range of epithelial tumour cells by human gamma delta T cells: involvement of NKG2D ligands and T-cell receptor- versus NKG2D-dependent recognition.* Scandinavian Journal of Immunology, 2007. **66**(2-3): p. 320-328.

77. Adams, E.J., S. Gu, and A.M. Luoma, *Human gamma delta T cells: Evolution and ligand recognition.* Cell Immunol, 2015. **296**(1): p. 31-40.

78. Wiemer, A.J., C.-H.C. Hsiao, and D.F. Wiemer, *Isoprenoid Metabolism as a Therapeutic Target in Gram-Negative Pathogens.* Current Topics in Medicinal Chemistry, 2010. **10**(18): p. 1858-1871.

79. Harwood, H.J., Jr., et al., *In vivo regulation of human leukocyte 3-hydroxy-3-methylglutaryl coenzyme A reductase: increased enzyme protein concentration and catalytic efficiency in human leukemia and lymphoma.* J Lipid Res, 1991. **32**(8): p. 1237-52.

80. Santolaria, T., et al., *Repeated systemic administrations of both aminobisphosphonates and human Vgamma9Vdelta2 T cells efficiently control tumor development in vivo.* J Immunol, 2013. **191**(4): p. 1993-2000.

81. Ryan-Payseur, B., et al., *Multieffector-functional immune responses of HMBPP-specific Vgamma2Vdelta2 T cells in nonhuman primates inoculated with Listeria monocytogenes DeltaactA prfA*.* J Immunol, 2012. **189**(3): p. 1285-93.

82. Fournie, J.J., et al., *What lessons can be learned from gammadelta T cell-based cancer immunotherapy trials?* Cell Mol Immunol, 2013. **10**(1): p. 35-41.

83. Messal, N., et al., *Differential role for CD277 as a co-regulator of the immune signal in T and NK cells.* Eur J Immunol, 2011. **41**(12): p. 3443-54.

84. Gu, S., W. Nawrocka, and E.J. Adams, *Sensing of Pyrophosphate Metabolites by Vgamma9Vdelta2 T Cells.* Front Immunol, 2014. **5**: p. 688.

85. Hsiao, C.H., et al., *Synthesis of a phosphoantigen prodrug that potently activates Vgamma9Vdelta2 T-lymphocytes.* Chem Biol, 2014. **21**(8): p. 945-54.

86. Kabelitz, D., *CD277 takes the lead in human gammadelta T-cell activation.* Blood, 2012. **120**(11): p. 2159-61.

87. Ran, F.A., et al., *Genome engineering using the CRISPR-Cas9 system.* Nat Protoc, 2013. **8**(11): p. 2281-308.

88. Holtmeier, W. and D. Kabelitz, *gammadelta T cells link innate and adaptive immune responses.* Chem Immunol Allergy, 2005. **86**: p. 151-83.

89. Goldberg, J.E., S.W. Sherwood, and C. Clayberger, *A novel method for measuring CTL and NK cell-mediated cytotoxicity using annexin V and two-color flow cytometry.* J Immunol Methods, 1999. **224**(1-2): p. 1-9.

90. Batzri, S. and E.D. Korn, *Interaction of phospholipid vesicles with cells. Endocytosis and fusion as alternate mechanisms for the uptake of lipid-soluble and water-soluble molecules.* J Cell Biol, 1975. **66**(3): p. 621-34.

91. Wernimont, S.A., et al., *PIPKI gamma 90 negatively regulates LFA-1-mediated adhesion and activation in antigen-induced CD4+ T cells.* J Immunol, 2010. **185**(8): p. 4714-23.

92. Gruenbacher, G., et al., *CD56+ human blood dendritic cells effectively promote TH1-type gammadelta T-cell responses.* Blood, 2009. **114**(20): p. 4422-31.

93. Holoshitz, J., et al., *Dual antigenic recognition by cloned human gamma delta T cells.* J Clin Invest, 1992. **89**(1): p. 308-14.

94. Kozbor, D., et al., *Human TCR-gamma+/delta+, CD8+ T lymphocytes recognize tetanus toxoid in an MHC-restricted fashion.* J Exp Med, 1989. **169**(5): p. 1847-51.

95. Thompson, K., et al., *Cytosolic entry of bisphosphonate drugs requires acidification of vesicles after fluid-phase endocytosis.* Mol Pharmacol, 2006. **69**(5): p. 1624-32.

96. Guenot, M., et al., *Phosphoantigen Burst Upon Plasmodium Falciparum Schizont Rupture Can Distantly Activate Vgamma9-Vdelta2 T-Cells.* Infect Immun, 2015.

97. Benzaid, I., et al., *High phosphoantigen levels in bisphosphonate-treated human breast tumors promote Vgamma9Vdelta2 T-cell chemotaxis and cytotoxicity in vivo.* Cancer Res, 2011. **71**(13): p. 4562-72.

98. Bukowski, J.F., et al., *Crucial role of TCR gamma chain junctional region in prenyl pyrophosphate antigen recognition by gamma delta T cells.* Journal of Immunology, 1998. **161**(1): p. 286-293.

99. Gong, G., et al., *Phosphoantigen-activated V gamma 2V delta 2 T cells antagonize IL-2-induced CD4+CD25+Foxp3+ T regulatory cells in mycobacterial infection.* Blood, 2009. **113**(4): p. 837-45.

100. Wang, H. and C.T. Morita, *Sensor Function for Butyrophilin 3A1 in Prenyl Pyrophosphate Stimulation of Human Vgamma2Vdelta2 T Cells.* J Immunol, 2015. **195**(10): p. 4583-94.

101. Riano, F., et al., *Vgamma9Vdelta2 TCR-activation by phosphorylated antigens requires butyrophilin 3 A1 (BTN3A1) and additional genes on human chromosome 6.* Eur J Immunol, 2014.

102. Davis, S.J. and P.A. van der Merwe, *The kinetic-segregation model: TCR triggering and beyond.* Nat Immunol, 2006. **7**(8): p. 803-9.

103. Espinosa, E., et al., *Synaptic transfer by human gamma delta T cells stimulated with soluble or cellular antigens.* J Immunol, 2002. **168**(12): p. 6336-43.

104. Autran, B., et al., *T cell receptor gamma/delta+ lymphocyte subsets during HIV infection.* Clin Exp Immunol, 1989. **75**(2): p. 206-10.

105. Huttunen, K.M. and J. Rautio, *Prodrugs - an efficient way to breach delivery and targeting barriers.* Curr Top Med Chem, 2011. **11**(18): p. 2265-87.

106. Fowler, D.W. and M.D. Bodman-Smith, *Harnessing the power of Vdelta2 cells in cancer immunotherapy.* Clin Exp Immunol, 2015. **180**(1): p. 1-10.

107. Caccamo, N., et al., *Gammadelta T cell modulation in anticancer treatment.* Curr Cancer Drug Targets, 2010. **10**(1): p. 27-36.

108. Wilhelm, M., et al., *Gammadelta T cells for immune therapy of patients with lymphoid malignancies.* Blood, 2003. **102**(1): p. 200-6.

109. Kobayashi, H. and Y. Tanaka, *gammadelta T Cell Immunotherapy-A Review.* Pharmaceuticals (Basel), 2015. **8**(1): p. 40-61.

110. Gogoi, D. and S.V. Chiplunkar, *Targeting gamma delta T cells for cancer immunotherapy: bench to bedside.* Indian J Med Res, 2013. **138**(5): p. 755-61.

111. Braza, M.S. and B. Klein, *Anti-tumour immunotherapy with Vgamma9Vdelta2 T lymphocytes: from the bench to the bedside.* Br J Haematol, 2013. **160**(2): p. 123-32.

112. Kunzmann, V., et al., *Tumor-promoting versus tumor-antagonizing roles of gammadelta T cells in cancer immunotherapy: results from a prospective phase I/II trial.* J Immunother, 2012. **35**(2): p. 205-13.

113. Lang, J.M., et al., *Pilot trial of interleukin-2 and zoledronic acid to augment gammadelta T cells as treatment for patients with refractory renal cell carcinoma.* Cancer Immunol Immunother, 2011. **60**(10): p. 1447-60.

114. Dieli, F., et al., *Targeting human {gamma}delta} T cells with zoledronate and interleukin-2 for immunotherapy of hormone-refractory prostate cancer.* Cancer Res, 2007. **67**(15): p. 7450-7.

115. Meraviglia, S., et al., *In vivo manipulation of Vgamma9Vdelta2 T cells with zoledronate and low-dose interleukin-2 for immunotherapy of advanced breast cancer patients.* Clin Exp Immunol, 2010. **161**(2): p. 290-7.

116. Bennouna, J., et al., *Phase I study of bromohydrin pyrophosphate (BrHPP, IPH 1101), a Vgamma9Vdelta2 T lymphocyte agonist in patients with solid tumors.* Cancer Immunol Immunother, 2010. **59**(10): p. 1521-30.

117. Zhou, J., et al., *Anti-gammadelta TCR antibody-expanded gammadelta T cells: a better choice for the adoptive immunotherapy of lymphoid malignancies.* Cell Mol Immunol, 2012. **9**(1): p. 34-44.

118. Tu, W., et al., *The aminobisphosphonate pamidronate controls influenza pathogenesis by expanding a gammadelta T cell population in humanized mice.* J Exp Med, 2011. **208**(7): p. 1511-22.

119. Huang, D., et al., *Antigen-specific Vgamma2Vdelta2 T effector cells confer homeostatic protection against pneumonic plaque lesions.* Proc Natl Acad Sci U S A, 2009. **106**(18): p. 7553-8.

120. Wang, H., et al., *Indirect stimulation of human Vgamma2Vdelta2 T cells through alterations in isoprenoid metabolism.* J Immunol, 2011. **187**(10): p. 5099-113.

121. Nada, M.H., et al., *Enhancing adoptive cancer immunotherapy with Vgamma2Vdelta2 T cells through pulse zoledronate stimulation.* J Immunother Cancer, 2017. **5**: p. 9.

122. Shippy, R.R., et al., *Phosphinophosphonates and Their Tris-pivaloyloxymethyl Prodrugs Reveal a Negatively Cooperative Butyrophilin Activation Mechanism.* J Med Chem, 2017.